BOOK OF ABSTRACTS



10th Scientific Meeting of PhD Students at UAB campus

Dates: November 25th-27th 2026

PLENARY SPEAKER, INVITED SPEAKERS, WORKSHOPS, SEMINARS AND ROUND TABLE

10th Scientific Meeting of PhD Students at the BNC-b
25-27 November 2026 · UAB campus

Plenary speaker

A material world:

From design to applications through life



Prof. Dr. Luisa De Cola

Full Professor at the Università degli Studi di Milano Statale (Unimi)
Head of the Materials for Health Unit at the Istituto di Ricerche Farmacologiche Mario Negri (IRCCS)

November 26th, 2026
17:15 to 18:15
Sala d'Actes - Facultat de Ciències i Biociències UAB

2026 JPhD
10th edition

ICMAB
INSTITUT DE CIÈNCIA DE MATERIALS DE BARCELONA
EXCELENCIA SEVERO OCHOA
CSIC
CONSEJO SUPERIOR DE INVESTIGACIONES CIENTÍFICAS

UAB
Universitat Autònoma de Barcelona

ICN2
Institut Català de Nanociència i Nanotecnologia

Centre Nacional de Microelectrònica
IMB
EXCELENCIA MARÍA DE MAEZTU
CSIC

SCQ
Societat Catalana de Química

MDPI
Academic Open Access Publishing
since 1996

10th Scientific Meeting of PhD Students at the BNC-b
25-27 November 2026 · UAB campus

Synthesis and catalysis– Invited speaker

Colloidal engineering of reticular materials



Dr. Inhar Imaz Gabilondo

CSIC Research Scientist at the Institut Català de Nanociència i Nanotecnologia (ICN2)
Subgroup Leader of the Supramolecular NanoChemistry and Materials group at ICN2

November 25th, 2026
9:15 to 10:00
Sala d'Actes - Facultat de Ciències i Biociències UAB

2026 JPhD 10th edition

ICMAB Institut de Ciència de Materials de Barcelona · Excelencia Severo Ochoa · CSIC Consejo Superior de Investigaciones Científicas

UAB Universitat Autònoma de Barcelona

ICN2 Institut Català de Nanociència i Nanotecnologia

CNM Centre Nacional de Microelectrònica · IMB · Excelencia María de Maeztu · CSIC

SCQ Societat Catalana de Química

MDPI Academic Open Access Publishing since 1996

10th Scientific Meeting of PhD Students at the BNC-b
25-27 November 2026 · UAB campus

Biomedicine– Invited speaker

From Biomaterials to Vaccines:

Innovative Strategies for Animal Health



Dr. Nerea Roher Armentia

Full Professor at the Universitat Autònoma de Barcelona (UAB)
Coordinator of the Evolutive Immunology group at the Institut de Biotecnologia i Biomedicina (IBB)

November 25th, 2026
10:45 to 11:30
Sala de Graus - Facultat de Ciències i Biociències UAB

2026 JPhD
10th edition

ICMAB
INSTITUT DE CIÈNCIA DE MATERIALS DE BARCELONA
EXCELENCIA SEVERO OCHOA
CSIC
UAB
Universitat Autònoma de Barcelona
ICN2
Institut Català de Nanociència i Nanotecnologia
Centre Nacional de Microelectrònica
IMB
EXCELENCIA MARÍA DE MAEZTU
CSIC
SCQ
Societat Catalana de Química
MDPI
Academic Open Access Publishing
since 1996

10th Scientific Meeting of PhD Students at the BNC-b
25-27 November 2026 · UAB campus

Electronic and Optical properties of Materials – Invited speaker

Vibrations from scratch:

A first-principles journey trough phonons', electric fields and magnetism



Dr. Miquel Royo Valls

Tenured Scientist at the Institut de Ciència de Materials de Barcelona (ICMAB-CSIC)

November 26th, 2026
9:00 to 9:45
Sala d'Actes - Facultat de Ciències i Biociències UAB

2026 JPhD 10th edition

ICMAB Institut de Ciència de Materials de Barcelona · Excelencia Severo Ochoa · CSIC

UAB Universitat Autònoma de Barcelona

ICN2 Institut Català de Nanociència i Nanotecnologia

CNM Centre Nacional de Microelectrònica · IMB · Excelencia María de Maeztu · CSIC

SCQ Societat Catalana de Química

MDPI Academic Open Access Publishing since 1996

10th Scientific Meeting of PhD Students at the BNC-b
25-27 November 2026 · UAB campus

Energy, sustainability and environment – Invited speaker

In situ (scanning) transmission electron microscopy for exploring the stability of catalytic materials



Dr. Alba Garzón Manjón

Assistant Professor at the Universitat Autònoma de Barcelona (UAB)

November 25th, 2026
14:30 to 15:15
Sala d'Actes - Facultat de Ciències i Biociències UAB

2026 JPhD
10th edition

ICMAB 40 ANYS
INSTITUT DE CIÈNCIA DE MATERIALS DE BARCELONA
EXCELENCIA SEVERO OCHOA · CSIC

UAB
Universitat Autònoma de Barcelona

ICN2
Institut Català de Nanociència i Nanotecnologia

CNM Centre Nacional de Microelectrònica · IMB
EXCELENCIA MARÍA DE MAEZTU · CSIC

SCQ
Societat Catalana de Química

MDPI
Academic Open Access Publishing
since 1996

10th Scientific Meeting of PhD Students at the BNC-b
25-27 November 2026 · UAB campus

Magnetism and quantum materials – Invited speaker

Amorphous Magnetic Microwires at Microwave Frequencies:

From Wireless Sensors to Electromagnetic Absorbers



Dr. Pilar Marín Palacios

Full Professor at the Universidad Complutense de Madrid (UCM)
Director of the Instituto de Magnetismo Aplicado (IMA)

November 26th, 2026
14:30 to 15:15
Sala d'Actes - Facultat de Ciències i Biociències UAB

2026 JPhD
10th edition

ICMAB
INSTITUT DE CIÈNCIA DE MATERIALS DE BARCELONA
EXCELENCIA SEVERO OCHOA
CSIC
CONSEJO SUPERIOR DE INVESTIGACIONES CIENTÍFICAS

UAB
Universitat Autònoma de Barcelona

ICN2
Institut Català de Nanociència i Nanotecnologia

CNM
Centre Nacional de Microelectrònica
IMB
EXCELENCIA MARÍA DE MAEZTU
CSIC
CONSEJO SUPERIOR DE INVESTIGACIONES CIENTÍFICAS

SCQ
Societat Catalana de Química

MDPI
Academic Open Access Publishing
since 1996

10th Scientific Meeting of PhD Students at the BNC-b
25-27 November 2026 · UAB campus

Thriving, Not Just Surviving – Redefining Success in Academia

Mental health in Academia:

Tools for Proactive Stress Management



Dr. Ingeborg Porcar Becker

Founder and Technical Director of the Unitat de Trauma, Crisis i Conflictes de Barcelona (UTCCB)
Associate Professor at the Universitat Autònoma de Barcelona (UAB)

November 25th, 2026
17:15 to 18:30
Sala d'Actes - Facultat de Ciències i Biociències UAB

2026 JPhD
10th edition

ICMAB 40 ANYS
INSTITUT DE CIÈNCIA DE MATERIALS DE BARCELONA
EXCELENCIA SEVERO OCHOA · CSIC

UAB Universitat Autònoma de Barcelona

ICN2
Institut Català de Nanociència i Nanotecnologia

CNM Centre Nacional de Microelectrònica · IMB
EXCELENCIA MARÍA DE MAEZTU · CSIC

SCQ Societat Catalana de Química

MDPI
Academic Open Access Publishing since 1996

10th Scientific Meeting of PhD Students at the BNC-b
25-27 November 2026 · UAB campus

From Submission to Acceptance – Demystifying the Peer Review and Open Access Landscape

Open access and peer-review

Scientific publishing at MDPI



Dr. María José Vermejo Valle

Deputy Managing Editor at MDPI Spain.

November 25th, 2026
11:15 to 11:45
Sala d'Actes - Facultat de Ciències i Biociències UAB

2026 JPhD 10th edition

ICMAB 40 ANYS
INSTITUT DE CIÈNCIA DE MATERIALS DE BARCELONA
EXCELENCIA SEVERO OCHOA · CSIC Consejo Superior de Investigaciones Científicas

UAB Universitat Autònoma de Barcelona

ICN2 Institut Català de Nanociència i Nanotecnologia

CNM Centre Nacional de Microelectrònica · IMB
EXCELENCIA MARÍA DE MAEZTU · CSIC Consejo Superior de Investigaciones Científicas

SCQ Societat Catalana de Química

MDPI
Academic Open Access Publishing since 1996

10th Scientific Meeting of PhD Students at the BNC-b
25-27 November 2026 · UAB campus

Honest Insights, Real Challenges, and the Path Ahead – Navigating Your Transition to Group Leader

The road to becoming a PI:

The good, the bad and the unexpected



Dr. Ana Victoria Lechuga Vieco

Junior Group Leader of the Mitochondrial Biology and Tissue Regeneration Research Group at the Institut de Recerca Biomèdica (IRB Barcelona)

November 26th, 2026
11:15 to 11:45
Sala d'Actes - Facultat de Ciències i Biociències UAB

2026 JPhD 10th edition

ICMAB 40 ANYS
INSTITUT DE CIÈNCIA DE MATERIALS DE BARCELONA
EXCELENCIA SEVERO OCHOA · CSIC

UAB Universitat Autònoma de Barcelona

ICN2
Institut Català de Nanociència i Nanotecnologia

CNM Centre Nacional de Microelectrònica · IMB
EXCELENCIA MARÍA DE MAEZTU · CSIC

SCQ Societat Catalana de Química

MDPI
Academic Open Access Publishing since 1996

10th Scientific Meeting of PhD Students at the BNC-b
25-27 November 2026 · UAB campus

A Journey of Discovery, Dialogue, and Direction – Building Your Future After the PhD.

Academia vs Industry:

Two Career Paths After the PhD



Dr. De-yi Wang
Academia
IMDEA Materials Institute, Mardrid



Dr. Nora Ventosa Rull
Academia & Industry
ICMAB-CSIC & CEO of Delbios Pharmaceuticals



Dr. Ana Lechuga
Academia
IRB Barcelona



Dr. Fabião Santos
Industry
Vecmedical, Barcelona

November 26th, 2026
12:00 to 13:30
Sala d'Actes - Facultat de Ciències i Biociències UAB

2026 JPhD
10th edition

ICMAB
INSTITUT DE CIÈNCIA DE MATERIALS DE BARCELONA
EXCELENCIA SEVERO OCHOA · CSIC

UAB
Universitat Autònoma de Barcelona

ICN2
Institut Català de Nanociència i Nanotecnologia

Centre Nacional de Microelectrònica · IMB
EXCELENCIA MARÍA DE MAEZTU · CSIC

SCQ
Societat Catalana de Química

MDPI
Academic Open Access Publishing
since 1996

ORAL PRESENTATIONS

Planar Oxygen ion ECRAMs for neuromorphic computing

Hemant Agarwal[1], Francesco Chiabrera[1], Albert Tarancon[1]

[1]*Department of Advanced Materials for Energy, Catalonia Institute for Energy Research (IREC), Jardins de les Dones de Negre1,2, Sant Adrià de Besòs, Barcelona 08193, Spain*

hagarwal@irec.cat

Keywords: neuromorphic, computing, transistors, ECRAMs, Oxygen-ion, memory, devices

Neuromorphic computing involves using non-Von Neumann architecture of in memory computing for accelerating neural networks employing analog memory devices as artificial synapses [1]. For this, various analog memory technologies have been heavily investigated over the past decade, including but not limited to memristors [2], ferroelectric transistors, organic field effect transistors [3] and electrochemical random-access memory (ECRAMs).

ECRAMs work by exchange of ions between the reservoir and the channel through an electrolyte, whereby different gate biases and bias time allow for different degrees of intercalation into the channel allowing for various analog states, this intercalation changes conductivity allowing analog computation. Oxygen ion Electrochemical Random Access Memories (OECRAMs) involve transport of oxygen ion between the channel and reservoir changing the oxidation stoichiometry of the oxide channel, changing its properties [1]. OECRAMs are interesting because they show linear and reliable conductance modulation during potentiation and depression, low operation voltage and true nonvolatile memory behavior enabled by high temperature writing and room temperature state reading.

This work investigates etch free planar OECRAMs as artificial synapses where lanthanum strontium ferrite (LSF50) was used as the oxide channel and BiCuVOx as the fast oxygen ion electrolyte. The results show 500-fold change in conductivity, clear change in optical properties, potentiation and depression response, low cycle to cycle variability, and device operation stability over 4 months. Consistent and stable performance allows it to be a benchmark against future architectures and etch-free fabrication allows scaling to neuromorphic arrays and further applications.

(1) P. Langner, F. Chiabrera, N. Alayo, P. Nizet, L. Morrone, C. Bozal-Ginesta, A. Morata, A. Tarancón, Solid-State Oxide-Ion Synaptic Transistor for Neuromorphic Computing. *Adv. Mater.* 2025, 37, 2415743. https://doi.org/10.1002/adma.202415743.

(2) M. Raveendra Kiran, Hemant Agarwal, Sharath P., Santosh Nayak, P. Srijyothi, Hidayath Ulla, Dibya Yadav, Syed Arshad Hussain, Casein-derived functional layers for electronic memory, sensing and energy storage applications: A comprehensive review,Next Materials,Volume 13,2026,103244,

(3) Bishwajit Mandal, Prashant Sonar, Samarendra Pratap Singh; Visible Light-Stimulated Artificial Synapse Based on an Organic Field-Effect Transistor for Imitating Human Emotions and Mood Swings. *ACS Appl. Electron. Mater.* 23 April 2024; 6 (4): 2420–2433. https://doi.org/10.1021/acsaelm.4c00079

Anisotropic spin dynamics in proximitized graphene

Patricia Aguilar Merino[1,2], Gabriel de Araújo Masanti[1,2], Josef Světlík[1,2], Juan F. Sierra[2], Sergio O. Valenzuela[2,3]

1 Catalan Institute of Nanoscience and Nanotechnology (ICN2), Bellaterra (Barcelona), Spain.

2 Universitat Autònoma de Barcelona (UAB), Bellaterra, Spain
3 Institució Catalana de Recerca i Estudis Avançats (ICREA), Barcelona, Spain
patricia.aguilar@icn2.cat

Keywords: Spintronics, Graphene, 2D materials, anisotropy, proximity effects.

While electronics exploits the charge degree of freedom of electrons, spintronics benefits from their spin to process and store information. Graphene stands out as a medium for spin transport due to its carbon-based composition, which ensures very low spin-orbit coupling (SOC) and allows spins to propagate over very long distances. However, weak SOC limits spin manipulation.

Two-dimensional (2D) layered materials, integrated into vertical van der Waals heterostructures, offer unique opportunities for engineering novel physical properties through proximity-induced phenomena. In this work, we investigate spin dynamics in hybrid graphene–transition metal dichalcogenide (TMDC) systems, where proximity-induced SOC is introduced into graphene by adjacent high-SOC TMDCs.

Prior studies have reported strong spin lifetime anisotropy in graphene with the hierarchy $\tau_z >> \tau_x$; ty and isotropic in-plane spin lifetimes $\tau_x = \tau_y$ for symmetric TMDCs such as WSe_2, WS_2, MoS_2 and $MoSe_2$ [1]. Low-symmetry TMDCs, such as pentagonal $PdSe_2$ [2], further modify this hierarchy, yielding in-plane spin lifetime anisotropy. As a novelty, our experiments reveal a directional dependence of the spin lifetimes across all spatial directions, underscoring the richness and versatility of proximity-induced phenomena in these systems [3].

[1] T S Ghiasi et al., Nano Lett. 17 (2017) 7528−7532; L A Benítez et al., Nat. Phys. 14 (2018) 303-308; F Herling et al., APL Mater. 8 (2020) 071103.
[2] J F Sierra, J Světlík et al., Nat. Mater., published online (2025) doi:10.1038/s41563-024-02109-2.
[3] P Aguilar-Merino et al., (unpublished 2026).

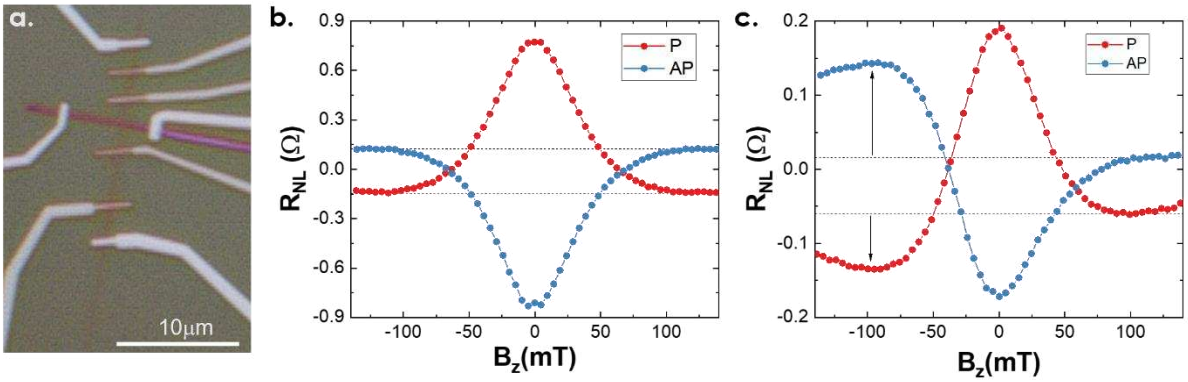

Figure 1: a. Graphene/TMDC spin valve. b. Parallel and antiparallel spin Hanle precession curves in bare graphene. c. Parallel and antiparallel Hanle spin precession curves in graphene showing in-plane anisotropy.

Molecular mechanism of iron recognition and domain closure in the periplasmic ferric-binding protein FbpA from *Mannheimia haemolytica*

Mercè Alemany-Chavarria[1,2], Chara Sarafoglou[3], Giorgos Gouridis[3], Jean-Didier Maréchal[1,2]

[1]*Department de Química, Universitat Autònoma de Barcelona, Cerdanyola del Vallès, Catalunya, Spain.*
[2] *Institut de Biotecnologia i de Biomedicina, Universitat Autònoma de Barcelona,Cerdanyola del Vallès, Catalunya, Spain*
[3] *Institute of Molecular Biology and Biotechnology, Heraklion, Crete, Greece*

merce.alemany@uab.cat

Keywords: Nutritional immunity, Ferric-binding protein, Metal-binding site prediction, Conformational change, Molecular dynamics

Iron is essential for nearly all organisms. Most pathogenic bacteria must obtain it from their host, which sequesters iron in proteins such as transferrin and lactoferrin. This defence, known as nutritional immunity, makes iron acquisition a key virulence determinant and fuels an evolutionary arms race between host and pathogen [1].

In Gram-negative bacteria, iron crossing the outer membrane is captured in the periplasm by solute-binding proteins (SBPs) and delivered to inner-membrane ABC transporters [2]. SBPs share a bilobal scaffold whose two domains close around the ligand through a hinge-bending motion, the "Venus flytrap" mechanism [3]. The ferric-binding protein FbpA, known as the "bacterial transferrin," belongs to this family [4]. In *Mannheimia haemolytica* FbpA, Fe^{3+} coordination involves a carbonate anion [5].

Here we investigate how Fe^{3+} binding to *M. haemolytica* FbpA is coupled to its conformational change. We use a multiscale computational approach that combines molecular docking, conventional and Gaussian accelerated molecular dynamics [6] and the metal-binding site predictor BioMetAll [7]. Our preliminary results identify the residues critical for recognition of the Fe^{3+}–carbonate complex and characterize the dynamics of the open-to-closed transition. These findings deepen our understanding of bacterial iron acquisition and may ultimately help identify new antibacterial targets.

References:

[1] Hood MI, Skaar EP. *Nat Rev Microbiol* 2012;10:525.
[2] Andrews SC, et al. *FEMS Microbiol Rev* 2003;27:215.
[3] Berntsson RP-A, et al. *FEBS Lett* 2010;584:2606.
[4] Bruns CM, et al. *Nat Struct Biol* 1997;4:919.
[5] Clarke TE., et al. *J Bacteriol* 2004 186 3903.
[6] Miao Y, et al. *J Chem Theory Comput* 2015;11:3584.
[7] Sánchez-Aparicio JE, et al. *J Chem Inf Model* 2021;61:311.

2026 JPhD 10th edition

Effect of BTO capping of ferroelectric La-Doped HfO_2 on energy storage performance

Neus Alert Peret, Tingfeng Song, Florencio Sánchez, Ignasi Fina Martínez

[1]*Institut de Ciència de Materials de Barcelona (ICMAB-CSIC), Campus UAB, Bellaterra, 08193 Barcelona, Spain*

nalert@icmab.es

Keywords: Ferroelectric, HfO_2, Electrostatic energy storage

Ferroelectrics are being studied as good candidates for next-generation electrostatic energy storage devices. The integration of these capacitors at chip level, next to logic and memory devices, would reduce the energy dissipation due to transport. Most studied materials for electrostatic energy storage based on perovskite structures are not compatible with industrial processes for electronic circuitry. Ferroelectric fluorite HfO_2 is an attractive and compatible alternative. However, the study of energy storage performance in these materials is still limited and the strategies available to improve it are still underdeveloped. Interface engineering is one of the promising strategies to tailor the functional properties of such devices. In this work, we will describe the impact of using perovskite ferroelectric $BaTiO_3$ as a capping layer on epitaxial La-doped HfO_2 thin films on the energy storage performance. Despite the lower polarizability of $BaTiO_3$ compared to HfO_2, a property that ultimately determines energy storage density (ESD), capped samples show an increase on ESD. Moreover, capping enhances the remanent polarization by 60% and reduces the coercive field relative to the uncapped ones. The coexistence of improved ESD with enhanced remanent polarization can be potentially leveraged in envisaged multifunctional devices that integrate energy storage and memory functionality in a single device and material.

Hybrid Graphene-Based Thin-Film Arrays for Bidirectional Neural Interfaces: Integration Challenges and Design Strategies

Nerea Alvarez de Eulate[1,3], Eduard Masvidal-Codina[2,3], Xavi Illa[1,3], Samuel M. Flaherty[4], Rob C. Wykes[4,5], Anton Guimerà-Brunet[1,3], Jose A. Garrido[2,6]

[1] Institut de Microelectrònica de Barcelona, IMB-CNM (CSIC), Campus UAB, Bellaterra, Spain
[2] Catalan Institute of Nanoscience and Nanotechnology (ICN2), CSIC and BIST, Campus UAB, Bellaterra, Spain
[3] Biomedical Research Networking Center in Bioengineering, Biomaterials and Nanomedicine (CIBER-BBN), Barcelona, Spain
[4] Division of Neuroscience, School of Biological Sciences, University of Manchester, UK
[5] UCL Queen Square Institute of Neurology, University College London, London, UK
[6] Institució Catalana de Recerca i Estudis Avançats (ICREA), Barcelona, Spain

nerea.alvarezdeeulate@imb-cnm.csic.es, anton.guimera@imb-cnm.csic.es, joseantonio.garrido@icn2.cat

Keywords: neural interfaces, bioelectronics, neuromodulation, graphene, neural recording and stimulation

Bidirectional neural interfaces capable of simultaneous recording and stimulation are critical for the development of adaptive neuromodulation therapies targeting neurological disorders. Recent advances in thin-film technologies have enabled hybrid devices that integrate active and passive components, offering new opportunities for high-resolution neural interfacing[1]. In particular, graphene-based solution-gated field-effect transistors (gSGFETs) provide wideband neural recording capabilities, including sensitivity to slow and infraslow activity such as DC shifts and oscillations below 0.1 Hz, which are highly relevant in conditions such as stroke and epilepsy. Complementarily, nanoporous graphene electrodes, especially those based on reduced graphene oxide (rGO), enable efficient and precise stimulation due to their high charge injection capacity and porous structure.

Despite the promise of combining these technologies within a single platform, significant challenges arise in their integration. Residual charge accumulation following stimulation pulses can degrade transistor performance, while crosstalk and insufficient protection in high-density arrays may lead to signal interference or damage to the graphene channels. These effects can compromise both the stability and longevity of the device.

This work investigates the compatibility between graphene-based recording and stimulation components in hybrid thin-film arrays and explores design strategies to mitigate stimulation-induced artifacts and degradation. By addressing key integration challenges, the proposed approach aims to enable robust, micrometer-thin platforms for reliable bidirectional neural interfacing. The results contribute to the development of next-generation neural devices with enhanced performance and stability, featuring wide-band neural recording and precise neuromodulation.

References

(1) M. Prokop, M. Esparza-Laizzo, E. Masvidal-Codina, et al., “An artefact-resilient wide bandwidth bidirectional graphene neural interface,” Nature Communications 17, no. 6536 (2026).

Unraveling Structure–Property Relationships in High-Entropy Oxide Solid oxide cell air electrodes Using Operando XPS and Freestanding Thin Films

Marlene Anzengruber[1], Kosova Kreka[1], Mai Hussein Hamed[2], Genrikh Shterk[2], Christoph Baeumer[2], Lluís Yedra[3], Ona Falcó Artero[3], Albert Tarancón[1,4]

[1]Catalonia Institute for Energy Research (IREC), Barcelona, Spain.
[2]MESA+ Institute, Faculty of Science and Technology, University of Twente, Netherlands.
[3]Laboratory of Electron Nanoscopies (LENS), Micro-Nanotechnology and Nanoscopies for electrophotonic Devices (MIND), Department of Electronics and Biomedical Engineering and Institute of Nanoscience and Nanotechnology (IN2UB), University of Barcelona, Barcelona, Spain.
[4]Catalan Institution for Research and Advanced Studies (ICREA), Barcelona, Spain.

manzengruber@irec.cat

Keywords: Freestanding Thin Films, HEO, Operando XPS

High-entropy oxides (HEOs) have emerged as a promising class of materials for electrochemical energy conversion technologies like solid oxide fuel cells (SOFCs) due to their exceptional compositional flexibility, structural robustness, and tunable functional properties. Despite these advances, the fundamental mechanisms governing the structure–property relationships in HEOs remain insufficiently understood[1,2]. For a better understanding of the origin of the good electrochemical performance of HEOs, operando studies in a near-ambient pressure X-ray photoelectron spectroscopy (NAP-XPS) setup were carried out on thin films synthesized by pulsed laser deposition PLD. By probing the electrode surface under operating conditions, direct observation of changes in electronic structure, surface composition, and phase stability could be achieved. Here, the growth of highly crystalline HEO thin films on $SrTiO_3$, utilizing a sacrificial $Sr_3CaAl_2O_6$ (SCAO) interlayer, could be achieved. The resulting freestanding HEO thin films were transferred onto functional supports for the evaluation of their electrochemical performance and stability. Additionally, comprehensive structural characterization by X-ray photoelectron spectroscopy (XPS) and transmission electron microscopy (TEM) provided further insight in the preservation of crystallinity, composition, and microstructural features following the transfer process. Overall, this work demonstrates how thin-film high-entropy oxides can serve as highly controlled model systems for the fundamental investigation of complex oxide materials.

1. Yang Y, Bao H, Ni H, Ou X, Wang S, Lin B, et al. J Power Sources. 2021; 482:228959

2. Dąbrowa J, Olszewska A, Falkenstein A, Schwab C, Szymczak M, Zajusz M, et al. J Mater Chem A Mater. 2020; 8(46): 24455–68

Near-Field Imaging of PN-Junction-Free Photoresponse in Graphene Constrictions

Mohibbul Aziz[1], Florian Ludwig[1], Bogdan Borodin[2], Ronny Omar De La Bastida[1], Petr Stepanov[2], Roshan Krishna Kumar[1*]

[1] *ICN2-Institut Català de Nanociència i Nanotecnologia, UAB Campus, 08193 Bellaterra, Barcelona, Spain*
[2] *Department of Physics & Astronomy, University of Notre Dame, 46556 Notredame (Indiana), USA*
*mohibbul.aziz@icn2.cat, *roshan.krishna@icn2.cat*

Converting light into electrical signals - photocurrent generation is at the heart of modern optoelectronics. To push technologies beyond intrinsic device limitations, fundamentally new materials and photocurrent generation mechanisms are needed. Graphene has proven an exceptional broadband photodetector over the last years owed to its high electronic quality, strong light-matter interactions and strong thermoelectric capabilities. Yet, detectors typically require the engineering of complex PN junctions using complex gating schemes. A photocurrent mechanism that generates current even without PN junctions could vastly simplify device architectures and accelerate application development. Here, we study a unique photocurrent mechanism in graphene heterostructures that does not require a PN junction. It is generated in asymmetric constrictions of a graphene channel exhibiting strong response at charge neutrality [1]. While robust across several devices, the mechanism is still heavily debated preventing further optimization for detectors. Here, we perform near-field photocurrent measurements in the mid-infrared and terahertz range in our devices, and observe unusual spatial patterns which shed light on the mechanism underlying this response. The results unveil new insights into the mechanisms governing PN-junction free photoresponses potentially driven by unconventional electronic properties including hydrodynamic electron flows [2].

Keywords: Photocurrent, heterostructure, constriction, near-field measurement, mid-infrared, terahertz, hydrodynamic electron flow

[1] Ma, Q.; Lui, C. H.; Song, J. C. W.; Lin, Y.; Kong, J. F.; Cao, Y.; Dinh, T. H.; Nair, N. L.; Fang, W.; Watanabe, K.; Taniguchi, T.; Xu, S.-Y.; Kong, J.; Palacios, T.; Gedik, N.; Gabor, N. M.; Jarillo-Herrero, P. Giant intrinsic photoresponse in pristine graphene. Nature Nanotechnology, 145-150.

[2] Krishna Kumar, R.; Bandurin, D. A.; Pellegrino, F. M. D.; Cao, Y.; Principi, A.; Guo, H.; Auton, G. H.; Ben Shalom, M.; Ponomarenko, L. A.; Falkovich, G.; Watanabe, K.; Taniguchi, T.; Grigorieva, I. V.; Levitov, L. S.; Polini, M.; Geim, A. K. Superballistic flow of viscous electron fluid through graphene constrictions. Nature Physics, 1182-1185.

2026 JPhD 10th edition

Optimized incident polarization and isotropic depolarization filtering for Stokes imaging of biological samples

Judit Bisbal-Amat[1], Irene Estévez[1], Juan Campos[1], Angel Lizana[1]

[1]*Universitat Autònoma de Barcelona, Facultat de Ciències, Grup Òptica, Edifici C, 08193, Bellaterra (Barcelona)*

judit.bisbal@uab.cat

Keywords: Polarimetry, Stokes-Mueller formalism, Biomedicine, Imaging, Isotropic Depolarization

In biological imaging, polarimetric techniques have proven able to reveal structures hidden to conventional methods, with applications ranging from brain structure identification to melanoma discrimination and plant pathology recognition [1-3]. Polarimetry probes optical properties such as dichroism, retardance and depolarization. Among them, depolarization has emerged as a particularly powerful contrast mechanism for identifying structures. In particular, recent works have shown that filtering isotropic depolarization can yield major image enhancement [4].

Stokes-Mueller formalism is widely used to describe light-matter interactions in terms of polarization [5]. The Mueller matrix contains the complete polarimetric information of a sample, but its acquisition time still limits real-time applications. Stokes polarimetry instead retrieves only the polarization of the emerging light, which is much faster. Although it does not contain the complete information of a sample, it depends on it and therefore retains part of it.

In this work, we optimize the generated incident polarization state of light specifically for each type of sample to enhance visualization of the emerging Stokes vector, a crucial preliminary step toward real-time methods based on Stokes polarimetry. In addition, we apply to Stokes measurements an isotropic depolarization filter analogous to the one already used in the literature on Mueller measurements [4], to improve contrast. Results show that the filtered Stokes components reveal more structures than the raw Mueller matrix elements.

[1] Gros, R.; Rodríguez-Núñez, O.; Felger, L.; et al. Characterization of Polarimetric Properties in Various Brain Tumor Types Using Wide-Field Imaging Mueller Polarimetry. *IEEE Trans. Med. Imaging* **2024**, *43* (12), 4120-4132.

[2] Montes-Gonzalez, I.; Bisbal-Amat, J.; Perez-Torres, A.; et al. Macroscopic Polarimetric Discrimination and Quantification of Antiangiogenic Effect of AGRO Aptamer and GK1 Peptide in a Preclinical Melanoma Model. *Sci. Rep.* **2026**, *16*, 14299.

[3] Rodríguez, C.; Garcia-Caurel, E.; Garnatje, T.; et al. Polarimetric Observables for the Enhanced Visualization of Plant Diseases. *Sci. Rep.* **2022**, *12*, 14743.

[4] Canabal-Carbia, M.; Estévez, I.; González-Arnay, E.; et al. Revealing Hidden Bioimaging Information by Isotropic Depolarization Filtering. *Opt. Laser Technol.* **2025**, *188*, 112956.

[5] Gil, J. J.; Ossikovski, R. *Polarized Light and the Mueller Matrix Approach*, 2nd ed.; CRC Press: Boca Raton, FL, **2022**.



Impact of physicochemical properties on drug release and *in vivo* biodistribution of PLGA nanocapsules

Adriana Bombón-Nuela[1], Irene Fernández-Folgueral[2], Carlos Lopez[1], Anna Solé-Porta[1], Anna Laromaine[1], Anna Roig[1], Jesús Ruiz-Cabello[2,3], Juan Pellico[1,3*]

[1]*Institut de Ciència de Materials de Barcelona (ICMAB-CSIC), Catalonia, 08193 Bellaterra, Spain*
[2]*CIC biomaGUNE, Basque Research and Technology Alliance (BRTA), 20014, Donostia San Sebastián, Spain*
[3]*CIBER Enfermedades Respiratorias (CIBERES). 28029 Madrid,*

E-mail abombon@icmab.es

Keywords: PLGA nanocapsules, physicochemical properties, drug delivery, biodistribution, PET imaging

The development of multifunctional nanocarriers for targeted drug delivery and imaging remains a significant challenge [1]. We report the synthesis and characterization of poly(lactic-co-glycolic acid) (PLGA) nanocapsules (NCs) and investigate the influence of their physicochemical properties on drug release, blood circulation, and short-term biodistribution [2].

We synthesized PLGA NCs using a double emulsion-solvent evaporation strategy and evaluate the influence of the emulsion parameters (time and amplitude) on key particle properties. While emulsion time had no significant effect, reducing the amplitude from 39% to 21% increased NC size from 247 ± 21 nm (39DE) to 325 ± 2 nm (21DE), while maintaining similar zeta potential (-30mV) and spherical morphology. To evaluate their drug delivery performance, NCs were loaded with bovine serum albumin conjugated to Alexa Fluor 488 (BSA-AF488) as a model protein. The 21DE formulation showed higher encapsulation efficiency (56 ± 18%) than 39DE (33 ± 5%) and a lower initial burst release (20 ± 3% vs. 43 ± 9%), followed by sustained and progressive BSA-AF488 release over 30 days (Figure 1A). Further toxicity tests using a *Caenorhabditis elegans* model were performed, with the NCs showing no adverse effects. Finally, Ga-68 radiolabeling enabled PET assessment of NCs circulation and short-term biodistribution in healthy mice, revealing predominant accumulation in the liver and spleen after 2h (Figure 1B).

Overall, this study highlights the critical role of the emulsion amplitude in the physicochemical properties of the NCs. The size of the NCs significantly affects their drug release profile but has limited impact on blood circulation and short-term biodistribution, suggesting that a higher size might be beneficial for an improved therapeutic outcome without altering the biodistribution.

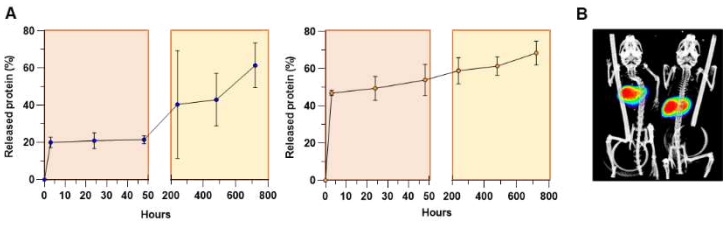

Figure 1. (A) Release profile. (B) PET imaging studies.

(1) C. Martins, F. Sousa, F. Araújo, B. Sarmento, Adv. Healthcare Mater. 2018, 7, 1701035.

(2) Solé-Porta, A.; Areny-Balagueró, A.; Camprubí-Rimblas, et al. *Small Science*, 2024, 4, 2400066

The Role of Reference and Counter Electrodes in the Stability of Graphene Solution Gated Field Effect Transistors (gSGFETs)

Laura Bono-Ros[1], Marc Tudela-Pi[1,2], Eva Casals Sanchez[1,2], Rosa Villa[1,2], Sergi Brosel-Oliu[1,2] Anton Guimerà-Brunet[1,2], Xavi Illa[1,2]

[1]Institute of Microelectronics of Barcelona, IMB-CNM (CSIC), Campus UAB, Bellaterra, 08193, Spain [2]CIBER-BBN, ISCIII, Bellaterra, 08193, Spain

laura.bono@imb-cnm.csic.es

Keywords: Graphene Solution Field Effect Transistor (gSGFET), reference electrode, long-term stability, biomedical applications

Graphene solution-gated field-effect transistors (gSGFETs) are promising platforms for biomedical applications due to their compatibility with aqueous environments, real-time monitoring capabilities, surface functionalization and multiplexed operation [1]. However, their long-term stability remains a significant challenge. Prolonged exposure to aqueous environments and repeated electrical operation can modify key device parameters, affecting reproducibility, reliability and sensing performance.

In the typical gSGFET configuration, current flows between the source and drain terminals through a graphene channel. The graphene-electrolyte potential is controlled by a gate electrode immersed in the electrolyte, which modulates the channel potential. The gate electrode serves simultaneously as the reference and counter electrode, providing the required current for charging graphene-electrolyte capacitance. Particularly, if the applied potential exceeds the electrochemical window of the graphene, faradaic currents can occur, leading to device degradation. Precise potential control is therefore crucial for reliable gSGFET operation, and Ag/AgCl electrodes are widely used due to their well-defined potential. However, passing current through an Ag/AgCl reference electrode, can change its potential and promote degradation, leading to Ag residues accumulation on the graphene channel. Alternatively, three-electrode configuration separates the reference and counter electrodes, using commonly Pt as a counter electrode. However, as a polarizable electrode, Pt can exhibit a potential drop when currents flow through it, potentially affecting the effective gate potential and the accuracy of extracted parameters such as the charge neutrality point (CNP), which is a crucial parameter for biosensing applications. Therefore, compensation of the counter-electrode potential drop is required to ensure reliable device characterization.

In this work, the impact of the electrode configuration on transfer characteristics and device parameters accuracy is evaluated. Ag/AgCl and Pt electrodes, together with a hydrogen reference electrode, are studied in conventional two-electrode and three-electrode configurations. The study is performed on arrays of 26 graphene microtransistors with 50 x 50 µm channel. The devices are electrically characterized, while scanning electron microscopy (SEM) is employed to investigate potential device contamination. These results provide insight into the role of the electrode system in gSGFET operation and contribute to the development of more stable and reliable graphene-based biomedical devices

(1) Masvidal-Codina, E. et al. High-resolution mapping of infraslow cortical brain activity enabled by graphene microtransistors. Nature Materials. 18, 280 (2019)

Gate-Current Monitoring in Frequency-Division Multiplexed gGFET Neural Interfaces

E. Casals Sanchez[1,2], M. Tudela Pi[1,2], X. Illa Vila[1,2] , A. Guimerà Brunet[1,2]

[1]*Institut de Microelectrònica de Barcelona (IMB-CNM),* [2]*Centro de Investigación Biomédica en Red (CIBER)*

eva.casals@imb-cnm.csic.es

Keywords:

Graphene solution-gated field-effect transistors (gSGFETs) offer an alternative approach for neural recording by converting extracellular electrical activity directly into changes in transistor current. One of their main features is the ability to preserve slow and quasi-DC potential variations, which can contain relevant physiological information and may be attenuated in conventional recording systems. This capability is of particular interest in applications such as epilepsy monitoring, where slow potential shifts can accompany seizure-related activity. However, their operation in direct contact with an electrolyte requires control of the electrical conditions at the graphene–electrolyte interface. In particular, gate current provides information about capacitive charging and leakage-related processes and can therefore be used to assess the electrochemical operating condition of the device.

Gate-current characterization was performed using step-based and ramp-based gate-source voltage protocols. Step measurements allowed the initial capacitive charging transient to be distinguished from the stabilized current, mainly associated with leakage or Faradaic processes. Continuous voltage sweeps at different rates were used to evaluate the dependence of these contributions on gate bias and sweep rate. In the FDM architecture, coupling capacitors block DC current paths, while a high-value bias resistor limits the current flowing through the electrolyte interface. This bias branch also enables gate-current monitoring through the voltage drop across the resistor.

The stabilized gate current increased with the applied gate-source voltage as the bias approached the limits of the electrochemical operating range. Ramp measurements produced wider current–voltage loops at higher sweep rates, reflecting the capacitive charging and discharging of the interface. At higher gate-source voltages, an additional nonlinear current increase was observed, consistent with a greater contribution from charge-transfer processes. In the FDM interface, increasing the bias resistance prolonged stabilization after changes in operating conditions. The measured transients departed from an ideal single-exponential response, suggesting that the array behaves as a distributed resistive-capacitive network. Once stabilized, the remaining current provided an estimate of the quasi-steady leakage contribution.

These results support gate-current monitoring as a complementary tool for assessing the electrochemical operating conditions of gSGFET arrays. The FDM coupling and biasing network provides DC isolation and current limitation while enabling monitoring, although stronger current limitation comes at the expense of longer stabilization times. This transient response must therefore be considered before interpreting gate-current measurements or acquiring transistor characteristics. Further long-term measurements and controlled electrical stress are needed to establish quantitative leakage-current limits and define stable operating conditions for scalable neural interfaces.

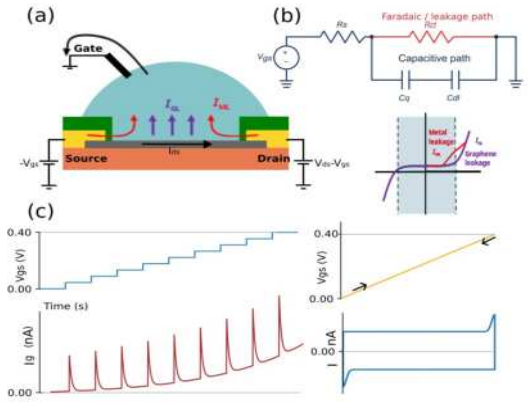

Figure 1: Gate-current characterization of the graphene–electrolyte interface. (a) gSGFET schematic and possible leakage paths. (b) Equivalent circuit and electrochemical operating window. (c) Step and ramp gate-voltage protocols with corresponding capacitive and leakage-related current responses.

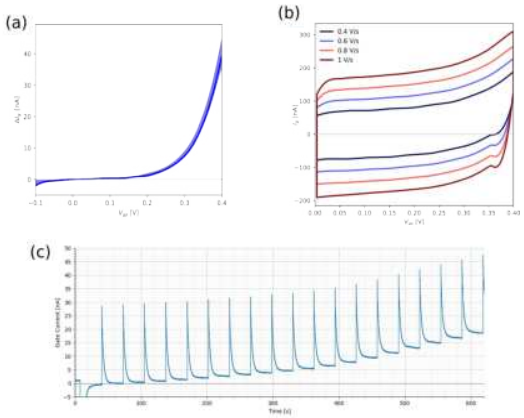

Figure 2: Experimental gate-current responses. (a) Stabilized gate current versus Vgs. (b) Gate current during Vgs sweeps at different rates. (c) Gate current during bias steps in the FDM interface, showing capacitive peaks and the quasi-steady current after stabilization.

Engineering biomimetic hydrogels for patient-derived lung cancer organoids and nanoparticle-assisted radiotherapy

Daniela Casamayor-Roberto[1]; Adrián R.Rodríguez; Anna Civit-Urgell; Marina Llenas; Esperanza Medina-Gutiérrez; Rubén García-Fontarosa; Judith Guasch; Gerard Tobías-Rosell

[1]*Smart Molecular, Inorganic and Hybrid Materials*
dcasamayor@icmab.es

Lung cancer remains one of the leading causes of cancer-related mortality worldwide, with non-small cell lung cancer (NSCLC) accounting for approximately 85% of all cases. Despite advances in current therapeutic strategies, radiotherapy remains limited by tumour resistance and potential damage to surrounding healthy tissues.

Gold nanoparticles (AuNPs) are being developed as promising radioenhancers for radiotherapy due to gold's high atomic number, which promotes radiation-induced electron emission, potentially increasing reactive oxygen species generation and tumour cell damage. However, their high cost may limit their widespread application. As an alternative to AuNPs, mesoporous silica nanoparticles (MSN) containing gold within their porous structure, provide a more cost-effective approach reducing the amount of gold required while maximizing the accessibility of gold to the incident radiation.

On the other hand, patient-derived tumour organoids (PDTOs) are promising 3D models that preserve relevant characteristics of the original tumour and are used to investigate tumour biology and therapeutic responses. Nevertheless, their culture commonly relies on biological scaffolds, such as Matrigel®, which present limitations including batch-to-batch variability, poorly defined composition and limited reproducibility. Thus, there is a need for more physiologically relevant systems that better recapitulate the complexity of NSCLC subtypes and their tumour microenvironment, as well as for novel therapeutic strategies to improve treatment outcomes.

To overcome these limitations, we aim to develop advanced subtype-specific NSCLC patient-derived tumour organoid platforms capable of reproducing the physicochemical and biological characteristics of the tumour microenvironment for testing novel radiation therapies.

In this study, biohybrid PEG-heparin hydrogels with tunable physicochemical properties to recapitulate tumour physiology have been developed. These hydrogels demonstrated their suitability for the establishment of 3D NSCLC models. Moreover, as an alternative radioenhancer to conventional AuNPs, gold-loaded MSN have been successfully synthesized and characterized. Their biocompatibility and radiosensitization potential have been evaluated in a patient-derived lung adenocarcinoma cell line. Altogether, these studies establish the basis for their future evaluation within the hydrogel-based 3D tumour model.

Design of Anisotropic Magneto-Opto-Mechanical Nanocapsules for Cancer Treatment

E. Casas-Aguilera[1,*], A. Lafuente[2], I. Cavaliere[1], C. Roscini[1], B. Sepulveda[2], D. Ruiz-Molina[1], J. Nogués[1,3] and A. G. Roca[1]

[1]Catalan Institute of Nanoscience and Nanotechnology – ICN2 (CSIC and BIST), Campus UAB, Bellaterra, 08193 Barcelona, Spain

[2]Instituto de Microelectrónica de Barcelona (IMB-CNM, CSIC), Campus UAB, Bellaterra, 08193 Barcelona, Spain

[3]ICREA, Pg. Lluís Companys 23, 08010 Barcelona, Spain

*Email: enric.casas@icn2.cat

Keywords: magnetic nanoparticles, encapsulation, immunomodulation, cancer treatment.

When trying to alter the magnetic and optical response or biological performance of magnetic nanoparticles (MNPs) shape tunning is often overlooked by other properties such as size and surface functionalization, even though anisotropic MNPs produce larger mechanical disruption on membranes or biofilms when subjected to an alternating magnetic field (AMF) and have better biodistribution and targeted cell interaction than spherical ones [1]. MNPs can be shaped during or after the synthesis However, MNPs achieved in the former are too small, and so, have low blood circulation [2], and, in the latter, uniform size and shape control can be challenging. Moreover, MNPs by themselves are not capable of drug loading, which limits the much-needed multifunctionality in nanomedicine [3]. In this work, a simple and cost-effective synthesis of anisotropic MNPs with drug loading ability is presented.

Cubic 18 nm MNPs were synthesized via thermal decomposition of iron (III) oleate and later incorporated in poly(lactic-co-glycolic acid) 150 nm nanocapsules by single emulsion evaporation. Finally, the nanocapsules were embedded in a film that was stretched and anisotropic magnetic nanocapsules (AMNCs) were easily recovered (Figure 1a). The AMNCs' possessed a superparamagnetic behaviour, presented a large photothermal response (Figure 1b), could rotate in the presence of an AMF and internalized inside THP-1 monocytes (Figure 1c). These anisotropic properties could be exploited for multitherapeutic magneto-mechanical, photothermal and chemical cancer treatments.

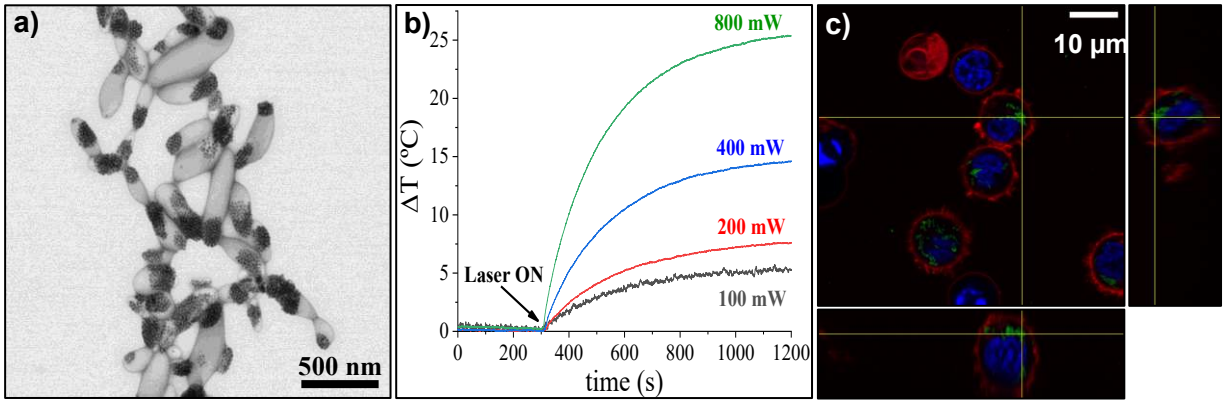

Figure 1. **(a)** Transmission electron microscopy image of the AMNCs. Average aspect ratio of 2.3. **(b)** Heating curves of AMNCs (0.1 mg/mL Fe) when irradiated with an 808 nm laser at different power values. **(c)** Confocal orthogonal views of AMNCs internalized in THP-1 cells. Red: cell membrane; Blue: nucleus; Green: AMNCs.

(1) Ben-Akiva *et al.*, Sci. Adv. 2020; 6(16):eaay035.
(2) El-Hammadi, *et al.*, Nanomaterials (Basel). 2022; 12(3):354.
(3) Kamaraj *et al.*, Med. Nov. Technol. Devices. 2025; 28:100400.

Simultaneous in-situ measurement of surface potential and heat capacity of organic semiconductors

Xavier Casi[1], C. Rodriguez-Tinoco[1], J. Fraxedas[2], J. Rodriguez-Viejo[1]

[1]*Universitat Autònoma de Barcelona (UAB), Bellaterra, Spain*

[2]*Institut Català de Nanociencia i Nanotecnologia, Bellaterra, Spain*

1531568@uab.cat

Keywords: Organic semiconductors, Spontaneous orientation polarization, Fast scanning calorimetry

Organic semiconductors display intricate polarization phenomena that have a strong impact on the generation, transport, and recombination of charge in optoelectronic devices. Specifically, when polar organic semiconductors are deposited as thin films, their molecules can spontaneously order in a preferred orientation, giving rise to a surface potential that alters the material's energy landscape. Such polarization effects may also affect excitonic processes, for instance exciton polarization quenching, in which the local electrostatic environment changes exciton dissociation and non-radiative decay pathways, and thereby influences device efficiency and stability. Even though molecular dipoles and spontaneous orientational ordering are recognized as key factors in shaping the internal electrostatic landscape of thin films, the connection between molecular orientation, thermodynamic transitions, and polarization dynamics is still not well understood, because there are no experimental techniques able to probe all these properties simultaneously and in situ.

In this work, we put forward a methodology for measuring surface potential and heat capacity simultaneously and in situ in thin films of organic semiconductors. The approach merges fast-scanning nanocalorimetry [1,2] with capacitor-based electrical measurements, allowing thermal signatures to be directly correlated with the evolution of polarization. Organic molecules with permanent dipole moments can orient spontaneously as the film grows, producing a macroscopic polarization and a measurable surface potential. By incorporating the film into a capacitor geometry while heat capacity is monitored at the same time, it is possible to determine how orientational ordering and phase behavior relate to changes in polarization.

This combined experimental platform offers a direct way to investigate the coupling among molecular arrangement, dipolar ordering, and phase transition processes in organic semiconductors. Being able to follow thermodynamic and electrostatic properties at once provides new insight into polarization-induced phenomena and may contribute to the development of more efficient organic electronic and photovoltaic devices.

(1) J. Rodriguez-Viejo and A. F. Lopeandía, Fast Scanning Calorimetry, Springer International Publishing, 105–149,(2016).
(2) A. Vila-Costa et al. Nature Physics, 19 (1), 114-119 (2023).

Mechanically responsive DNA-MOP sponges for enhanced molecular uptake

Caterina Caules[1,2], Alba Cortés-Martínez[1,2], Partha Samanta[1,2], Andrea Escobar-Peña[3], Sergio Royuela[3], Daniel Maspoch[1,4], Arnau Carné-Sánchez[2]

[1]*Catalan Institute of Nanoscience and Nanotechnology (ICN2), CSIC and The Barcelona Institute of Science and Technology, Bellaterra, Barcelona, Spain*
[2]*Departament de Química, Facultat de Ciències, Universitat Autònoma de Barcelona (UAB), Cerdanyola del Vallès, Barcelona, Spain*
[3]*Departamento de Química Inorgánica and Condensed Matter Physics Institute (IFIMAC), Universidad Autónoma de Madrid, Ciudad Universitaria de Cantoblanco, Madrid, Spain*
[4]*ICREA, Barcelona, Spain*

ccaules@icn2.net

Keywords: Metal-Organic Polyhedra (MOPs), DNA biomass, Ice-templating, Molecular uptake.

DNA biomass is an abundant and renewable natural polymer that offers a versatile platform for the design of sustainable functional materials through diverse molecular interactions [1]. In particular, rhodium-based metal-organic polyhedra (Rh-MOPs) provide well-defined coordination sites through the Rh(II)-Rh(II) paddlewheel clusters that selectively bind to adenine nucleobases in DNA [2]. Herein, we report the formation of macroporous DNA-MOP sponges through adenine coordination to hydroxyl-functionalized Rh-MOPs. The sponge-like matrix is generated by ice-templating via lyophilization of the aqueous DNA-MOP mixture, yielding an interconnected macroporous network (see Figure 1) [3].

The resulting DNA-MOP sponges exhibit excellent mechanical stability in the hydrated state, withstanding repeated compression under water while maintaining their structural integrity and fully recovering their original shape after deformation. Remarkably, cyclic mechanical compression while immersed in water actively enhances molecular transport through the network by inducing convective flow, resulting in up to a 70-fold increase in the uptake rate of cationic molecules, as demonstrated using methylene blue as a model compound. Therefore, mechanical stimulation provides a means to accelerate molecular capture while preserving the intrinsic selectivity of the DNA-MOP network.

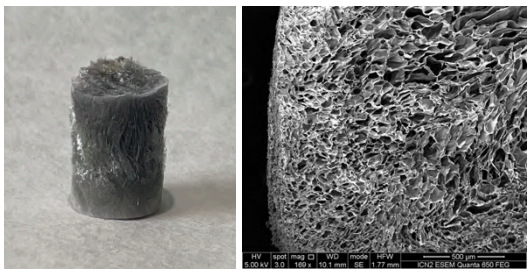

Figure 1. Optical photograph (left) and SEM image (right) of the ice-templated DNA-MOP sponge.

(1) Wang, D; et al. *J. Am. Chem. Soc*. 2020, *142*, 10114-10124.
(2) Hernández-López, L; et al. *J. Am. Chem. Soc*. 2025, *147*, 16560-16567.
(3) Buchtová, N.; et al. *Soft Matter*. 2019, *15*, 7901-7908.

The antiferromagnetic transition of β-Fe_2O_3 iron oxide

Chenjun Tang [1,*], Malina Ondrej [2], Martí Gich [1], José Luis García-Muñoz [1]

1. *Institut de Ciència de Materials de Barcelona (ICMAB-CSIC), Campus UAB, 08193 Bellaterra, Barcelona, Spain*
2. *School Regional Centre of Advanced Technologies and Materials, DEPPC, Faculty of Science, Palacky University, 17. 771 46 Olomouc, Czech Republic.*

** chenjuntang@icmab.es*

Keywords:

Iron oxide's phases are well known multifunctional materials for many technological applications. The ubiquitous Iron (III) Fe_2O_3 oxide is a canonical polymorphic example. At ambient pressure, the best-established crystalline polymorphs are α-Fe_2O_3 (hematite), γ-Fe_2O_3 (maghemite), ε-Fe_2O_3, and β-Fe_2O_3, while pressure treatment can stabilize additional forms such as ζ-Fe_2O_3 [1]. Across these polymorphs, magnetic properties are largely controlled by exchange topology, magnetocrystalline anisotropy and electronic structure, without changing chemical composition.

Within this polymorph family, β-Fe_2O_3 is exceptional as, in sharp contrast to α-, γ-, and ε-Fe_2O_3, it is magnetically disordered at room temperature, and becomes antiferromagnetic below T_N ≈112 K (θ_C=-757 K) [2]. The magnetic structure of this polymorph had not yet been determined, being the only unsolved order of this family [1,3]. Here, we have investigated the Néel transition, the origin of frustration and the magnetic properties of nanosized β–Fe_2O_3 particles, with bixbyite-type cubic structure (Ia-3). We present the magnetic structure of β–Fe_2O_3, a noncollinear spin arrangement with commensurate propagation vector and a single active magnetic irrep [4]. The spins are also non-collinear within each of the two magnetic orbits of the magnetic configuration. The implications of the magnetic symmetry for its physical properties will be discussed, as well as the origin of magnetic frustration in this iron oxide polymorph. A deviation from ideal antiferromagnetic behavior below T_N has been previously invoked to account for a small net ferromagnetic component inferred from magnetization measurements.

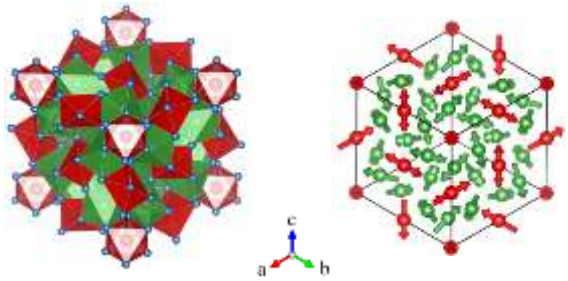

Fig.1: [111] projection of the crystal and magnetic structure of the cubic β–Fe_2O_3 iron oxide.

We acknowledge financial support from the Ministerio de Ciencia, Innovación y Universidades (MINCIU), through Projects PID2021-124734OB-C22 and PID2024-159457OB-C22, cofunded by ERDF from EU, and "Severo Ochoa" Programme (Grant No. CEX2023-001263-S). We also thank the Institut Laue-Langevin (ILL) and the Spanish CRG access program.

References

(1) L. Machala et al., Chem. Mater. 23, 3255 (2011)

(2) O. Malina et al., RSC Adv. 5, 49719 (2015)

(3) J. L. García-Muñoz et al., Chem. Mater. 29, 9705 (2017)

(4) Chenjun Tang et al., submitted (2026)

Structural basis of covalent inhibition of ALDH1A3 by the acrylamide-based compound Z34

Daniela Covaleda[1,7], David Vizarraga[2,3,7], Tulsi Upadhyay[4], Jiyun Zhu[4], Daniel Abegg[5], Raquel Pequerul[1], Tsvetelina Baryakova[4], Martín Hugo[6], Alexander Adibekian[5], Ignacio Fita[3], Xavier Parés[1], Francesc Xavier Avilés[1], Matthew Bogyo[4,*], Jaume Farrés[1,*]

[1]Department of Biochemistry and Molecular Biology, Faculty of Biosciences, Universitat Autònoma de Barcelona, 08193 Bellaterra, Cerdanyola del Vallès, Barcelona, Spain.
[2]Centre for Genomic Regulation (CRG), The Barcelona Institute of Science and Technology, 08003 Barcelona, Spain.
[3]Instituto de Biología Molecular de Barcelona (IBMB-CSIC), Parc Científic de Barcelona, Barcelona, Spain
[4]Department of Pathology, Stanford University School of Medicine, Stanford, California, USA.
[5]Department of Chemistry, University of Illinois Chicago, Chicago, IL, USA.
[6]Serra Húnter Fellow, Departament de Bioquimica i Biologia Molecular, Universitat Autònoma de Barcelona, Bellaterra, 08193 Barcelona, Spain.
[7]These authors contributed equally

Daniela.Covaleda@uab.cat

Keywords: ALDH1A3; covalent inhibition; Z34; cryo-electron microscopy; covalent fragments; structural biology

Aldehyde dehydrogenase 1A3 (ALDH1A3) catalyzes the NAD^+-dependent oxidation of aldehydes to their corresponding carboxylic acids and is overexpressed in several cancers, making it a potential therapeutic target. However, the development of covalent inhibitors targeting ALDH1A3 remains relatively unexplored. Here, we used the esterase activity of ALDH1A3 to establish a high-throughput screening assay for cysteine-reactive compounds and screened a library of 3,200 covalent fragments. This approach identified Z34, an acrylamide-based compound that inhibited ALDH1A3 and the closely related isoform ALDH1A1 at sub-micromolar concentrations. Biochemical and biophysical characterization showed that Z34 acts as a time-dependent, covalent, and irreversible inhibitor by modifying the catalytic cysteine. By using high-resolution cryo-electron microscopy, we elucidated the 3D structure of human ALDH1A3 in complex with Z34 at 2.26-Å resolution. The structure revealed two mutually exclusive covalent binding modes, in which Z34 engages the same catalytic cysteine through either the substrate-binding or cofactor-binding pocket. These findings reveal an unexpected mode of covalent interaction in the ALDH1A3 active site and provide structural insights that may guide the development of covalent inhibitors targeting ALDH enzymes.

A preprint version of this work is available on bioRxiv (DOI: https://doi.org/10.64898/2026.07.14.738401). This work was partially funded by the National Institutes of Health grant R01 EB037592 (to MB) and by the Spanish Ministerio de Ciencia, Innovación y Universidades (Agencia Estatal de Investigación; grant PID2023-150696NB-I00/MCIU/AEI/10.13039/501100011033/FEDER, UE).

2026 JPhD 10th edition

Engineering cooling dynamics in graphene by screening effects in twisted trilayer graphene

Ronny de la Bastida[1], Anand Nivedan[1], Daria Belotcerkovtceva[2], Anand Nivedan[1], Roshan Krishna[1], Alexey Berdyugin[2], Klaas-Jan Tieelroij[1,3]

[1]*Catalan Institute of Nanoscience and Nanotechnology (ICN2), Barcelona Institute of Science and Technology, Campus UAB, Bellaterra, Barcelona, 08193, Spain*

[2]*Department of Materials Science and Engineering, National University of Singapore, Singapore, Singapore*

[3]*Department of Applied Physics, TU Eindhoven, Den Dolech 2, Eindhoven, 5612 AZ, Netherlands*

ronny.delabastida@icn2.cat

Keywords: cooling dynamics, screening effects, hot carriers

The new promising THz technologies demand high speed detectors and high responsivity for 6G technologies, being graphene one of the most promising materials due to broadband absorption, fast detection, room temperature operation and high responsivity. During the last decades, photothermoelectric (PTE) THz graphene detectors have been widely studied due to the low energy consumption, fast response, and high responsivity at room temperature [1]. Its fast response and high responsivity arise mainly due to its cooling dynamics, where fast cooling thermalization happens around one to two picoseconds, enabling fast detection but limiting the thermal gradient produced in the electronic system [2]. Recently, placing a metal close to an encapsulate graphene [3] and using a large angle twisted graphene systems [4] show an improvement in the electronic transport in graphene due to the screening effects in the system, and more important, screening effects in graphene shows a way to control the cooling dynamics [5]. Here, we show a modification of the cooling dynamics in a twisted trilayer graphene due to screening effects where the three layers are electronic decoupled by twisting in an angle of 20º and acting as three independent monolayer graphene layers, opening a new way to enhance the thermal gradient and the detector performance.

References

(1) Sebastián Castilla, Bernat Terrés, Marta Autore, Leonardo Viti, Jian Li, Alexey Y. Nikitin, Ioannis Vangelidis, Kenji Watanabe, Takashi Taniguchi, Elefterios Lidorikis, Miriam S. Vitiello, Rainer Hillenbrand, Klaas-Jan Tielrooij, Frank H.L. Koppens. Fast and Sensitive Terahertz Detection Using an Antenna-Integrated Graphene pn Junction. Nano Lett. **19** (5), 2765–2773 (2019).

(2) Mathieu Massicotte, Giancarlo Soavi, Alessandro Principi, Klaas-Jan Tielrooij; Hot carriers in graphene – fundamentals and applications. *Nanoscale* **13** (18), 8376–8411 (2021).

(3) M. Kim, S. G. Xu, A. I. Berdyugin, A. Principi, S. Slizovskiy, N. Xin, P. Kumaravadivel, W. Kuang, M. Hamer, R. Krishna Kumar, R. V. Gorbachev, K. Watanabe, T. Taniguchi, I. V. Grigorieva, V. I. Fal'ko, M. Polini, and A. K. Geim. Control of electron-electron interaction in graphene by proximity screening. *Nat Commun.* **11**, 2339 (2020)

(4) I. Babich, I. Reznikov, I. Begichev, A. E. Kazantsev, S. Slizovskiy, D. Baranov, M. Šiškins, Z. Zhan, P. A. Pantaleon, M. Trushin, J. Zhao, S. Grebenchuk, K. S. Novoselov, K. Watanabe, T. Taniguchi, V. I. Fal'ko, A. Principi and A. I. Berdyugin. Milli-Tesla quantization enabled by tuneable Coulomb screening in large-angle twisted graphene. *Nat Commun* **16**, 7389 (2025).

(5) H. I. Wang, X. Jia, A., Nivedan, M. Bonn, A. W. Cummings, A. Principi, and K.-J. Tielrooij. Dielectric control of ultrafast carrier dynamics and transport in graphene. Preprint at https://arxiv.org/abs/2604.00217 (2026)

2026 JPhD 10th edition

Tunable gelatin-chitosan hydrogels for tumor microenvironment-inspired 3D models in cancer immunotherapy

Fajardo-García A[1,2,3], Guasch J[3], Garcia-Torres J[1,2,4]

[1]*Department of Materials Science and Engineering and Institute for Research and Innovation in Health, Universitat Politècnica de Catalunya–BarcelonaTech, Barcelona, Spain*

[2]*Barcelona Research Center in Multiscale Science and Engineering, Universitat Politècnica de Catalunya–BarcelonaTech, Barcelona, Spain*

[3]*Institute of Materials Science of Barcelona (ICMAB-CSIC), Barcelona, Spain*

[4]*Centro de Investigación Biomédica en Red de Bioingeniería, Biomateriales y Nanomedicina (CIBER-BBN), Instituto de Salud Carlos III, Madrid, Spain*

andrea.fajardo@upc.edu

Keywords: gelatin-chitosan hydrogels; tumor microenvironment; 3D models; biomaterials; cancer immunotherapy

Introduction. Cancer remains one of the leading causes of death worldwide, and its progression and response to therapy are strongly influenced by the tumor microenvironment (TME), a dynamic milieu comprising cancer cells, stromal cells, immune cells and extracellular matrix (ECM). However, conventional *in vitro* models poorly reproduce the three-dimensional and biomechanical complexity of native tissues. In this context, hydrogels offer a promising platform for developing physiologically relevant 3D models to investigate immune-related processes and evaluate immunotherapeutic strategies. Among natural polymers, gelatin and chitosan are attractive candidates due to their biocompatibility and biodegradability, with gelatin providing cell-adhesive motifs and chitosan contributing structural tunability.

Aim. This work aims to engineer and optimize gelatin-chitosan hydrogels with tunable properties to mimic the TME, with the final goal of generating 3D platforms for the study of cancer immunotherapy.

Materials and Methods. Hydrogels were prepared by mixing 1:1 gelatin in water and chitosan in 1% v/v acetic acid, casting, cooling overnight at 4 °C and treating with NaOH. Three final chitosan/gelatin concentrations (1.0/1.4, 1.4/1.9 and 1.8/2.4% w/v) were combined with 0.25, 0.75 or 2.00 M NaOH. ESEM, micro-CT, ATR-FTIR, swelling, mechanical properties and degradation tests assessed internal architecture, chemical structure, hydration, mechanics and stability. Preliminary cytocompatibility of the three 0.25 M formulations was evaluated by flow cytometry and confocal microscopy at days 1 and 3.

Results. The resulting hydrogels exhibited composition-dependent physicochemical and mechanical properties. Swelling decreased consistently with NaOH concentration, while immersion medium and polymer formulation modulated the response. Young's modulus ranged from 4.91 to 20.9 kPa and generally increased with polymer content, whereas NaOH effects were non-monotonic. ESEM and micro-CT revealed porous internal architectures, and ATR-FTIR showed characteristic bands of both polymers. Higher NaOH was associated with pronounced early mass loss, while 0.25 M formulations showed a more progressive response. Mean cell viability remained above 80% at days 1 and 3, without significant differences from the control.

Conclusion. These results demonstrate that gelatin–chitosan hydrogels provide tunable physicochemical and mechanical properties within ranges relevant to the TME, supporting their potential as 3D models to study tumor–immune interactions and evaluate immunotherapeutic strategies.

Unravelling the intermediate phase in voltage-controlled $SrFeO_{3-\delta}$ thin films

Ona Falcó [1], Paul Nizet, Francesco Chiabrera, Alicia Ruiz-Caridad, Albert Tarancón, Sònia Estradé, Francesca Peiró, Catalina Coll, Lluís Yedra

[1] *LENS-MIND Department of Electronics and Biomedical Engineering and Institute of Nanoscience and Nanotechnology (IN2UB), University of Barcelona, Spain*

ona.falco@ub.edu

Keywords: $SrFeO_{3-\delta}$; oxygen vacancies; phase coexistence; electron microscopy; STEM-HAADF; EELS

Oxygen stoichiometry strongly influences the structural and functional properties of transition metal oxides. $SrFeO_{3-\delta}$ is a model system for studying oxygen-driven topotactic transitions between perovskite (PV) and brownmillerite (BM) structures. However, the structural nature of intermediate oxidation states and their local phase distribution remain poorly understood. Here, we investigate voltage-controlled $SrFeO_{3-\delta}$ thin films to resolve their structural and chemical evolution at the nanoscale.

Epitaxial SFO thin films were subjected to solid-state electrochemical gating to control oxygen stoichiometry between the brownmillerite $SrFeO_{2.5}$ and perovskite $SrFeO_3$ end members (Figure 1). Cross-sectional lamellas were characterized by complementary electron microscopy and spectroscopy techniques. Structural characterization reveals a progressive evolution with oxygen content, including the coexistence of an intermediate phase (IPh) and BM domains. The IPh exhibits different oxygen-vacancy ordering and reduced lattice distortion, while correlated variations in oxygen and iron distributions are observed.

These results demonstrate that intermediate oxidation states in $SrFeO_{3-\delta}$ involve nanoscale structural heterogeneity and phase coexistence, with oxygen redistribution and vacancy ordering governing the local structural response.

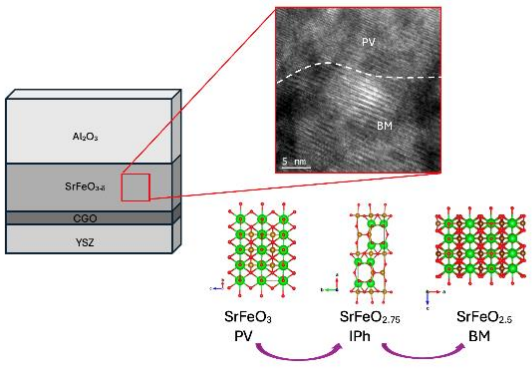

Figure 1: Nanoscale phase evolution in voltage-controlled $SrFeO_{3-\delta}$ thin films.

(1) Nizet, P.; Chiabrera, F.; Ruiz-Caridad, A.; et al. *Unlocking stable intermediate states in $SrFeO_{3-\delta}$ through voltage control of oxygen non-stoichiometry*. Nature Communications (2026).

2026 JPhD 10th edition

Towards the preparation of stacked single-crystalline oxide membranes

L. Fan[1], M. Ramis[1], R. Guzman[1], M. Coll[1].

[1]*1Institut de Ciència de Materials de Barcelona (ICMABCSIC) Campus UAB 08193 Bellaterra - Barcelon*

longyifan@icmab.es

Keywords: freestanding complex oxide, membranes transfer, stack, $La_{0.7}Sr_{0.3}MnO_3$

Abstract

Freestanding single-crystalline complex oxide membranes provide a route to artificial heterostructures beyond the constraints of conventional epitaxial growth. Here, we investigate polymer-assisted transfer and stacking of $La_{0.7}Sr_{0.3}MnO_3$ (LSMO) membranes as a model strongly correlated oxide system, focusing on surface quality and stacking interfaces. Several polymer supports were evaluated in terms of adhesion, peeling behavior, surface roughness, and residual contamination. Both poly(propylene carbonate) (PPC) and polyethylene terephthalate (PET) enabled transfer onto SiO_2/Si substrates. However, X-ray photoelectron spectroscopy revealed residual carbon-containing species after PPC removal, while additional cleaning treatments could damage the membranes. PET-assisted transfer produced membranes with improved surface morphology and was therefore selected for preparing LSMO/LSMO stacks. X-ray diffraction confirmed (00l)-oriented LSMO on SiO_2/Si, while cross-sectional transmission electron microscopy and electron energy-loss spectroscopy revealed interfacial gaps and carbon contamination in the as-stacked samples. High-temperature post-annealing reduced interfacial carbon contamination and narrowed the gaps. Local crystallographic alignment between the two layers after annealing was consistent with interfacial reconstruction. These results demonstrate progress towards stacked oxide membranes and highlight residual contamination and membrane roughness as key challenges for improving interface quality in future twisted and multilayer structures.

Electroactive Self-Assembled Monolayers: Three Viologen Derivatives for Generation of Potential Gradients

Aysha Fasna[1,2], David B. Amabilino[2], Lluïsa Pérez-García[1]

[1] *Departament de Farmacologia, Toxicologia i Química Terapèutica, Universitat de Barcelona, Av. Joan XXIII 27-31, Barcelona, 08028, Spain and Institut de Nanociència i Nanotecnologia UB (IN2UB)*

[2] *Institut de Ciència de Materials de Barcelona (ICMAB-CSIC), Carrer dels Til·lers, 08193 Cerdanyola del Vallès,Spain*

afasna@icmab.es

Keywords: Electron acceptors, Surfaces, π-Functional materials

Electroactive self-assembled monolayers (SAMs) on surfaces provide versatile platforms for designing responsive surfaces and switchable supramolecular systems [1]. Viologens (4,4′-bipyridinium derivatives) are particularly attractive units in these systems because of their reversible single-electron reduction from the dication to the radical cation [2]. In addition to their redox response, these states exhibit distinct *π*-electron donor/*π*-electron acceptor interactions, where the viologen units act as electron-deficient *π*-electron acceptors capable of engaging in switchable interactions with electron-rich *π*-electron donors [3].

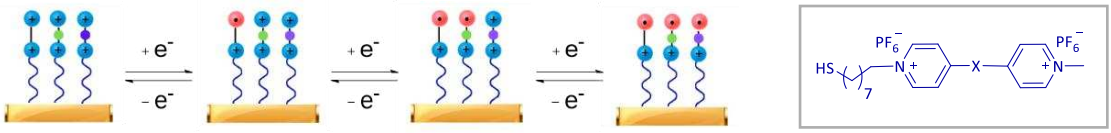

Figure 1: Schematic representation of the sequential, reversible single-electron reduction ($V^{2+} \rightleftharpoons V^{+\cdot}$) of three distinct viologen derivatives assembled on gold (left) and chemical structure of thiol-functionalized viologen derivative (right, x = variable spacer).

In this work, we investigate the assembly and electrochemical behavior of monolayers prepared from three distinct viologen derivatives (with different spacers between the pyridinium unit) on gold. The different substituents on the viologen core shift the reduction potential while maintaining their reversibility. These distinct redox potential across these three derivatives provides the electroactive foundation to generate potential gradient (Figure 1), opening pathways for the controlled, surface-driven transport of nano- and microscale objects, the final goal of this project.

Acknowledgments: We thank the MICIU/AEI/10.13039/501100011033 and FEDER, EU for financing project PID-2023-146658NB-C32 and MCIN/AEI/10.13039/501100011033 for PID2024-160803NB-C31 as well as the "Severo Ochoa" program CEX2023-001263-S.

References

(1) Singh, M.; Kaur, N.; Comini, E. J. Mat. Chem. C 2020, 8, 3938-3955.
(2) Hünig, S.; Berneth, H. Angew. Chem. Int. Ed. Engl. 1980, 19, 247–267.
(3) Sluysmans, D.; Zhang, L.; Li, X.; Garci, A.; Stoddart, J. F.; Duwez, A.-S. *J. Am. Chem. Soc.* 2020, *142*, 21153–21159

Adsorption of nitrogen based ligands on Ru nanoparticles and their effect on hydrogen evolution reaction: A DFT study.

Hmad Fatihi[1,2], Hakima Ouhenou[1,2], Luis Rodríguez-Santiago[1], Xavier Solans-Monfort[1]

1*Departament de Química, Universitat Autònoma de Barcelona, 08195 – Bellaterra, Spain.*

2*Multidisciplinary Research Laboratory in Physics, Faculty of Applied Sciences, Sultan Moulay Slimane University, Beni Mellal, Morocco*

Hmad.fatihi4@gmail.com

Keywords: DFT, Ruthenium nanoparticles, Hydrogen evolution reaction

The development of efficient electrocatalysts for hydrogen production is essential for the transition towards sustainable energy technologies. Ruthenium-based materials have attracted considerable interest for the hydrogen evolution reaction (HER), and their catalytic properties can be influenced by the local environment of the Ru surface as well as the presence of capping ligands. In this work, density functional theory (DFT) calculations are used to investigate the interaction of several nitrogen-based ligands with realistic Ru-based nanoparticle models including various sites (B, C and F) differing on the local environment of the Ru centers (Figure 1). Results reveal a clear dependence of ligand adsorption on the Ru site and ligand structure that mixes electronic and steric effects of both the metal center and the ligand. These results provide insight into how the ligand structure tunes its adsorption on the nanoparticle, while the consequences on the electrocatalytic hydrogen production will examined in a recent future.

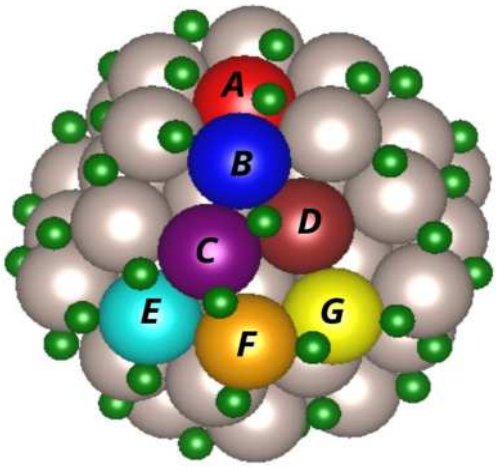

Figure 1: Ligands and Ru Nanoparticle model Considered in this work. Labelling describes the different sites of the Np model.

Copper-Modified Hydroxyapatite Surfaces as Catalysts in Environmental Processes: A Computational Perspective

Paolo Fichera[1], Eric Mates-Torres[3], Albert Rimola[3], Sebastiano Campisi[2], Antonella Gervasini[2], Marta Corno[1]

[1] *Department of Chemistry, University of Turin, Turin, Italy.*
[2] *Department of Chemistry, University of Milan, Milan, Italy.*
[3] *Department of Chemistry, Universitat Autònoma de Barcelona, Bellaterra, Spain.*
paolo.fichera@autonoma.cat

Keywords: Catalysis, DFT, Environmental Chemistry, Computational Chemistry, Innovative Materials.

In recent years, hydroxyapatite (HA, $Ca_{10}(PO_4)_6(OH)_2$) has emerged as a promising material in green chemistry, owing to its feasible synthesis from waste-derived resources [1]. Its tunable acid-base properties, non-toxicity, adsorption capability, and ion-exchange behaviour, make HA an attractive support for eco-friendly heterogeneous catalysts aimed at the abatement of environmental pollutants [2]. In this context, the nature and strength of molecule-surface interactions play a key role in determining catalytic performance. Computational methods have therefore become an essential tool to accurately describe these interactions and to support rational catalyst design [3], benefitting from the continuous advancement in computational power [4].

In this contribution, a periodic quantum mechanical approach is employed to investigate the interaction between small reactive molecules and the most stable hydroxyapatite surfaces. Copper-modified HA models are considered to enhance catalytic activity while preserving the structural integrity of the material [5]. Specifically, the interaction of formaldehyde, taken as a benchmark volatile organic compound, with the (001), (010), and (101) HA facets is analysed for both pristine and Cu-substituted surfaces. In addition, ammonia selective catalytic reduction (NH_3-SCR) is examined in comparison with experimentally driven data, with particular attention to the effect of water. Variations in structural, energetic, and vibrational properties are discussed to establish a computational framework for the investigation of environmentally relevant catalytic processes. This approach can be readily extended to other cationic substitutions, such as iron, highlighting hydroxyapatite as a versatile and highly promising material for environmental catalysis.

(1) Kong, L. Liu, X.; Lv, G.; Liu, T.; Zhang P.; Li Y.; Chen B.; Liao L. Adv. Civ. Eng., 2022.
(2) Campisi, S.; Galloni, M. G.; Marchetti, S. G.; Aouroux, A.; Postole, G.; Gervasini A. Chem. Cat. Chem. 1676-1690.
(3) Corno, M.; Rimola, A.; Bolis, V.; Ugliengo, P. *Phys. Chem. Chem. Phys.*, 6309-6329.
(4) Cutini, M.; Corno, M.; Costa, D.; Ugliengo, P. J. Phys. Chem. C., 7540−7550.
(5) Ibrahim, M.; Labaki, M.; Giaoudon J.-M.; Lamonier J.-F. J. Hazard. Mater., 383.

2026 JPhD 10th edition

Semiconductor nanoelectronic devices based on single dopants

Mihaela Floruc Darie[1], Francesc Pérez-Murano[1], Xavier Oriols Pladevall[2]

[1] *Institut de microelectrònica - Centre Nacional de Microelectrònica (IMB-CNM)*

[2] *Departament d'Enginyeria Electrònica, Universitat Autònoma de Barcelona.*

Mihaela.Floruc@imb-cnm.csic.es

Keywords: Single-donor devices, phosphorus dopants, atomistic simulation, quantum transport

At the atomic scale, the precise position of individual dopant atoms can significantly influence the electrical and quantum behaviour of semiconductor devices. Controlled single-dopant incorporation in silicon offers potential applications in quantum technologies, spin-based qubits and ultra-low-power electronics. [1]

This PhD research aims to develop simulation tools to guide the design and optimisation of single-donor devices. The work investigates how dopant position, device geometry and electrostatic environment affect their electronic and transport properties. After the design and simulation phase, devices will be fabricated in the context of an international collaboration with EPFL and University of Basel. [2]

A simulation framework based on NEMO5 [3] was developed and validated for atomistic electronic structure and quantum transport calculations, and subsequently extended to include individual phosphorus donors in silicon. Preliminary results show the modification of the local electrostatic potential induced by a single dopant (Figure 1). In parallel, a master-equation approach is being implemented to study sequential tunnelling and Coulomb blockade in single-donor single-electron transistors that will provide the electronic transport characteristics.

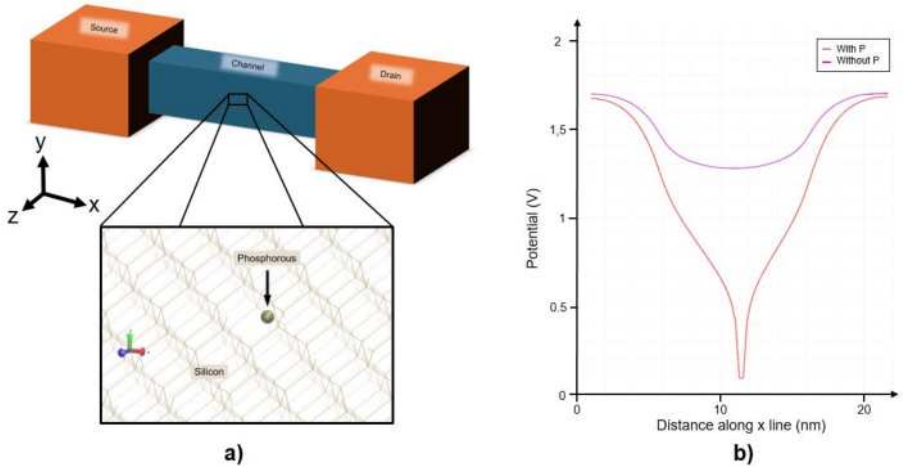

Figure 1. (a) Three-dimensional view of the device, with a zoom of the central channel region showing the phosphorus dopant. (b) Comparison of the electrostatic potential with and without the phosphorus dopant.

[1] Fuechsle, M., Miwa, J., Mahapatra, S. *et al.* A single-atom transistor. *Nature Nanotech* **7**, 242–246 (2012). https://doi.org/10.1038/nnano.2012.21

[2] EPFL. (2026). *EPFL*. https://www.epfl.ch/ University of Basel. (2026). *University of Basel*. https://www.unibas.ch/

[3] Klimeck Group. (s. d.). *NEMO5*. Purdue University. https://engineering.purdue.edu/gekcogrp/software-projects/nemo5/

Photonic Biosensor for Rapid, Urine-based Screening of Sexually Transmitted Infections

Celia Galindo-Martin[1], Yannick Hoyos-Mallecot[2], Juan José González-López[2], Laura M Lechuga[1], Maria Soler[1*]

[1] *Nanobiosensors and Bioanalytical Applications Group (NanoB2A), Catalan Institute of Nanoscience and Nanotechnology (ICN2), CSIC, BIST and CIBER-BBN. Barcelona (Spain)*
[2] *Microbiology Research Group, Vall d'Hebron Institut de Recerca (VHIR), Vall d'Hebron Barcelona Hospital Campus, Barcelona, Spain*
speaker: celia.galindo@icn2.cat,
corresponding author: maria.soler@icn2.cat

Keywords: Sexually transmitted infections (STIs), Gonorrhoea, Chlamydia, Photonic biosensor, Bimodal Waveguides (BiMW), Silicon photonics, Point-of-care diagnostics, Urine-based testing, Ultrasensitive detection, Decentralized screening.

Reported cases of sexually transmitted infections (STIs) have increased sharply in recent years, with gonorrhoea incidence rising by approximately 300% since 2014. Globally, over 1 million people acquire an STI every day, with *Chlamydia trachomatis* and *Neisseria gonorrhoeae* representing the two most prevalent bacterial pathogens. These infections remain asymptomatic in up to 80% of infected women, contributing to ongoing transmission and increasing the risk of severe reproductive and systemic health complications.

Rapid, accessible diagnostics are essential to enable early detection and interrupt transmission chains. However, current PCR-based methods rely on centralized laboratory infrastructure and trained personnel, limiting their suitability for decentralized or point-of-care screening. Moreover, urethral or vaginal swab collection can be challenging or uncomfortable, whereas urine represents an ideal, non-invasive, easily self-collected specimen.

Here, we present an integrated photonic biosensor based on bimodal waveguide (BiMW) interferometers for the ultrasensitive detection of *C. trachomatis* and *N. gonorrhoeae* directly in urine samples. The assay is completed in 20 minutes and enables rapid, label-free pathogen detection down to 4 CFU/mL. Validation using a cohort of 125 clinical samples demonstrated statistically significant discrimination and accurate pathogen identification. The *C. trachomatis* sensor achieved a diagnostic sensitivity of 97.5% and 93.9% specificity, while the *N. gonorrhoeae* sensor reached 96.9% sensitivity and 93.8% specificity.

By combining a simplified workflow with scalable silicon photonic chip technology, this platform represents a practical point-of-care alternative to conventional molecular diagnostics for large-scale STI screening and control.

Acknowledgements: The research has been funded by Barcelona City Council and "La Caixa" Foundation (DIGITS). CGM acknowledges financial support from AGAUR FI (2025 FI-1 00274), backed by the Department of Research and Universities of the Generalitat of Catalonia, as well as the European Social Plus Fund.

Development of MEMS-Based Silicon Carbide Detectors for Beam Monitoring in Advanced Radiotherapy

Pol Gaya Salas[1], Consuelo Guardiola[1], Celeste Fleta[1]

[1]*Institut de microelectrònica - Centre Nacional de Microelectrònica (IMB-CNM)*

pol.gaya@csic.es

Keywords: Silicon Carbide (SiC) MEMs, FLASH radiotherapy, Beam monitoring, SiC manufacturing

FLASH therapy has emerged as a promising radiotherapy modality due to its ability to control de tumour while potentially reducing damage to healthy tissues by delivering ultra-high dose rates. In this context, achieving accurate real-time beam monitoring with high spatial and temporal resolution is essential because the dose is delivered within milliseconds, leaving minimal error margins. Reliable monitoring systems are therefore critical to guarantee dose accuracy, patient safety, and treatment reproducibility under ultra-high dose-rate conditions. However, the extreme irradiation conditions involved, and high particle fluences, come with significant technology challenges for conventional dosimetry and real time beam monitoring.

Silicon-based detectors may suffer from radiation-induced degradation when operating under such demanding conditions [1]. In this context, silicon carbide (SiC) has attracted increasing interest as an alternative semiconductor material for radiation detection because of its wide bandgap, high radiation hardness, low leakage current, fast response, and excellent thermal and electrical stability. These properties make SiC suitable for the development of beam monitors capable of operating in FLASH radiotherapy environments [2][3].

This work presents the fabrication of the first SiC MEMS detectors designed for beam monitoring applications in advanced radiotherapy, such as FLASH and proton therapy. The proposed devices are fabricated using 4H-SiC epitaxial wafers and combine optimized SiC processing with advanced micromachining techniques to obtain radiation detectors with controlled ultra-thin sensitive volumes.

The fabricated detectors are expected to provide fast temporal response, high radiation tolerance, and stable operation under FLASH conditions. These characteristics make them suitable candidates for next-generation quality assurance systems in FLASH radiotherapy.

[1] doi: 10.1016/j.radphyschem.2026.114172

[2] doi: 10.1088/1361-6560/ad37eb

[3] doi: 10.1016/j.radmeas.2026.107660

From 6-inch Wafer to Brain: Scalable Fabrication of Graphene SGFETs for Neural Recording

Anna W. Graf[1], Eduard Masvidal-Codina[1], Xavi Illa[2,3], Neela Codadu[4], Anton Guimera-Brunet[2,3], Marc Tudela-Pi[2,3], Elena del Corro[1], Rob Wykes[4,5], Jose A. Garrido[1,6]

[1]Catalan Institute of Nanoscience and Nanotechnology (ICN2), CSIC and BIST, Campus UAB, Bellaterra, Barcelona, Spain, [2]Instituto de Microelectrónica de Barcelona, IMB-CNM (CSIC), EsferaUAB, Bellaterra, Spain, [3]Centro de Investigación Biomédica en Reden Bioingeniería, Biomateriales y Nanomedicina (CIBER-BBN), Madrid, Spain [4]Department of Clinical and Experimental Epilepsy, Queen Square Institute of Neurology, University College London, London, UK. [5]Nanomedicine Lab, National Graphene Institute and Faculty of Biology Medicine and Health, University of Manchester, Manchester, UK., [6]ICREA, Barcelona, Spain

anna.graf@icn2.cat

Graphene solution-gated field-effect transistors (gSGFETs) have emerged as a powerful technology for neural interfaces, offering a significant advantage over traditional passive electrodes with their on-site signal amplification, DC-coupled wide-bandwidth recording, and scalable multiplexing for high-density brain mapping [1],[2]. Moving this technology closer to the industry depends heavily on the scalability of the overall manufacturing process.

Moving from rodent models to large animals or human applications requires significantly larger probes with higher channel counts, consistent performance, and high-throughput batch production - capabilities that small-scale laboratory prototyping cannot achieve.

Here we demonstrate the upscaling of graphene SGFET technology to 6-inch wafers with high homogeneity, reproducibility, and yield across the full wafer, with physiological reliability validated in vivo using mouse epilepsy models. With intracortical probes, we show successful capture of high-fidelity, wide-bandwidth neural activity across deep brain layers. Overall, this paves the way for the industrial-scale manufacturing of graphene-based neural interfaces.

1) Masvidal-Codina, E. *et al. Nat. Mater.* **18**, 280–288 (2019).

2) Schaefer, N. *et al. 2D Mater.* **7**, 025046 (2020).

2026 JPhD 10th edition

Quatsomes nanovesicles as active antimicrobial ingredients for advanced wound care: combining antimicrobial activity with tissue regeneration

Elba Guasch [1,2], Xavier Castellví[3], Judit Tomsen[1,2], Arnau Güell[3], Elisabet González[2,1], Mariana Köber[2,1], Imma Ratera[2,1], Alba Córdoba[3], Nora Ventosa[2,1,3]

[1] *CIBER-BBN, Madrid, Spain;* [2]*ICMAB-CSIC, Cerdanyola del Vallès, Spain;* [3]*Nanomol Technologies SL, Cerdanyola del Vallès, Spain.*

eguasch@icmab.es

Keywords: Quatsomes, Antimicrobial, Biomaterials, Wound Healing, Silver Alternatives, Dual-Action

Tissue regeneration in chronic wounds is frequently hindered by persistent bacterial infections. Standard antimicrobial therapies rely heavily on silver-based dressings; however, they have associated local cytotoxicity and high treatment costs. To overcome these limitations, safer and cost-effective alternatives are urgently needed. This study achieved the integration of quatsomes (QS), small unilamellar nanovesicles composed of cholesterol and commercial surfactants with proven intrinsic antimicrobial activity [1], into tissue-regenerative matrices for wound healing. By incorporating QS as active antimicrobial ingredients, we provided these tissue-regenerative products with infection-control properties, achieving a dual-action therapeutic system [2].

QS nanovesicles were synthesized using the green, scalable DELOS-susp methodology [3] and incorporated into matrices of diverse physicochemical natures including bacterial cellulose-based dressings, hydrogel ointments, and resorbable skin-mimetic matrices (Figure 1). Physicochemical characterization confirmed the successful integration of QS into these different biomaterial formats. Evaluation with cellular assays and skin explant models confirmed that the intrinsic antimicrobial activity of QS was fully preserved across all formulations. Furthermore, preliminary toxicity studies demonstrated excellent safety and biocompatibility. Crucially, trials with animal models proved that adding QS nanovesicles did not alter or compromise the inherent wound healing performance of the matrices.

Overall, we have successfully provided antimicrobial activity to various wound healing products with distinct properties, establishing QS nanovesicles as a versatile, effective, and safe active ingredient. The broad spectrum of tested matrices enables the creation of an array of products tailored to different wound types, advancing toward personalized chronic wound care. By integrating wound healing and infection control into single, dual-action formulations using readily accessible and economical raw materials, this platform offers a promising cost-effective alternative that overcomes the toxicity and economic limitations of silver-based dressings. Crucially, the robust product validation achieved in this study represents a significant step forward in the clinical translation of these multifunctional biomaterials for real-world therapeutic applications in wound care.

Acknowledgements: This research is the result of a collaborative effort among all partners of the NABIHEAL project consortium, supported by the European Union's Horizon Europe program (GA No. 101092269).

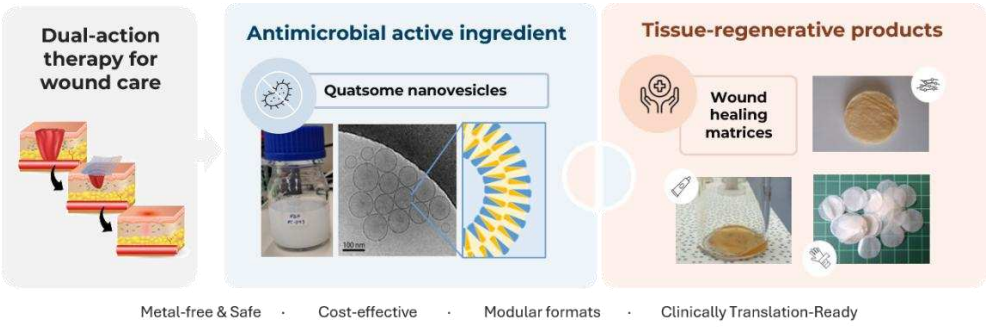

Figure 1: Dual-action wound care system combining antimicrobial quatsome nanovesicles with tissue-regenerative matrices.

(1) Köber, M.; Gallardo-Moreno, A. M.; Ferrer-Tasies, L., et al. Colloids Surf. B Biointerfaces, 2026, 267, 115932.
(2) European Patent Application EP26383247.9, 2026 (pending),European Patent Application EP26383248.7, 2026 (pending)
(3) Córdoba, A. Method for obtaining nano-disperse systems. Patent WO2026032777, 2026.

Spray-Deposited and Water-Activated Batteries for IoT Surveillance System

Júlia González-Sanz[1], Maria Hadid[1], Jaume Esteve[1], Neus Sabaté*[1], Carme Martínez-Domingo*[1]

[1]*Institut de Microelectrònica de Barcelona, IMB-CNM (CSIC), Campus UAB, 08193 Bellaterra, Spain*

*neus.sabate@imb-cnm.csic.es, carme.martinez@imb-cnm.csic.es

Keywords: Flexible batteries, Spray coating, Aqueous zinc-ion primary batteries, Internet of Things (IoT)

The deployment of IoT systems for environmental hazard detection requires autonomous energy sources capable of operating for decades in remote and harsh environments without maintenance. Sensor nodes remain inactive for most of their lifetime and must deliver sudden high-current pulses during emergency events to activate wireless communication modules. Rechargeable batteries suffer from self-discharge and limited lifetime stability, while primary lithium-based coin cells often struggle to sustain high pulse-power delivery after prolonged aging.

This work presents a flexible primary battery for event-driven hazard monitoring, featuring an Ag/AgCl cathode and a Zinc (Zn)-on-Copper (Cu) anode. All components are spray-deposited onto a flexible PET substrate and dried at room temperature. As directly deposited Zn films are highly resistive (~MΩ/square), a spray-deposited Cu underlayer was introduced: 6 Cu layers minimized internal resistance (<1Ω/square), and a single Zn top layer yielded the best electrochemical performance, with an open-circuit voltage of ~0.97V in 1M NaCl. This bilayer architecture enables a maximum current density of ~250μA/mm^2 (power density of 17.5mW/cm^2), satisfying the pulse transmission demands of LoRaWAN and NB-IoT modules, with vastly superior current and power capabilities compared to a screen-printed zinc-carbon counterpart (***Fig. 1***).

Due to their open architecture, these cells remain dormant until an aqueous electrolyte bridges the electrodes. The system thus acts directly as a flood sensor: when printed on river walls, rising water serves as the electrolyte to instantly trigger power. In standby, the cell maintains an absolute open circuit with zero self-discharge, offering a compact, maintenance-free, zero-standby-current solution for remote environmental monitoring networks.

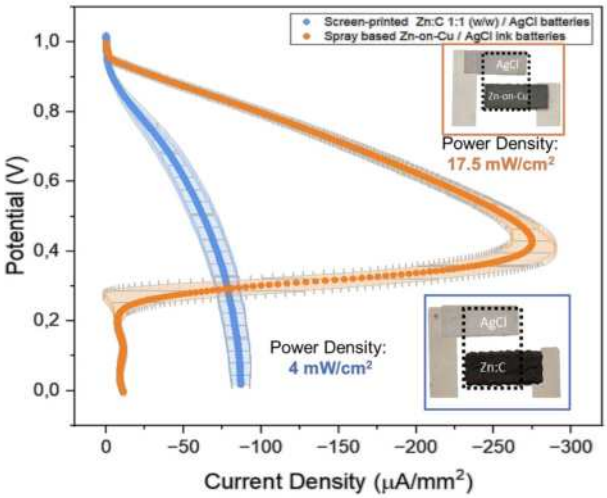

Fig. 1. *Linear sweep voltammetry (LSV) profiles comparing spray-coated Zn-on-Cu//Ag/AgCl and screen-printed Zn:C//Ag/AgCl batteries in* ***1M NaCl*** *electrolyte, with corresponding optical images. The active area for both batteries is 100mm^2 (dashed rectangle). Data evaluated in triplicate (N=3) for each device.*

2026 JPhD 10th edition

Surface functionalization of Ruthenium Nanoparticles for the Hydrogen Evolution Reaction

Eduarda Carolina Hagemann Lopes[1], Álvaro Lozano-Roche[1], *Marcos Gil-Sepulcre* [1,2] *Jordi García-Antón*[1], *Xavier Sala*[1]

[1] *Inorganic Chemistry Unit, Chemistry Department, Faculty of Science of the UAB, 08193, Cerdanyola del Vallès (Barcelona), Spain.*
[2] *Chemistry Department, University of Valencia, 46100, Burjassot (Valencia), Spain.*
EduardaCarolina.Hagemann@UAB.CAT

Keywords: Electrolysis, nanocatalysts, hydrogen evolution

Hydrogen is considered a clean fuel and a good alternative to fossil fuels, especially when produced via water-splitting. Nevertheless, water splitting is a thermodynamically demanding process and involves significant kinetic barriers. Thus, the use of catalysts is necessary to make this reaction more favorable.(1) In the hydrogen evolution reaction (HER), the metal-hydrogen (M-H) bond is a key descriptor of the performance of hydrogen evolution catalysts. In this regard, Pt-based materials are the state-of-the-art catalysts for HER because the Pt-H bond energy is very close to the ideal value of 0 kcal/mol. However, other metals can be tuned with ligands to achieve optimal M-H bond energies.

In particular, Ru nanoparticles (NPs) functionalized with ligands are a good example. An interesting method to synthesize ligand-capped Ru NPs is the organometallic approach, since it produces NPs with a narrow size distribution and a very clean surface.

The control of the surface composition enables the study of the role of the ligands on their catalytic performance. Recent works from our group using Ru NPs functionalized with 4-phenylpyridine (3) and 2,2′-bipyridine (bpy) showed good catalytic performance in the HER, comparable to that of commercial Pt/C.(1, 2) In one of these previous works, our group demonstrated that the coordination mode of bpy (**σ** or **π)** has an effect on the HER activity of specific sites. Inspired by this, we have synthetized Ru NPs by an organometallic approach using a series of bpy-based ligands trying to control the coordination mode using different substituents. Physicochemical and electrochemical characterization has been used to investigate the relationship between the coordination mode of the ligands and the catalytic performance in the HER reaction in surface functionalized NPs.

(1) Lozano-Roche, A., et al. Fine-Tuning HER Activity Through the Interplay Between Nanoparticle Size and Ligand Coordination Mode in Surface-Functionalized Nanocatalysts. ACS Catalysis. 2026, vol. 16, no 11, p. 10337-10347.

(2) Martí, G., et al. Surface-Functionalized Nanoparticles as Catalysts for Artificial Photosynthesis. *Advanced Energy Materials*, 2023, 13(21), Article 2300282.

(3) Creus, J., et al. Ligand-capped Ru nanoparticles as efficient electrocatalyst for the hydrogen evolution reaction. ACS Catalysis, (2018), 8(12), 11094-11102.

Early-Stage Life Cycle Assessment of Magnetic Iron Oxide Nanoparticles for Biohybrid Microrobots

Mehrafarin Hossein panah[1,2], Mario Guyon[3], Alba Bala[4], Pere Fullana[4], Victor Oliva[1], Alessandro Digregorio[3], Gianluca Maria Farinola[3]

[1]*MOVIC WEARE SL, Tarragona, Spain*

[2]*University of Barcelona (UB), Department of Physical Chemistry, Barcelona, Spain*

[3]*Department of Chemistry, University of Bari Aldo Moro, Bari, Italy*

[4]*UNESCO Chair of Life Cycle and Climate Change - Escuela Superior de Comercio Internacional - Pompeu Fabra University, Barcelona, Spain*

Mehrafarin@movic.eu

Throughout the last decades, micro- and nanorobots have emerged as promising technologies for a wide range of applications[1]. Biohybrid systems combine biological structures with exogeneous functionalities to provide either novel class of properties or to improve already existing native biological features., [1,2]. Diatoms are promising building blocks due to their naturally structured biosilica cell walls and present potential for functionalization. Incorporation of magnetic properties enables their controlled motion under an external magnetic field. However, the environmental performance of emerging technologies cannot be assumed from their intended applications or use of bio-based components. Integrating environmental assessment at early development stages allows process configurations to be modified before technological choices become increasingly fixed [3,4]. This study performs a cradle-to-gate LCA of magnetic iron oxide nanoparticle fabrication for diatom functionalization. Laboratory data are used to develop the foreground inventory and identify environmental hotspots. A prospective scale-up approach is additionally applied to estimate energy requirements at larger production scales. The study evaluates the main contributors to environmental impacts and identifies opportunities for process improvement, supporting the integration of environmental considerations into the early design of biohybrid robotic systems.

Keywords: Life cycle assessment, Magnetic properties, Biohybrid microrobots, and Environmental analysis

(1) Lin, Z., Jiang, T. & Shang, J. The emerging technology of biohybrid micro-robots: a review. Bio-Design and Manufacturing 5, 107–132 (2022

(2) Zhang, F., Li, Z., Chen, C., Luan, H., Fang, R.H., Zhang, L. & Wang, J. Biohybrid Microalgae Robots: Design, Fabrication, Materials, and Applications. Advanced Materials 36, 2303714 (2024).

(3) Arvidsson, R., Tillman, A.-M., Sandén, B.A., Janssen, M., Nordelöf, A., Kushnir, D. & Molander, S. Environmental Assessment of Emerging Technologies: Recommendations for Prospective LCA. Journal of Industrial Ecology 22, 1286–1294 (2018).

(4) Bergerson, J.A. et al. Life cycle assessment of emerging technologies: Evaluation techniques at different stages of market and technical maturity. Journal of Industrial Ecology 24 (2020).

Controlling emission with Hybrid Plasmonic Modes

Afroditi Koutsogianni[1], David B. Amabilino[1], Agustín MihiMai[1]

[1]*Institute of Materials Science of Barcelona, ICMAB-CSIC, 08193 Bellaterra, Catalonia, Spain*

akoutsogianni@icmab.es

Integrating distinct plasmonic phenomena within a single platform offers new opportunities to control light-matter interactions at the subwavelength scale. We present a scalable nanoparticle-array-on-mirror (NPAoM) metasurface fabricated via template-assisted self-assembly [1]. Colloidal silver nanoparticles are organized into ordered two-dimensional clusters on a silver mirror, separated by a 20 nm dielectric spacer. This architecture combines grating-coupled surface plasmon polaritons (SPPs), surface lattice resonances (SLRs), and localized gap plasmons. By varying array geometry, we tune the diffractive and localized modes. Angular reflectance spectroscopy and finite-difference time-domain simulations reveal pronounced anti-crossing behavior, indicating strong mode hybridization and enhanced nanogap field confinement. Furthermore, integrating an emitter with the metasurface enables modification of its emission, demonstrating the potential of this architecture to control light-matter interactions. This scalable platform offers opportunities for enhanced surface-enhanced Raman spectroscopy, fluorescence, and phosphorescence through active-material integration within the nanogap.

(1) Koutsogianni, A.; Qi, X; Mendoza-Carreño, J.; Moronta, P.; Alonso, M.L.; Amabilino, D.B.; et.al. Advanced Optical Materials, Hybridization of Gap Plasmons and Grating-Coupled Surface Plasmon Polaritons in Metal Nanoparticle Cluster Arrays on a Mirror. **2026**. doi:10.1002/adom.71842.

Neuromorphic Electrochemical Imagers for Advanced OrganModeling and Medical Discovery on Chip

Jitendra Kumar[1,2], Josep Maria Margarit Taulé[1]

[1] *Integrated Circuits and Systems Group (ICAS), Institute of Microelectronics of Barcelona (IMB-CNM, CSIC)*

[2] *Universitat Autonoma de Barcelona (UAB)*

jitendra.kumar@imb-cnm.csic.es

Keywords: Organoid-on-chip, CMOS biochips, Neuromorphic engineering, Event-driven sensing, Closed-loop bio-control, In-sensor computing.

Organoid-on-chip (OoC) platforms present a transformative tool for personalized medicine and disease modeling, yet continuous, real-time assessment and modulation of microphysiological environments remain fundamental bottlenecks [1]. Standard bio-monitoring relies on off-chip, bulky analytical systems that lack local feedback mechanisms and cannot account for biological variability in real time. In this work, we propose a new class of autonomous, intelligent OoC platforms that seamlessly integrate CMOS-compatible electromechanical multi-sensor arrays with embedded neuromorphic processing units on a single biochip (Figure 1).

The platform leverages event-driven readouts to achieve real-time, low-latency electromechanical imaging of dynamic physiological biomarkers, including ion concentrations and hormone fluxes. To minimize latency and power consumption within the stringent dimensional and thermal constraints of the OoC, we introduce an in-sensor recurrent neural network architecture that directly reuses front-end sensing circuitry for neuropredictive modelling and edge computing [2]. This architecture enables the biochip to sense, perceive, and modulate organoid microenvironments in a closed loop. We validate the platform's performance in in-situ neurodegenerative disease models, demonstrating enhanced experimental reproducibility, sub-millisecond adaptive response, and robust tracking across diverse biological phenotypes. This integrated edge-biochip framework lays the groundwork for self-regulating in vitro diagnostic and therapeutic testing platforms.

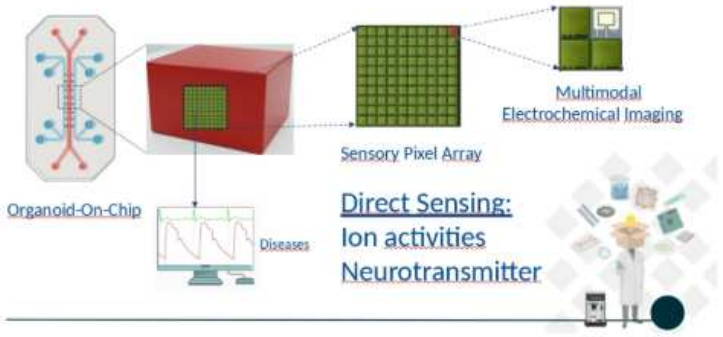

Figure 1: System-level overview of the autonomous organoid-on-chip platform, illustrating the monolithic integration of CMOS multi-sensor arrays, event-based neuromorphic processing, and closed-loop biochemical actuation.

(1) Leung, C.M.; et.al. Nature Reviews, 2022. DOI: 10.1038/s43586-022-00118-6

(2) Park, S.E.; et.al. Science, 2019. DOI: 10.1126/science.aaw7894

2026 JPhD 10th edition

Photovoltaic Response in Epitaxial $GdFeO_3$ Thin Films

Shubham Kumar[1,2], David Pesquera[1], Kumara Cordero-Edwards[1], José Santiso[1], Gustau *Catalan[1,3]*

[1] Catalan Institute of Nanoscience and Nanotechnology (ICN2), CSIC and BIST, Campus UAB, Bellaterra, Barcelona, 08193, Catalonia, Spain

[2] Universitat Autònoma de Barcelona, Plaça Cívica, Bellaterra, Barcelona, 08193, Catalonia, Spain

[3] ICREA – Institució Catalana de Recerca i Estudis Avançats, Barcelona, 08010, Catalonia, Spain

shubham.kumar@icn2.cat

Keywords: epitaxial thin films, photovoltaics effect, composition gradient, flexo-photovoltaics

$GdFeO_3$(GFO) is a centrosymmetric perovskite-structured orthoferrite with a range of interesting physical properties. Its visible bandgap makes it an attractive material for studying photovoltaic responses [1]. In this work, we investigate the photovoltaic response of epitaxial GFO thin films grown on orthorhombic $NdGaO_3$(110) substrate, using $La_{0.66}Sr_{0.33}MnO_3$ (LSMO) as the conducting bottom electrode and ITO as the top electrode. The optimized GFO film shows a clear photoresponse under illumination, with a short-circuit current density of approximately 4.7 mA/cm^{-2} and an open-circuit voltage of -0.35 V. The observed photovoltaic response is associated with the asymmetric electrode configuration and the formation of interfacial Schottky barriers arising from the difference in work functions between the electrodes. These results establish epitaxial GFO as a promising platform for further investigation of other types of photovoltaic responses, such as the strain gradient-induced flexophotovoltaic effect [2], which we are doing through compositional gradient engineering.

(1) Zhu, X.-H.; Xiao, X.-B.; Chen, X.-R.; Liu, B.-G. *Electronic structure, magnetism and optical properties of orthorhombic $GdFeO_3$ from first principles*. RSC Advances, 4054–4061

(2) Yang, M.-M.; Kim, D. J.; Alexe, M. Flexo-photovoltaic effect. *Science*, 904–907

Synthesis of Citrate-Stabilized Iron Oxide Nanowires: From Experimental Design to Predictive Synthesis

Ana C. Leyva-Castro[1], Karen Mejía-Carmona[1], Muriel F. Gustà[1], Jielin Zhang[1], Aziz Genç[1], Jordi Arbiol[1], Víctor Puntes[1,2], Neus G. Bastús[1].

[1] *Catalan Institute of Nanoscience and Nanotechnology (ICN2), CSIC and BIST, Barcelona 08193, Spain*

[2] *Vall d'Hebron Institut de Recerca (VHIR), Barcelona 08035, Spain*

anacecilia.leyva@icn2.cat

Keywords: iron oxide nanowires; cerium cations; anisotropic nanostructures; design of experiments; coprecipitation synthesis; magnetic nanomaterials; nanowire morphology

The morphological control of nanomaterials has gained increasing attention due to the strong influence of shape and size on their physicochemical properties. In particular, anisotropic iron oxide nanowires are of interest because of their magnetic behavior and potential catalytic, electronic, and biomedical applications. Understanding how synthesis parameters influence anisotropic growth is therefore important for controlling nanowire formation and tuning their magnetic properties for specific applications. In this work, we investigate the formation of citrate-stabilized iron oxide nanowires promoted by high cerium concentrations. A Design of Experiments (DoE) approach was used to develop a quadratic response surface model to systematically evaluate the influence of the main synthesis parameters, as well as their interactions. In particular, the study focuses on identifying the conditions that favor anisotropic growth over the formation of isotropic nanoparticles or poorly defined aggregates. The nanostructures were characterized to establish correlations between synthesis conditions and their morphological and magnetic properties. Distinct morphologies spanning two orders of magnitude in size (100 nm–10 µm) were observed, ranging from loosely connected single-particle chains to more compact and branched multi-particle nanowires.

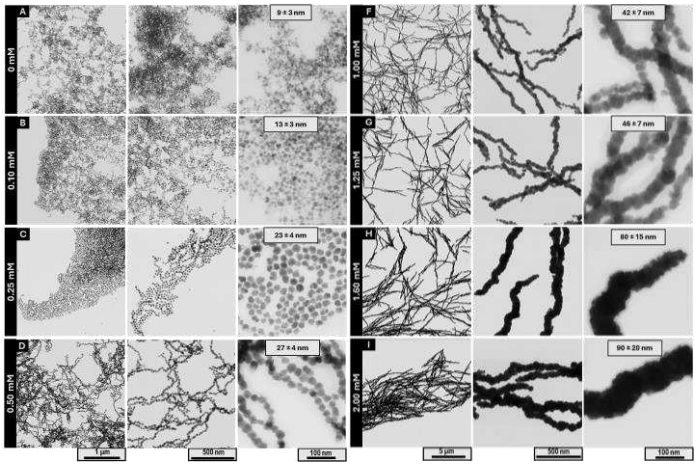

Figure 1: Morphological evolution of iron oxide nanostructures with increasing Ce^{3+} concentration.

(1) Mejía-Carmona, K.; Gustà, M.F.; Guardia, P.; Spadaro, M.C.; Arbiol, J.; Puntes, V.; Bastús, N.G. Size Control of Highly Monodisperse Citrate-Stabilized Magnetite Nanoparticles in Aqueous Media: The Role of Cerium Cations. Chemistry of Materials 2025, 37, 7846–7857, doi:10.1021/acs.chemmater.5c01492.

(2) Williamson, E.M.; Sun, Z.; Mora-Tamez, L.; Brutchey, R.L. Design of Experiments for Nanocrystal Syntheses: A How-To Guide for Proper Implementation. Chemistry of Materials 2022, 34, 9823–9835, doi:10.1021/acs.chemmater.2c02924.

2026 JPhD 10th edition

A Carborane-Based Platform for Multifunctional, Composition-Tunable Lanthanide Metal–Organic Frameworks

Xiaoming Liu[1], Ana Arauzo[2], Sara Fuertes[2], José Giner Planas[1*], and Elena Bartolomé[1*]

[1]*Institut de Ciència de Materials de Barcelona (ICMAB-CSIC), Campus UAB, 08193 Bellaterra, Spain*

[2]*Instituto de Nanociencia y Materiales de Aragón (INMA-CSIC), Dep. Física de la Materia Condensada, CSIC-Universidad de Zaragoza, 50009-Zaragoza, Spain*

[3]*Departamento de Quı´mica Inorga´nica, Facultad de Ciencias, Instituto de Sı´ntesis Quı´mica y Cata´lisis Homoge´nea (ISQCH), CSIC-Universidad de Zaragoza, Pedro Cerbuna 12, Zaragoza, 50009, Spain*

xiaomingliu@icmab.es

Keywords: lanthanide metal–organic frameworks; carborane linker; single-molecule magnets; magnetocaloric effect; near-infrared luminescence

Metal-organic frameworks (MOFs), built from organic linkers and metal ions arranged in crystalline, porous structures, have gained widespread attention for their versatility in applications such as catalysis, gas storage, and sensing. Lanthanide (Ln)-based MOFs, in particular, stand out for their unique magnetic, electronic, and optical properties, making them attractive for advanced technologies including information storage and processing, magnetic refrigeration, and luminescence. We recently achieved the unprecedented synthesis of multivariate MOFs from the bulky, carborane linker *m*CB-L, enabling the incorporation of customizable combinations of multiple lanthanides within a single isostructural framework. Here we exploit this versatile platform to design two new mixed-Ln members with deliberately contrasting functionality. In {Ce/Er}, doping Er^{3+} into the emissive Ce^{3+} host unlocks simultaneous, independently-addressable visible and near-infrared emission alongside field-induced single-molecule magnet (SMM) behaviour and a sizeable magnetocaloric effect (MCE).[1] In {Nd/Yb}, the same strategy instead yields a dual-NIR emitter, where partial $Nd^{3+}\rightarrow Yb^{3+}$ energy transfer enables radiometric tuning of the emission colour, together with SMM and MCE behaviour.[2] These results highlight carborane-based multivariate lanthanide MOFs as powerful platform for multifunctional materials, with exciting prospects for optical tagging, ratiometric NIR sensing/thermometry, and bioimaging.

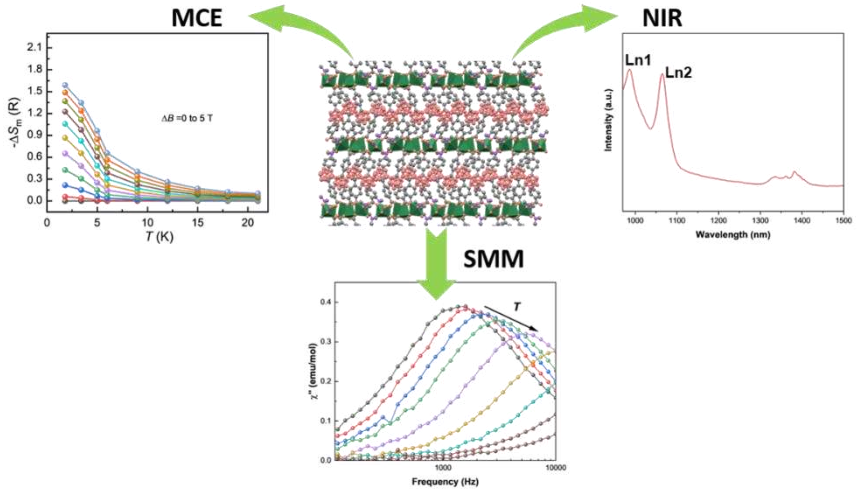

Figure 1. A carborane-linker (*m*CB-L) platform for multifunctional lanthanide MOFs, showing field-induced SMM, NIR behaviour and additive magnetocaloric response.

[1] Liu, X.; Arauzo, A.; Fuertes, S.; Giner Planas, J.; Bartolomé, E. Tunable {Er/Ce} carborane-based metal–organic frameworks combining slow magnetic relaxation, magnetocalorics and multi-band visible-NIR emission. *J. Mater. Chem. C* **2026**. https://doi.org/10.1039/d6tc01235c

[2] Liu, X.; Arauzo, A.; Fuertes, S.; Giner Planas, J.; Bartolomé, E. Pure and mixed {Nd/Yb} carborane-based metal–organic frameworks integrating slow magnetic relaxation, magnetocaloric effect and NIR emission. *J. Mater. Chem. C* **2026**, 14 (19), 8085–8098. https://doi.org/10.1039/d5tc03820k

Enabling Low-Pressure Methanol Synthesis from CO_2 through Copper Confinement in ZIF-8 Frameworks: Role of Metal-Support Interactions and Cu Active Sites

Adrià López-Pontanilla[1], Alejandro Borrás, Concepción Domingo

[1]*Materials Science Institute of Barcelona (ICMAB-CSIC) Campus UAB s/n, 08193 Bellaterra (Spain)*

alopez5@icmab.es

Keywords: CO_2 hydrogenation, Methanol synthesis, ZIF-8, Copper confinement, Low-pressure catalysis

The continuous increase in atmospheric CO_2 levels has intensified efforts to develop sustainable carbon capture and utilization strategies. Among them, the thermocatalytic hydrogenation of CO_2 to methanol (MeOH) is particularly attractive, as methanol is both a key chemical feedstock and an energy carrier. Since catalyst design strongly determines process performance, copper-based systems remain the state of the art due to their high activity and selectivity under relatively mild conditions [1]. This work investigates the role of zeolitic imidazolate frameworks (ZIFs), a class of highly microporous MOFs, in the thermocatalytic hydrogenation of CO_2 to methanol. In particular, ZIF-8, formed by Zn^{2+} ions tetrahedrally coordinated to 2-methylimidazolate linkers, is employed to stabilize Cu nanoparticles (NPs) and Cu single-atom sites [2], enhancing catalytic efficiency and MeOH selectivity through improved intermediate stabilization and metal-support interactions [3]. To address water accumulation, Cu@ZIF-8 is dispersed on a reduced graphene oxide (rGO) aerogel with extended hydrophobic character [4]. To improve sustainability, reactions are performed at 10 bar, significantly below industrial pressures (>50 bar). Although lower pressures generally favor CO formation via reverse water–gas shift (RWGS) reaction and reduce methanol yield, improved metal-support interactions and Cu confinement within ZIF-8 enable practical low-pressure operation. The microporous framework enhances CO_2 adsorption, increases local reactant concentration and stabilizes reaction intermediates. Supercritical CO_2 is used for both ZIF-8 synthesis and GO aerogel preparation. Compared with benchmark $Cu/ZnO/Al_2O_3$ catalysts [5], the developed materials achieve near-100% methanol selectivity at 10 bar, while Cu confinement prevents catalyst deactivation by nanoparticle sintering.

(1) M. Kubovics, A. Trigo, A. Sánchez, G. Marbán, A. Borrás, J. Moral-Vico, A.M. López-Periago, C. Domingo, ChemCatChem 14, e202200607, 2022.
(2) A. Rosado, I.M. Popa, A.A. Markeb, J. Moral-Vico, E.M. Naughton, H.G. Eckhardt, J.A. Ayllón, A.M. López-Periago, C. Domingo, L. Negahdar, J. Mater. Chem. A 12(33) 21758-21771, 2024.
(3) V.K. Velisoju, J.L. Cerrillo, R. Ahmad, H.O. Mohamed, Y. Attada, Q. Cheng, X. Yao, L. Zheng, O. Shekhah, S. Telalovic, J. Narciso, L. Cavallo, Y. Han, M. Eddaoudi, E.V. Ramos-Fernández, P. Castaño, Nat. Commun. 15, 2045, 2024.
(4) M. Kubovics, A. Borrás, A.A. Markeb, G. Marbán, J. Moral-Vico, A. Sánchez, A.M. López Periago, C. Domingo, ACS Sustainable Chem. Eng. 12(28), 10634–10646, 2024.
(5) M. Behrens, F. Studt, I. Kasatkin, S. Kühl, M. Hävecker, F. Abild-Pedersen, S. Zander, F. Girgsdies, P. Kurr, B.L. Kniep, M. Tovar, R.W. Fischer, J.K. Nørskov, R. Schlögl, Science 336, 893–897, 2012.

2026 JPhD 10th edition

Biological Effects of 5G Millimeter Wave Electromagnetic Fields at 26 GHz on *Caenorhabditis elegans*: Toward a New Approach Methodology for Health Hazard Assessment

Carlos López-Orts[1], Amanda Muñoz-Juan[1], Pol Alonso[1], Núria Alonso[1], Mariateresa Allocca[2], Fulvio Schettino[3], Olga Zeni[2], Anna Laromaine[1]

[1]*Institute of Material Science of Barcelona (ICMAB-CSIC), Spain*
[2]*Institute for Electromagnetic Sensing of Environment (IREA-CNR), Italy*
[3]*Department of Electrical and Computer Science Engineering, University of Cassino, Italy*

clopez2@icmab.es, alaromaine@icmab.es

Keywords:

Owing to its transparent body, short life cycle, low maintenance costs, and significant genetic homology with humans, the nematode *Caenorhabditis elegans* serves as a powerful in vivo model. By focusing on its well described physiology, we have used it as a subject in in toxicology studies using electromagnetic radiation in the 5G frequency range. We exposed wild-type (N2) and cuticule-sensitive (CB6055) worms, mimicking Wi-Fi exposure in humans at 26.5 GHz, maintaining a specific absorption rate (SAR) of 1 W/kg, adapted to worm size and volume. We compared various organismal health endpoints, between exposed and non-exposed worms across two generations, and our findings reported a notable absence of effects due to RF-EMF exposure in parameters such as survival, egg hatching, length (Figure 1A, 1B, 1C; respectively), motility, and reproductive toxicity. Further studies, at the cellular level, studied oxidative damage by assessing the antioxidant capacity of exposed worms, which was not determined to be depleted by ROS production. Lastly, delving deeper into the genetic expression, functional enrichment analysis of exposed worms failed to show activation of stress-response genetic pathways that could indicate detrimental effects.

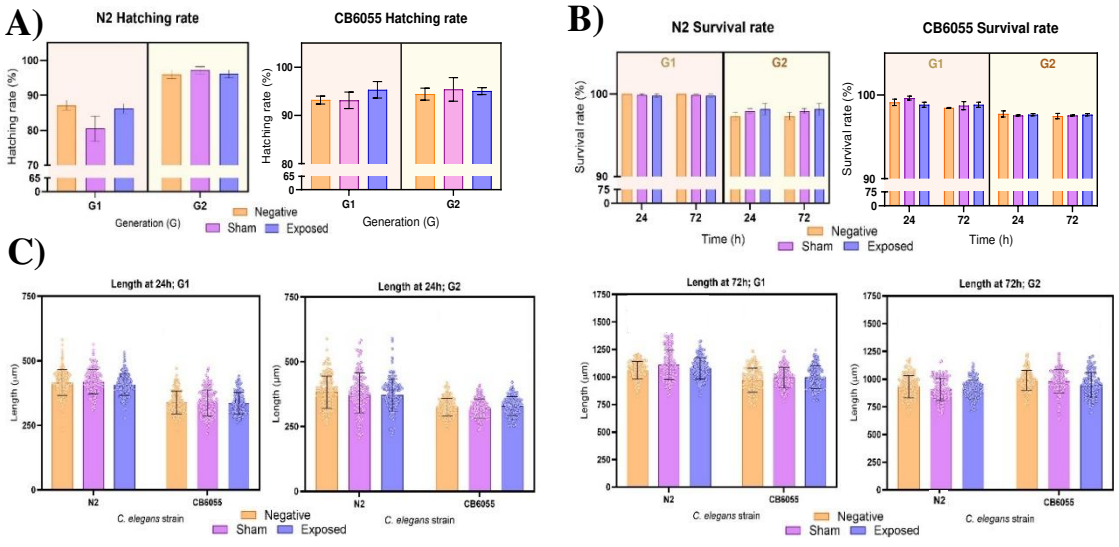

Figure 1: Organismal health endpoints in two generations of *C. elegans*. (A) Hatching rate (B) Survival rate (C) Length

Integration of vertical topologies in silicon-based technologies

H. Lozano-Fuster*, A. del Moral, A. Guerrero, J. Bausells, J. Llobet and E. Amat

Institute of Microelectronics of Barcelona (IMB-CNM, CSIC), 08193Bellaterra, Spain

*corresponding author: hugo.lozano@imb-cnm.csic.es

Keywords: Silicon-based technologies, semiconductors, CFET, IC, EBL, RIE, nanopillars, footprint

The aim of Complementary-FET (CFET) technology is to minimize the footprint of integrated circuits (IC) by stacking the circuit devices. Currently, their implementation is based on nanosheet devices as core element (**Fig. 1**), following a 2D configuration [1]. In this context, we propose a more aggressive reduction in area by presenting a novel CFET implementation paradigm based on stacking devices in a vertical configuration within the same silicon pillar (**Fig. 2**), becoming the Stack-in-Pillar (SiP) configuration. [2] **Fig. 3** shows the highest area footprint reduction (80%) of our proposal in front of other architectures [3]. The PhD aim is, in the framework of EnVertIC (*#PID2024-15871OB-C31*) national project, to validate the SiP proposal by implementing, as proof of concept, a CMOS inverter with p- and n-type devices sharing the same nanopillar. In this structure, the same potential will be applied to both gates. This will result in a depletion region forming in one side of the nanopillar while a conducting region forms in the other, thereby enabling the inverter behaviour (**Fig. 4**).

Several techniques are being combined to fabricate the device: electron beam lithography (EBL) followed by reactive ion etching (RIE) for top-down nanopillar fabrication; several techniques for the deposition of the interlayer dielectric (ILD); evaporation or sputtering for the metal gate integration; and a combination of ion implantation and polymeric precision doping (PPD) for controlled doping.

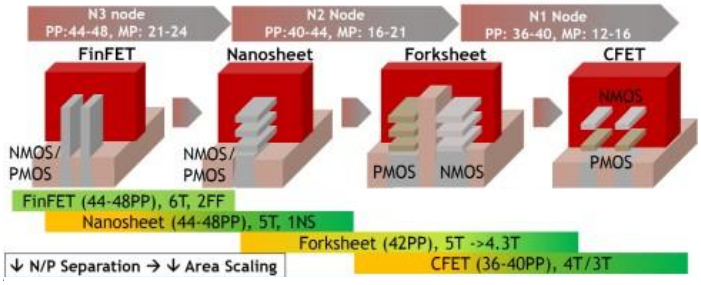

Fig. 1. Schematic of the evolution of CMOS technology. [1]

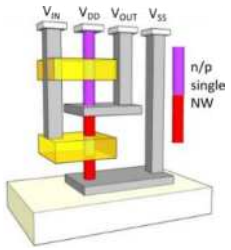

Fig. 2. Conceptual draw of a SiP-based CMOS inverter. [2]

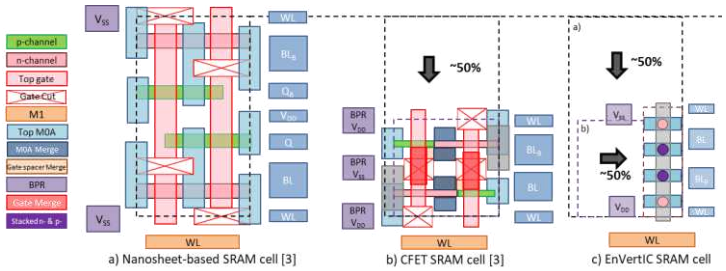

Fig. 3. Area footprint reduction when a SRAM cell is implemented using different strategies. [3]

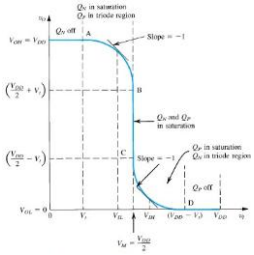

Fig. 4. Voltage transfer curve of a CMOS inverter.

References

(1) J. Ryckaert *et al.*, IEDM, pp. 29.4.1-29.4.4, 2019
(2) E. Amat *et al.*, IEEE Trans. Nanotechnol, vol. 23, pp. 435–440, 2024
(3) H.-H. Liu *et al.*, IEEE TED, vol. 70, pp. 883–890, 2023.

Optimization of Reduced Graphene Oxide Microelectrodes for Efficient and Biocompatible Muscle Stimulation

M. Madrid[a], M. Rovira,[b] M. Martí,[a] F. Lezcano,[b] X. Illa,[c] M. Crespo,[b] A. Guimerà,[c] K. Bhorkar,[a] S. Sánchez,[b] J.A. Garrido,[a] E. Del Corro [a]

[a] *Institut Català de Nanociència i Nanotecnologia (ICN2)*

[b] *Institute for Bioengineering of Catalonia (IBEC)*

[c] *Instituto de Microelectrónica de Barcelona - Centro Nacional de Microelectrónica (IMB-CNM)*

miquel.madrid@icn2.cat

Keywords:

Graphene-based microelectrodes represent a new generation of bioelectronic interfaces, combining high electrochemical performance with outstanding biocompatibility and mechanical flexibility. Unlike conventional metallic electrodes, which are rigid and non-conformal, reduced graphene oxide (rGO) microelectrode arrays (MEAs)[1] provide efficient, localized, and stable electrical stimulation thanks to their high surface area and large volumetric capacitance, enabling effective charge storage and delivery at low power consumption.

In this work, the Advanced Electronic Materials and Devices (AEMD) group at ICN2 developed and characterized rGO MEAs designed to interface with 3D bioengineered muscle tissues[2] created by the Smart Nano-Bio-Devices group at IBEC. The flexibility of the graphene-based electrodes allows intimate integration with soft biological constructs, while their biocompatibility ensures long-term stability for stimulation and recording. When tested with 3D muscle models, the rGO MEAs successfully delivered localized and reproducible electrical stimulation without inducing any detectable damage or adverse effects on the tissue, demonstrating their safety and functional reliability.

Building on these results, our current research focuses on the optimization of the rGO layer thickness, which plays a crucial role in defining the electrochemical performance of the electrodes. By systematically tuning the film thickness, we aim to understand its impact on ion transport, charge storage, and tissue response, ultimately optimizing both the stimulation efficiency and the bio-integration of graphene-based interfaces for future applications in muscle regeneration and rehabilitation.

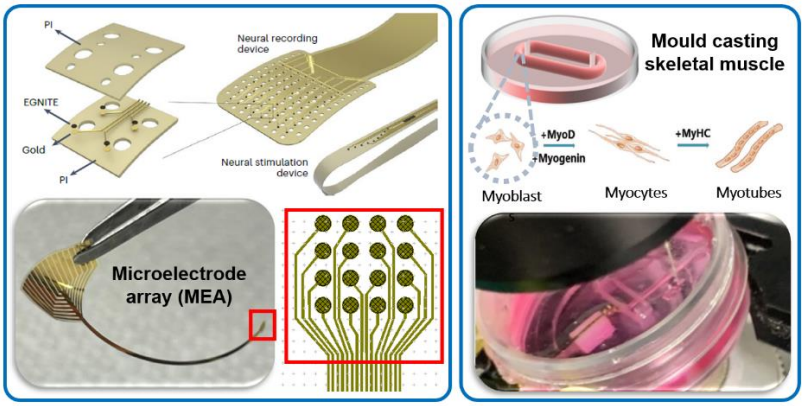

Figure 1: Flexible microelectrode array with rGO and skeletal muscle model.

(1) Viana, D., Walston, S.T., Masvidal-Codina, E. et al. Nanoporous graphene-based thin-film microelectrodes for in vivo high-resolution neural recording and stimulation. Nat. Nanotechnol. 19, 514–523 (2024).

(2) Mestre R, García N, Patiño T, Guix M, Fuentes J, Valerio-Santiago M, Almiñana N, Sánchez S. 3D-bioengineered model of human skeletal muscle tissue with phenotypic features of aging for drug testing purposes. Biofabrication. 2021 Aug 16;13(4).

Sperm and seminal extracellular vesicle proteomes of the gilthead seabream (*Sparus aurata*), a comparative model of male fertility

Leonardo Madsen[1,2], Jaxaira Maggi[3,4], François Chauvigné[1,2], Montserrat Carrascal[3,4], Joan Cerdà[1,2]

[1] *Institute of Marine Sciences, ICM/CSIC, Spain*
[2] *Institute of Biotechnology and Biomedicine, IBB/UAB, Spain*
[3] *Biological and Environmental Proteomics Group, Institute of Biomedical Research of Barcelona, IIBB-CSIC, Spain*
[4] *CSIC/UAB Proteomics Laboratory, Spain*

Leonardo.Madsen@autonoma.cat; madsen@icm.csic.es

Keywords: male fertility; spermatozoa; proteomics; extracellular vesicles; orthology; *Sparus aurata*

Defining the sperm proteome is key to understanding the molecular basis of fertilization and male infertility. The gilthead seabream (*Sparus aurata*), a teleost whose spermatozoa mature after leaving the testis, offers a comparative vertebrate model of conserved sperm functions, but its sperm proteome has remained scattered across analyses searched against different databases. Here, we integrated five shotgun LC-MS/MS services into a single inventory in which every protein carries a graded level of evidence. The 23 samples included immature (efferent-duct) and mature (ejaculated) spermatozoa, analyzed whole or as total-membrane, plasma-membrane, nuclear, mitochondrial and flagellar fractions. Keeping medium- or high-confidence identifications, the inventory comprises 6,907 proteins (3,571 seabream genes). Enrichment analysis through seabream–human orthologs yielded 329 GO and KEGG terms, including oxidative phosphorylation, glycolysis with the sperm-type GAPDHS, fatty-acid oxidation, the sperm flagellum, peroxiredoxins and the proteasome, including its spermatoproteasome subunit PSMA8. Both GAPDHS and PSMA8 are required for male fertility in mice [1]. A sequence-based comparison with the zebrafish and human sperm proteomes detected homologs in both for 78% of the seabream sperm genes and reciprocal orthologs for 44%. This shared core comprised the axoneme, energy metabolism, the proteasome and a translation apparatus including all 24 detected aminoacyl-tRNA synthetases, consistent with protein synthesis in post-testicular spermatozoa [2]. In parallel, seminal-fluid extracellular vesicles from three tank pools yielded 1,342 high-confidence proteins (counted per gene) detected in all three, including the EV markers CD9-like, CD63, CD81, ALIX and syntenin; 78% were also in the sperm inventory. Current efforts address the remodeling of the sperm phosphoproteome during the hyperosmotic activation of motility. Altogether, these data provide a curated resource to study conserved mechanisms of sperm function across vertebrates and to search for sperm-quality biomarkers and paternal contributions to offspring health.

(1) Gómez-H, L. et al. *PLoS Genet.* 2019, 15, e1008316.

(2) Castro-Arnau, J. et al. *iScience* 2025, 28, 111537.

2026 JPhD 10th edition

Tailoring Bacterial Cellulose Scaffolds to Support Limbal Stem Cells for Corneal Regeneration

Mina Maleki[1], Anna Roig[1]

[1]*Institut de Cie`ncia de Materials de Barcelona (ICMAB, CSIC), Bellaterra, Spain*

Mmaleki@icmab.es

Keywords: Bacterial Cellulose, Corneal Tissue Engineering, Limbal Stem Cells, Surface Modification

In Europe, 30 million people suffer from corneal disease. If limbal stem cells are damaged by injury, infection, or genetic disease, the cornea cannot heal and may result in permanent blindness. Few treatment options, such as cornea transplantation and artificial corneas, are currently available. However, they have limitations such as high costs, donor availability, infection, and immune responses. In order to overcome these challenges, corneal tissue engineering has emerged as a promising alternative by minimizing immune rejection with natural biomaterials *(1–3)*. Amniotic membrane (AM) serves as a clinical reference. Although AM is advantageous, it is also limited by poor optical transparency, donor scarcity, and significant batch-to-batch variability *(4)* . In this study, we explore bacterial cellulose (BC) as a potentially reproducible, donor-independent candidate for delivering limbal stem cells, as a previous study by our group showed promising results *(5).* As a biosynthetic compound, BC has been reported to have biocompatibility, low immunogenicity, mechanical strength, optical transparency, and high-water retention capabilities that are advantageous for this application. Nevertheless, native BC lacks intrinsic cell-adhesion motifs, so cell attachment is limited for delivering limbal stem cells. As a preliminary evaluation, we will assess modified BC scaffolds through in vitro cellular attachment, viability, and proliferation, together with mechanical properties. In addition, to gain an initial insight into clinical handleability and surgical suitability, we have started a collaboration to examine sutureability and application of the scaffold in a mouse eye model. These investigations are intended to support the further development of modified BC as a scaffold for limbal stem cell therapy.

1. Palchesko, R. N.; Carrasquilla, S. D.; Feinberg, A. W. Advanced Healthcare Materials 2018, 7(16).

2. Tafti, M. F.; Aghamollaei, H.; Moghaddam, M. M.; Jadidi, K.; Alio, J. L.; Faghihi, S Journal of Tissue Engineering and Regenerative Medicine. John Wiley and Sons Ltd August 1, 2022, pp 683–706.

3. Di Girolamo, N. Advanced Materials. John Wiley and Sons Inc October 17, 2024.

4. Li, Y.; Wang, Z. Advanced Science. John Wiley and Sons Inc February 10, 2025.

5. Anton-Sales, I.; Koivusalo, L.; Skottman, H.; Laromaine, A.; Roig, A. Small 2021, 17(10), 2003937.

2026 JPhD 10th edition

Computational Mueller Matrix Microscopic Pathology Based on Mueller Decomposition for Medical Reference Mapping

Yuxuan Mao[1], Irene Estevéz[1], Armando Pérez-Torres[2], Juan Campos[1], Angel Lizana[1]

[1]*Optics Group, Department of Physics, Universitat Autònoma de Barcelona, Bellaterra 08193, Spain*

[2]*Cellular and Tissue Biology Department, Faculty of Medicine, Universidad Nacional Autónoma de México,Ciudad de México, 04510, México*

Angel.lizana@uab.cat

Keywords: Polarimetric imaging, Computational bioimaging, Differential Mueller matrix decomposition, Image stitching, Multi-parametric pseudo-color mapping

Label-free quantitative polarimetric imaging provides access to tissue properties beyond conventional intensity-based microscopy, offering a means to extract physically interpretable bioinformation for computational pathology [1]. Mueller matrix imaging enables spatially resolved characterization of optical mechanisms, including diattenuation, birefringence, and depolarization, thereby providing complementary physical information for the characterization and diagnosis of biological tissues [2]. However, its application to tissue-scale analysis remains challenging because high-resolution acquisition restricts the field of view [3], while the high-dimensional polarimetric information is difficult to interpret and relate to conventional histological references.

Here, we present a physics-informed computational framework, termed Computational Mueller Matrix Microscopic Pathology. The framework integrates differential decomposition [4], wide-field Mueller matrix image stitching, and mechanism-specific multi-channel pseudo-color visualization into a unified computational pipeline. By combining physically interpretable Mueller matrix image with SIFT-based stitching strategy [5], the framework extends high-resolution Mueller matrix imaging to large tissue areas while preserving spatial consistency and physical interpretability. Mechanism-specific pseudo-color mappings further transform decomposed optical responses into spatially distinguishable representations, facilitating visual and quantitative comparison with conventional histological references.

The framework was evaluated on paired H&E-stained murine melanoma specimens under untreated (Trt-) and treated (Trt+) conditions using complementary physical, quantitative, and histological analyses. Differential and Lu-Chipman decompositions produced comparable tissue representations in thin pathological sections, while mechanism-specific pseudo-color mappings revealed distinct spatial contrasts associated with different optical mechanisms. Among these, depolarization consistently exhibited tumor-associated spatial contrast across numerical distributions, spatial heterogeneity, and visual representations, with preliminary correspondence to H&E-defined tissue regions.

Overall, the proposed framework demonstrates the feasibility of integrating large-field Mueller matrix imaging with physically interpretable decomposition and bioinformation-oriented visualization. Rather than serving solely as an imaging enhancement strategy, it provides a computational route for linking tissue histology with quantitative optical properties and extracting spatially resolved polarimetric features relevant to tissue characterization. This framework establishes a foundation for exploiting Mueller matrix polarimetry as a label-free source of biologically relevant information in computational pathological analysis.

[1] J. C. Ramella-Roman and T. Novikova, (2022), Polarized Light in Biomedical Imaging and Sensing: Clinical and Preclinical Applications, Springer Nature.

[2] J. J. Gil and R. Ossikovski , (2022), Polarized Light and the Mueller Matrix Approach (CRC Press)

[3] F. Ghaznavi, A. Evans, A. Madabhushi, and M. Feldman, (2013). “Digital imaging in pathology: whole-slide imaging and beyond,” Annual Review of Pathology: Mechanisms of Disease, vol. 8, no 1, p. 331-359.

[4] Arteaga, O. and Kahr, B. (2013). Characterization of homogenous depolarizing media based on mueller matrix differential decomposition. Optics Letters 38, 1134–1136.

[5] D. G. Lowe, “Distinctive image features from scale-invariant keypoints,” International journal of computer vision, 60(2), 91-110.

[6] Hernandez-Aceves, J. A., Cervantes-Torres, J., Torres-Garcia, D., Zuniga-Flores, F. J., Patino-Chavez, O. J., Pe˜na Agudelo, J. A., et al. (2023). Gk-1 effectively reduces angiogenesis and prevents t cell exhaustion in a breast cancer murine experimental model. Cancer Immunology,Immunotherapy 72, 3825–3838.

Formulation of amorphous solid dispersions of a poorly water-soluble anticancer drug using Compressed Fluid and Spray Drying technologies

Andrés Eduardo Márquez Chacón[1,3], David Piña[1,3]; Xavier Castellvi[2]; Mariana Köber[1,3]; Ramón Berenguer[4]; Marta Racamonde[4]; Santi Sala[2]; Alba Córdoba[2]; Nora Ventosa[2]

[1]*Instituto de Ciencia de Materiales de Barcelona (ICMAB), CSIC; 08193, Bellaterra*
[2]*Nanomol Technologies S.L.; 08193, Bellaterra*
[3]*Centro de Investigación Biomédica en Red de Bioingeniería, Biomateriales y Nanomedicina, 28029, Madrid*
[4]*Esteve Química S.A; 08030, Barcelona*

amarquez2@icmab.es

Keywords:

Poor aqueous solubility remains a major challenge in the formulation of orally administered drugs, limiting the bioavailability of many active pharmaceutical ingredients (APIs) [1,2]. However, advancements in formulation strategies, such as amorphous solid dispersion (ASDs), have been crucial in overcoming these solubility challenges, allowing the successful development of many poorly water-soluble drugs [3]. This study investigates Precipitation with a Compressed Antisolvent (PCA) using CO_2 as a green, single-stage approach, and Spray Drying, as the most widely used technology in the industry for this purpose, for the ASD development of the poorly water-soluble anticancer drug Ibrutinib (IBR).

IBR was co-precipitated with two cellulosic polymers, hydroxypropyl methylcellulose (HPMC-E15) and hydroxypropyl methylcellulose acetate succinate (HPMCAS). PCA processing conditions were optimized to achieve efficient precipitation and homogeneous API–polymer incorporation. The resulting particles were characterized in terms of morphology, particle size, solid-state properties, and dissolution performance. Equivalent formulations were prepared by conventional Spray Drying (SD) for performance comparison.

CO_2-based PCA successfully produced amorphous Ibrutinib ASDs with distinct microstructural characteristics. The HPMC-E15/IBR (1:1, w/w) formulation formed highly porous, sponge-like microparticles composed of coalesced primary particles. Compared with spray-dried formulations, the compressed-fluid-processed dispersions exhibited faster and enhanced dissolution, highlighting the potential of PCA to improve the dissolution performance of poorly water-soluble APIs. Overall, these results demonstrate that compressed-fluid precipitation can generate microstructures that offer advantages over conventional spray drying for the development of polymer-based ASDs.

[1] Bárdos, V.; Szolláth, R.; Tőzsér, P.; Mirzahosseini, A.; Sinkó, B.; Angi, R.; Takács-Novák, K. Study of the Influence of Pharmaceutical Excipients on the Solubility and Permeability of BCS Class II Drugs. Sci. Pharm. 93, 19, 2025.

[2] Rabia, I.; Omer S.; Abid M.; Syed A.; Hafiz S.; Gul S.; Uzma S.; Muhammad F. Enhanced solubility and biopharmaceutical performance of atorvastatin and metformin via electrospun polyvinylpyrrolidone-hyaluronic acid composite nanoparticles. European Journal of Pharmaceutical Sciences. Volume 161. 2021, 105817, ISSN 0928-0987.

[3] Dhavalkumar, M.; Dudhat, K.; Shah, S. Role of polymeric carriers in amorphous solid dispersions: comprehensive review of stabilization mechanisms, dissolution behavior, and FDA-approved formulations. Polym. Bull. 83, 285, 2026.

Cellulose-Based Conductive ECG Electrodes for Sustainable Electrophysiological Monitoring

A. Martí Maymó[1,2], M. Iordanoglou[3], F. Vilaseca[4], MT. García[5], A. Fabregat Sanjuan[6], P. Fullana-i-Palmer[3], A. Guimerà Brunet[1,2], G. Gabriel Buguña[1,2]

[1] Institut de Microelectrònica de Barcelona, IMB-CNM (CSIC), Campus UAB, Bellaterra, Spain

[2] Centro de Investigación Biomédica en Red de Bioingeniería, Biomateriales y Nanomedicina, Spain

[3] UNESCO Chair in Life Cycle and Climate Change, Escola Superior de Comerç International (ESCI-UPF), Pg. Pujades 1, 08003 Barcelona, Spain

[4] Advanced Biomaterials and Nanotechnology, University of Girona, Maria Aurèlia Capmany 61, 17003 Girona, Spain

[5] Institut de Química Avançada de Catalunya, IQAC-CSIC, C/ Jordi Girona 18–26, 08034 Barcelona, Spain

[6] Departament d'Enginyeria Mecànica, Universitat Rovira i Virgili (URV), Av. Països Catalans, 26, 43007, Tarragona, Spain

Aleix.marti@imb-cnm.csic.es

Keywords: electrocardiography, cellulose, PEDOT, sustainable electrodes, biodegradability.

Electrocardiography (ECG) is widely used for cardiovascular monitoring, but conventional disposable electrodes generate environmental burdens due to their multi-material composition and limited end-of-life options [1]. This work presents a paper-based ECG electrode as a more sustainable alternative to conventional Ag/AgCl electrodes. The proposed design combines a cellulose substrate with PEDOT as the conductive component while maintaining a conventional configuration compatible with standard ECG connectors and recording systems.

The developed electrode was characterized in terms of its electrical, electrochemical, mechanical, and skin–electrode interfacial properties, and its performance was evaluated through three-lead ECG recordings in comparison with a commercial electrode. The optimized electrode showed a sheet resistance of 52.1 Ω/sq and stable open-circuit potential values close to 0 V at the hydrogel–skin interface. Impedance measurements on skin showed values comparable to those obtained with the commercial reference, with both electrodes reaching approximately 65 kΩ at 10 Hz. ECG recordings from three subjects showed comparable waveform morphology and amplitude, with similar signal-quality performance between both electrodes. The environmental performance was assessed through life-cycle assessment of the complete electrode, showing a 35% reduction in carbon footprint compared with the commercial Ag/AgCl electrode. In addition, regulated biodegradability testing showed that almost all tested components exceeded 60% biodegradation within the first days, while the remaining components reached this threshold before 40 days. These results demonstrate the potential of conductive cellulose-based materials to replace conventional sensing components in disposable ECG electrodes while maintaining functional performance and improving their environmental and end-of-life profile.

(1) H. Wu, G. Yang, K. Zhu, S. Liu, W. Guo, Z. Jiang, Z. Li. *Materials, Devices, and Systems of On-Skin Electrodes for Electrophysiological Monitoring and Human–Machine Interfaces*. Advanced Science, 8, 2001938 (2021).

Ultrathin Al_2O_3 Encapsulation for Scalable, Long-Term-Stable van der Waals Quantum Devices

Fereshteh Masoudinia[1], Gervasi Herranz Casabona, Gyanendra Singh

[1]*Laboratory of Multifunctional Oxides and Complex Structures (MULFOX), Institut de Ciència de Materials de Barcelona (ICMAB-CSIC), Campus UAB, 08193 Bellaterra, Barcelona, Spain*

fmasoudinia@icmab.es

Keywords: van der Waals heterostructures; air-sensitive materials; oxide encapsulation; Ising superconductivity; anomalous Hall effect

Van der Waals (vdW) heterostructures offer a versatile platform for combining superconductors, ferromagnets, and insulators without lattice-matching constraints, but many technologically relevant vdW materials such as the superconductor $NbSe_2$ and the itinerant ferromagnets Fe_3GeTe_2 and Fe_3GaTe_2 degrade rapidly in air. While hexagonal boron nitride (hBN) is the standard encapsulant, it requires the entire device stack to be assembled inside a glovebox, limiting scalability. Here we present an exposure-minimized Al_2O_3 encapsulation strategy in which a single flake is exfoliated and capped with a 10 nm oxide layer immediately after exfoliation, confining glovebox handling to this initial step alone and enabling standard, wafer-compatible photolithography for the remainder of the fabrication process. We test this strategy across four materials with markedly different physics. For $NbSe_2$, encapsulated Hall-bar devices show sharp superconducting transitions and a thickness-dependent upper critical field consistent with Ising superconductivity, unchanged after eight months of ambient storage. For Fe_3GeTe_2, the anomalous Hall effect reveals robust ferromagnetic hysteresis together with a bulk-like resistive anomaly at the Curie temperature rarely reported in exfoliated devices, while Fe_3GaTe_2 retains a clear anomalous Hall signal up to nearly 350 K. In contrast, superconductivity in Al_2O_3-capped BSCCO is strongly suppressed or absent, in stark contrast with an hBN-capped reference device (Tc ≈ 90 K), because superconductivity in this cuprate is set directly by the oxygen stoichiometry of the CuO_2 planes [1], which the oxide interface disturbs. These results establish a practical design rule: ultrathin Al_2O_3 encapsulation is a scalable, wafer-compatible alternative to hBN for metallic van der Waals materials, but is unsuitable for oxygen-sensitive cuprate superconductors, for which encapsulant choice must instead be matched to the chemistry of the material being protected.

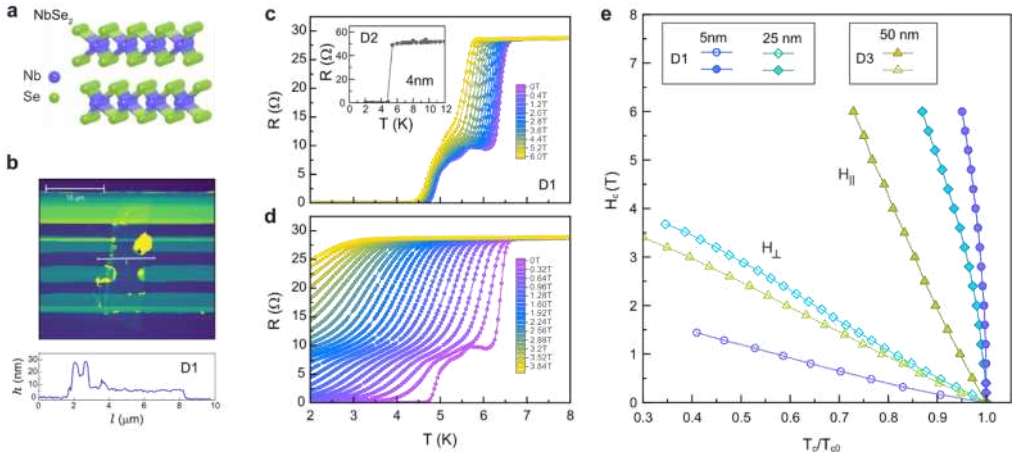

Figure 1: Al_2O_3-encapsulated $NbSe_2$ Hall-bar device. **a.** Crystal structure. **b.** AFM image showing coexisting 5 and 25 nm-thick regions. **c–e.** Thickness-dependent superconducting transitions and upper critical field, $Hc_2(T)$, consistent with Ising superconductivity.

(1) Lee, P. A.; Nagaosa, N.; Wen, X.-G. Doping a Mott Insulator: Physics of High-Temperature Superconductivity. Rev. Mod. Phys. 2006, 78, 17–85.

2026 JPhD 10th edition

Growth rate dependence on nucleation, microstructure and vortex pinning in TLAG REBCO films

O. Mola-Bertran[1], C. Torres[1], M. Voulhoux[1], V. Fuentes[1,2], E. Ghiara[1], V. Bertini[1], E. Pach[1,2], K. Gupta[1], R. Vlad[1], C. Pop[1], E. Solano[2], L. Simonelli[2], J. Gutierrez[1], X. Obradors[1], T. Puig[1]

[1]*Institut of Materials Science of Barcelona, ICMAB-CSIC, Campus UAB, 08193 Bellaterra, Barcelona, Spain*

[2]*ALBA Synchrotron, 08290 Bellaterra, Barcelona, Spain*

omola@icmab.es

Keywords: REBCO superconductors, growth rate, thin films, defect microstructure, vortex pinning, Transient Liquid Assisted Growth (TLAG)

Nowadays, REBCO production is limited by high costs and increasing demand. The high-throughput growth technique Transient Liquid Assisted Growth (TLAG) [1-3] addresses both challenges, as it enables lower-cost production compared to conventional REBCO growth techniques and achieves ultrahigh growth rates while maintaining high critical current densities [4]. In TLAG, a Ba-Cu-O transient liquid dissolves the rare earth element, enabling rapid REBCO crystallization over a wide range of oxygen partial pressures (P_{O2}) and temperatures. This work investigates the impact of growth rate on nucleation, crystal growth, defect microstructure, and vortex pinning in TLAG films. In-situ resistivity measurements are used to determine the growth rate, revealing a clear correlation between higher growth rates and increased P_{O2} and temperature, with values ranging from 10 to 5000 nm/s for RE = Y, Er. Nucleation and growth mechanisms under different conditions are further analyzed by correlating in-situ resistivity with in-situ XRD and XAS measurements at the ALBA Synchrotron. TEM analysis show that higher growth rates produce a cleaner microstructure with less secondary phases and porosity and increased number of twin boundaries. Transport measurements reveal enhanced pinning at high magnetic fields and low temperatures for samples grown at higher P_{O2}.

(1) Soler, L. et al., Nat Commun 11, 344 (2020).
(2) Rasi, S. et al., Advanced Science 9, 2203834 (2022).
(3) Saltarelli, L. et al., Advanced Materials e10660 (2025).
(4) Puig, T.; Gutierrez, J & Obradors, X., Nat. Rev. Phys. 6, 132-148 (2023).

2026 JPhD 10th edition

Bacterial cellulose containing iron oxide nanocubes for magnetically-triggered oil separation membranes

Roger Morales-Pérez[1], Asier R. Muguruza[1], Anna Roig[1], Pablo Guardia[*1]

[1]*Institut de Ciència de Materials de Barcelona (ICMAB-CSIC), Campus UAB, Bellaterra, 08193, Spain*

Email of corresponding author: pguardia@icmab.es

Keywords: iron oxide nanoparticles, bacterial cellulose, magnetic hyperthermia, biocomposites.

Magnetic hyperthermia relies on a temperature increase generated by a heat mediator under an external alternating magnetic field [1]. Among magnetic nanoparticles, iron oxide nanoparticles stand out as heat mediators due to their excellent biocompatibility, non-toxicity, and potential for functionalization [2]. It has been reported that nanoparticle shape and size play a key role in the final heating efficiency, with 20-25 nm nanocubes showing the highest specific abortion rate (SAR) values [3]. Noteworthy, the use of nanoparticles for magnetic hyperthermia entails localized heating, which limits its implementation for large-area applications. However, attempts to create large areas of assembled nanoparticles often result in regions where nanoparticles form large aggregates, which limits their heating efficiency and spatial coverage for effective thermal treatment [4]. Bacterial cellulose (BC) could serve as an excellent substrate to overcome these limitations due to its unique characteristics: biocompatibility, high surface area, remarkable mechanical strength, water retention capacity, and facile functionalization [5]. While hyperthermia and BC have mostly been applied to the biomedical field, this work attempts to approach other possible applications focusing on environmentally significant issues, such as oil contamination in water caused in industries [6].

In this work, we present an approach for the functionalization of BC films with iron oxide nanocubes. The composition, microstructure and magnetic properties of the composite were analyzed, as well as its heating response under an alternating magnetic field. The iron oxide nanocubes completely cover the BC fibers leading to a BC composite showing excellent magnetic properties. Indeed, the produced magnetic BC composites show outstanding heating efficiencies under an alternating applied magnetic field. The resulting nanocomposites show limited lipophilicity at room temperature, not allowing the flow of oil through the membrane. However, when exposing the membrane to an alternating magnetic field; the local temperature of the membrane is raised and the lipophilicity of the material improves, increasing the flow of oil allowed and achieving water/oil separation.

[1] Jordan, A.; Scholz, R.; Wust, P.; Fak, H.; Felix, R. *J. Magn. Magn. Mater.* **1999**, 201, 413–419.

[2] Gupta, A.; Gupta, M. *Biomaterials*, **2005**, 26, 18, 2995-4021.

[3] Guardia, P.; Di Corato, R.; Lartigue, L.; Wilhelm, C.; Espinosa, A.; Garcia-Hernandez, M.; Gazeau, F.; Manna, L.; Pellegrino, T. *ACS Nano*, **2012**, 6, 4, 3080-3091.

[4] Jiang, C.; Mei Ng, S.; Leung, C. W.; Pong, P. W. T. J. Mater. Chem. C, **2017**, 5, 252-263.

[5] Meslier, T.; D'Antin, J. C.; Jlio, G.; Roig, A., *Adv. Healthcare Mater.*, **2025**, e02189.

[6] Teng, T.; Zhao, Y.; Yang, H.; Gao, Y.; Zhou, X.; Wang, G.; Guo, P.; Zhang, H. *Carbohydr. Polym.* **2026**, 389, 125665.

Development of Atomically precise Nanoporous Graphene Membranes for molecular filtration

Bushra Naz[1,2], Emigdio Chavez-Angel[1], Aitor Mugarza[1,3]

[1] Catalan Institute of Nanoscience and Nanotechnology (ICN2), CSIC and BIST, Campus UAB,

[2] Universitat Autònoma de Barcelona (UAB), Plaça Cívica, 08193 Bellaterra, Barcelona

Bellaterra, 08193 Barcelona, Spain

[3] ICREA − Institució Catalana de Recerca i Estudis Avançats, Pg. Lluís Companys 23, 08010

Barcelona, Catalonia, Spain

bushra.naz@icn2.cat

Keywords: Graphene, filtration, nanoscience, material science

Recent advancements have highlighted atomically precise nanoporous graphene (NPG), synthesized via a bottom-up scientific method [1], as a promising candidate due to its exceptional mechanical strength, chemical stability, and well-defined pore architecture. Unlike pristine graphene, which is impermeable to all molecules, this bottom-up synthesized NPG intrinsically contains uniformly distributed subnanometer pores that enable selective molecular transport, making it highly suitable for desalination applications. In this study, we report the development and evaluation of a NPG based membrane system for efficient desalination of saline water. The membranes were fabricated through on-surface synthesis, a bottom-up “Lego chemistry” approach in which molecular building blocks self-assemble to form atomically precise nanoporous graphene with uniformly distributed pores. The size, density, morphology, and chemical composition of these pores are controlled through the rational design of molecular precursors. The structural integrity of the resulting nanoporous graphene and the formation of the pore network were characterized using scanning tunneling microscopy (STM) and Raman spectroscopy. The synthesized nanoporous graphene was subsequently transferred onto silicon nitride (SiN) support membranes with a pore size of 300 nm to fabricate the final filtration membrane. The resulting system will be used to evaluate molecular transport across the nanoporous graphene layer for filter and sensor applications.

[1] Moreno, César, Manuel Vilas-Varela, Bernhard Kretz, Aran Garcia-Lekue, Marius V. Costache, Markos Paradinas, Mirko Panighel et al. Science 360.6385 (2018): 199-203

Fully Integrated pH-Triggered Microbatteries for Smart Bioelectronics via ALD-alumina Growth

Orlane Nicolardot[1], Sandra Perez-Jimenez[1], Julia Gonzalez[1], Jaume Esteve[1], Neus Sabaté[1], Ferran Pujol-Vila[1]

[1] *Institut de Microelectrònica de Barcelona (IMB-CNM, CSIC), Campus UAB, Bellaterra, 08193 Barcelona, Spain.*

orlane.nicolardot@imb-cnm.csic.es

Keywords: Microbatteries, Alumina, pH-triggered, bioelectronics, smart-devices.

Biological systems feature dynamic chemical microenvironments characterized by pH variations that signal critical physiological or pathological processes *(e.g.*, bacterial activity, tumour acidosis or metabolic shifts). *[1][2]*

On the other hand, conventional microbatteries (MBs) are the cornerstone of autonomous bioelectronic microsystems, but lack the intelligence required for tailored adaptive actions in response to these variations. In general terms, electrochemical MBs begin operating upon contact with fluids, being unable of environmental adaptation and spaciotemporal control. Herein, a novel aluminum-platinum (Al-Pt) microbattery, engineered with an atomic layer deposited (ALD) alumina (Al_2O_3) layer to govern pH-triggered electrochemical activation, is introduced (**Figure 1a**).

Results demonstrate that ALD-Al_2O_3-coated MBs exhibit intrinsic responsiveness to pH changes, functioning as adaptive switches, i.e., they remain fully passivated at physiological pH 7.4 and "switch on" only under acidic (pH 1.5) or alkaline conditions (pH 13) reaching **current density up to 72 µA/mm² and 61 µA/mm², respectively and within seconds** (**Figure 1b**). This pH-sensitive platform functions as biocompatible self-contained, sensor-free transducer. The fast, pH-dependent activation of these microbatteries enables autonomous, rapid and localized electrochemical sensing and modulation of biological environments, with potential applications in monitoring inaccessible sites, enabling localised interventions and developing bioelectrochemical interface for targeted therapies. *[3][4]*

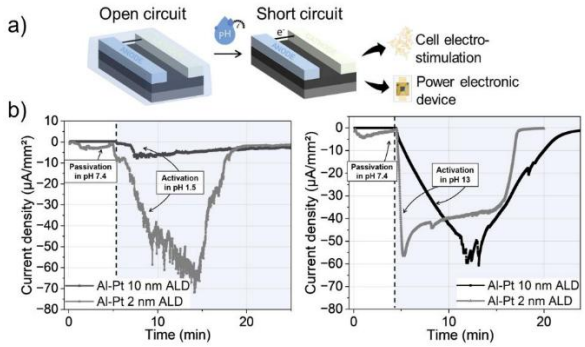

Figure 1: **a)** Simplified scheme of the pH-triggered ALD-Al_2O_3-coated MBs
b) Acidic (left) and alkaline (right) activation chronoamperometry at 0V for Al_2O_3-coated Al-Pt MBs during immersion in buffer at pH 7.4, followed by immersion in pH 1.5 or pH 13 solutions.

[1] Yamamura R, Inoue KY, Nishino K and Yamasaki S. Intestinal and fecal pH in human health. Front. Microbiomes. 2, 1192316 (2023).
[2] Hosonuma M, Yoshimura K. Association between pH regulation of the tumor microenvironment and immunological state. Front Oncol. 13, 1175563 (2023).
[3] Xiaoran Ding et al., Tumor microenvironment–activated Zn//MnO2 battery for sustained and local electrochemical immunotherapy. Sci. Adv. 11, eadu1647 (2025).
[4] Sunil K. Sailapu et al., Self-activated microbatteries to promote cell death through local electrical stimulation. Nano Energy 83, 105852 (2021).

Base-directed room-temperature synthesis of ultrasmall CeO_2 nanozymes: tuning properties and redox activity for MASH therapy

Ana Otero Bello[1], Endris Yibru Hanurry[1], Gregori Casals[2,3,4], Guillermo Fernández-Varo[2,3] Muling Zeng[1]

[1] *Insitut de Ciencia de Materiales de Barcelona (ICMAB)*
[2] *Biochemistry and Molecular Genetics Service, Hospital Clínic of Barcelona, University of Barcelona*
[3] *Centro de Investigación Biomédica en Red de Enfermedades Hepáticas y Digestivas (CIBERehd)*
[4] *Department of Fundamental and Clinical Nursing, Faculty of Nursing, University of Barcelona*

aotero@icmab.es

Metabolic dysfunction-associated steatohepatitis (MASH), the progressive form of metabolic dysfunction-associated steatotic liver disease (MASLD), is characterized by steatosis, inflammation, hepatocellular injury and fibrosis. Oxidative stress and redox imbalance are to the central drive of MASH progression, yet conventional antioxidant therapies are limited by poor bioavailability, rapid degradation, and insufficient liver targeting [1].

Cerium oxide nanozymes (CeO_2 NZs) offer a promising alternative through their regenerable antioxidant activity, mediated by reversible Ce^{3+}/Ce^{4+} cycling at oxygen-vacancy-rich surfaces [2]. CeO_2 NZs display superoxide dismutase- and catalase-like activities and have demonstrated reductions in lipid accumulation, oxidative stress and inflammation in hepatocyte and rodent models of fatty liver disease. Their catalytic activity is strongly influenced by particle size, Ce^{3+} fraction, surface species and colloidal stability, which are determined during synthesis. The base used to hydrolyze Ce(III) precursors is known to control ceria nucleation, growth and size distribution in sol–gel/hydrothermal routes [3]; however, its role in ultrasmall (<5 nm) CeO_2 prepared under mild aqueous conditions, where surface effects and adsorbed counter-ions become particularly relevant, remains poorly understood.

Here, we prepared ∽4nm CeO_2 NZs from $Ce(NO_3)_3{\cdot}6H_2O$ by a facile room-temperature aqueous route, using either an organic base, tetramethylammonium hydroxide (TMAOH), or an inorganic base, ammonium hydroxide (NH_4OH) [4], [5], while keeping all other parameters constant. The resulting nanoparticles were characterized in terms of size and morphology (TEM), crystal structure (XRD), colloidal stability (DLS), elemental composition (EDX, EELS) and surface Ce^{3+}/Ce^{4+} ratio (XPS), and their ROS-related catalytic activity was evaluated with the ABTS assay. This side-by-side comparison directly links the reaction medium to surface chemistry, defect structure and nanozyme performance (Figure 1). This work identifies the alkaline medium as a simple and inexpensive handle, requiring no heating, pressure or post-synthetic modification, to tailor the surface chemistry and catalytic behavior of ultrasmall CeO_2 NZs. The resulting synthesis-structure-activity framework supports the rational and scalable design of ceria nanozymes for MASH and other oxidative-stress-related diseases for the next steps.

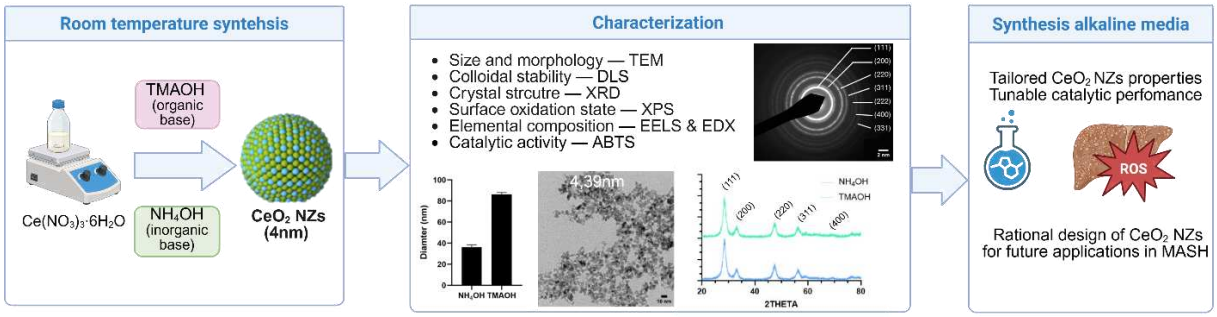

Figure 1. Synthesis–Property–Activity Relationship of Ultrasmall CeO_2 Nanozymes. *Schematic representation of the synthesis using TMAOH and NH_4OH and subsequent physicochemical and catalytic characterization.*

[1] Lu, H.; Huang, J.; Wang, Y.; Casals, E.; Casals, G.; Zeng, M. *Redox Biology*, 103933. doi: 10.1016/j.redox.2025.103933.
[2] Casals, E.; et al. *Small*, 1907322. doi: 10.1002/smll.201907322.
[3] Yeşil Acar, Z.; Asiltürk, M.; Arpaç, E. *Chem. Pap.*, 4927–4939. doi: 10.1007/s11696-022-02217-w.
[4] Zeng, M.; et al. *Nanoscale*, 14365–14379. doi: 10.1039/D3NR03524G.
[5] Parra-Robert, M.; et al. *Biomolecules*, 425. doi: 10.3390/biom9090425.

2026 JPh 10th edition

Design of Push–Pull Curcuminoids for Molecular Electronic Applications

Joseth Pachacama-Ruiz[1], Daniel Herrera[1], Esther Barrena[1] and Núria Aliaga-Alcalde[1,2]

1. Institutde Ciènciade Materials de Barcelona (ICMAB-CSIC), CarrerdelsTil.lers, 08193 Cerdanyoladel Vallès, Spain
2. 2. ICREA (InstitucióCatalanade RecercaiEstudisAvançats), PasseigLluísCompanys, 23, 08018 Barcelona, Spain.

pachacama@icmab.es

Keywords: Boron difluoride curcuminoids, push-pull molecules, optoelectronic properties, donor and acceptor moieties.

Recent advances in Materials Chemistry and Engineering have focused on organic π-conjugated systems that exhibit exceptional optoelectronic properties[1]. Among these architectures, push-pull molecules (D-π-A) are molecular architectures composed of electron donor units (D) and electron acceptor moieties (A) interconnected through a π-conjugated spacer. The excellent semiconducting properties of these molecules are directly from this structural configuration and the electronic features.

Boron difluoride curcuminoid systems (BF_2-CCMoids) are considered optimal materials to satisfy the above optoelectronic criteria. The main structure is derived from curcumin, a natural substance found in turmeric[2]. Upon coordination with BF_2 units, the CCMoid blackbone becomes more rigid and simultaneously, the acceptor capacity of this new segment drives significant variations in the optical gap. This modification allows the flow of electrons and tunes the light response for the creation of modern electronics[3]. BF_2-CCMoids exhibit notable properties including fluorescence, high photostability[4], with potential applications in bioimaging[5], sensing, optoelectronic devices[6], and organic light-emitting diodes[7].

Here, we report a new family of BF_2-CCMoids containing strong donor-acceptor conjugated molecules providing a set of extended push–pull electronic structures. We present their syntheses and a comparative analysis of their photophysical properties. Our results open up new possibilities for this novel family of organic semiconductor materials with potential application in sensing technologies.

[1] J. Kulh´anek, O.Pytela, et al. European Journal of Organic Chemistry 2021 (2021).

[2] Kocaadam, B., & Şanlier, N. *Critical reviews in food science and nutrition*, *57*(13), 2889-2895 (2017).

[3] B.Madhav, V.Anunanda, et al. Applied Physics 131 (2025).

[4] Bhuskute, Kaustubh R., Jiayi Fan, and Amandeep Kaur. Aggregate 131 (2025).

[5] Tavera-Hern´andez, Rosario, et al. ChemistrySelect 10 (2025).

[6] A. Felouat, A. D'Al´eo, and F.Fages. The Journal of Organic Chemistry 78 (2013).

[7] Kim, H. U., Kim, T., Kim, C., Park, T., and Sohn, S Dyes and Pigments 211 (2023).

2026 JPhD 10th edition

Correlative Multi-Edge MCR Analysis of Mn-Ni Evolution in Operando Layered Oxide Cathodes

Pol Pérez Quer, [1] Oleg Usoltsev, [2] Laura Simonelli [2] and Dino Tonti[1]

[1] *Institut de Ciència de Materials de Barcelona (ICMAB-CSIC)*

[2] *ALBA Synchrotron Light Facility*

pperez2@icmab.es

Keywords: Operando XAS · Multivariate Curve Resolution (MCR) · Multi-Edge Correlation · Charge Compensation · Layered Oxide Cathodes

Rechargeable batteries rely on chemical reactions in their electrode materials to store and release energy. Understanding these reactions is important for improving battery performance, but the changes occurring inside battery materials can be difficult to follow during operation. X-ray absorption spectroscopy (XAS), a technique that probes the chemical environment of specific elements, can provide this information. Previous work has shown that Multivariate Curve Resolution (MCR), a statistical method for separating complex combinations of species in experimental spectra into meaningful contributions, can be used to identify and follow different chemical environments in operando XAS (measurements performed while the battery is operating) [1]. Building on this approach, we combine operando XAS with MCR to investigate how the chemical environments of Mn and Ni evolve across different cathode materials.

We apply this approach to Mn and Ni in 14 different layered oxide cathode materials, covering a range of compositions, structures and Li- and Na-based batteries. By comparing how the Mn and Ni environments change during battery operation, we identify common patterns despite the differences between the materials. In particular, the analysis shows that the initial Ni environments can be separated into distinct groups, and that these groups are associated with different patterns of Ni evolution during cycling. This demonstrates that the initial chemical environment of Ni directly determines its subsequent behavior, and not other evolutions in its surroundings.

The correlation between evolutions of Mn and Ni also reveals two recurring patterns across the cathode materials: a continuous, approximately linear evolution and a stepwise evolution in which Mn-associated changes precede significant Ni changes. While a deeper understanding of the solid state chemistry of these materials is underway, these results show how combining operando spectroscopy with statistical analysis can help classify chemical environments and identify common behavior across diverse battery materials.

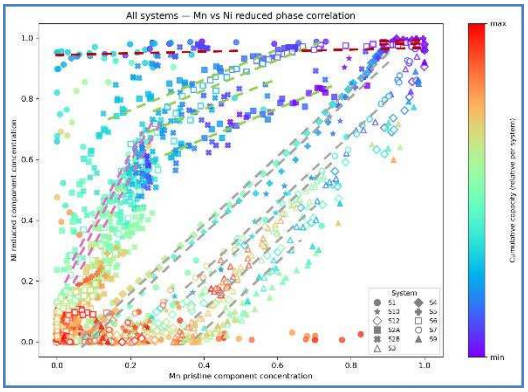

Figure 1: Figure captions should be below the figure.

(1) Oleg Usoltsev et al., Operando multi-edge XAS to reveal the effect of Co in Li- and Mn-rich NMC Li-ion cathodes, Materials Today Energy Volume 50, June 2025, 101853.

2026 JPhD 10th edition

Applying graphene solution-gated field-effect transistors (gSGFETs) for the detection of MUC1-specific antibodies tumoral biomarkers.

Sandra Pérez-Jiménez[1], Sergi Brosel-Oliu[1,2], Xavi Illa[1,2], Anton Guimerà-Brunet[1,2], Fayna García-Martin[3], Elisabet Prats-Alfonso[2,1]

[1]*IMB-CNM, C/ dels Til·lers. Campus UAB, 08193 Cerdanyola del Vallès, Spain*
[2]*CIBER BBN, Instituto de Salud Carlos III, 28029 Madrid, Spain*
[3]*IQUR, UR, Complejo Científico Tecnológico*
C/ Madre de Dios, 53, 26006 Logroño, La Rioja, Spain

Sandra.perez.jimenez@imb-cnm.csic.es

Keywords: graphene field-effect transistor; biosensing; MUC1; anti-MUC1; peptide functionalization; tumoral biomarkers

The ongoing development of personalized and precision medicine is driving the demand for rapid and decentralized detection of disease-associated molecular signatures, motivating the development of biosensors that directly translate molecular recognition into electrical signals. Among these, graphene solution-gated field-effect transistors (gSGFETs) enable label-free sensing with small sample volumes and potential multiplexing by translating molecular interactions at the graphene–liquid interface into electrical responses [1,2]. However, reliable detection depends on controlling the graphene–biomolecule interface, as the functionalization strategy influences recognition and coupling to electrical transduction. This is particularly relevant to cancer applications, where circulating molecular signatures could support early and minimally invasive diagnosis. Mucin 1 (MUC1) is a cancer-associated biomarker whose altered expression and glycosylation can promote the generation of circulating MUC1-specific antibodies (anti-MUC1), providing a potential serological molecular signature [3]. In this work, we investigated how graphene–peptide interface architecture affects the electrical detection of anti-MUC1. A MUC1-derived peptide previously shown to contain an epitope recognized by anti-MUC1 was used as the recognition element [4]. Two functionalization strategies were compared: an indirect graphene–PBASE–peptide architecture using PBASE, and a direct approach using a Fmoc-modified peptide immobilized on graphene through π–π interactions [5]. The variations in the charge neutrality point (CNP) were monitored as the main electrical parameter. Additionally, PBS and non-specific anti-IgG were used as controls. Both strategies produced concentration-dependent negative CNP shifts upon anti-MUC1 exposure, consistent with antibody–peptide recognition, with the PBASE-mediated interface showing a response distinguishable from PBS and anti-IgG, while the direct Fmoc-based interface yielded a comparable anti-MUC1 response with partial overlap with anti-IgG, indicating some non-specific contribution. These findings highlight the graphene–peptide interface as a key determinant of antibody detection specificity and support gSGFETs for sensing cancer-associated molecular signatures, while motivating further optimization of the simplified Fmoc-based strategy to improve specificity without an intermediate linker.

(1) R. Forsyth et al., Diagnostics, 7(3) (2017) 45.
(2) Q. Zhang et al., Adv. Sci., 11(39) (2024) 2401796.
(3) A. Montero-Calle et al., Front. Immunol., 15 (2024) 1455602.
(4) P. A. Guillen-Poza et al., J. Med. Chem., 63(15) (2020) 8524–8533.
(5) S. Brosel-Oliu et al., Small, 20(18) (2024) 2308857.

Development of an SPR biosensor for detection of Candida albicans virulence-associated biomarkers

Piotr Poręba[1], Mari Carmen Estévez[1]*, Laura M. Lechuga[1]

[1]*ICN2 – Institut Català de Nanociència i Nanotecnologia, Universitat Autònoma de Barcelona, Bellaterra, Spain*

Speaker Email: piotr.poreba@icn2.cat mcarmen.estevez@icn2.cat

Corresponding author Email: mcarmen.estevez@icn2.cat

Keywords: *Candida albicans*; Als3; Hwp1; surface plasmon resonance; biosensor; invasive candidiasis; multiplex detection

Invasive candidiasis remains a major clinical challenge, particularly in critically ill and immunocompromised patients, while current diagnostic approaches can be slow and may not adequately distinguish invasive infection from colonisation. Here, we investigated a surface plasmon resonance (SPR)-based biosensing approach for the detection of immune responses against two *Candida albicans* hypha-associated virulence proteins, Als3 and Hwp1.*C. albicans* ATCC 10231 was differentiated into yeast, pseudohyphal and hyphal morphotypes, followed by sequential protein extraction and ELISA characterisation of native Als3 and Hwp1 immunoreactivity. Recombinant Als3 and Hwp1 were subsequently used to characterise antibody recognition and concentration-dependent responses. SPR surface chemistry and immobilisation conditions were systematically optimised, followed by evaluation of nonspecific serum interactions and antifouling strategies. Both singleplex and multiplex SPR configurations were successfully established. Concentration-dependent responses were obtained for both target-specific antibody interactions, with detection limits in the ng/mL range. An ex situ immobilisation strategy was developed to enable preparation of functionalised sensor chips prior to integration into the multiplex platform. Simultaneous immobilisation of Als3 and Hwp1 bioreceptors on the same sensor enabled detection of the corresponding antibody responses while maintaining limited cross-reactivity. Overall, these results demonstrate the feasibility of using Als3- and Hwp1-targeted SPR sensing for the detection of *C. albicans*-associated immune responses and establish the technical basis for further validation using clinical samples. The developed approach represents a step towards rapid, label-free and multiplexed detection of biomarkers associated with invasive candidiasis.

Novel materials for the development of organic phototransistors for NIR detection

Nerea Río-Grela[1], Marta Mas-Torrent[1], Esther Barrena-Villas[1]

[1]*Institut de Ciència de Materials de Barcelona (ICMAB-CSIC), Bellaterra, Spain*

***Email**: nriogrela@icmab.es*

Keywords: organic field-effect transistors, near-infrared photodetectors, charge-transfer complexes, co-crystals

Organic phototransistors are appealing devices for the fabrication of low cost, light-weight and highly sensitive photodetectors. Upon absorption of incident light by the organic semiconductor (OSC), Frenkel excitons, consisting of bound electron–hole pairs, are generated [1]. These excitons can either recombine or dissociate into free charge carriers, which can modify the conductivity of the transistor channel, leading to an increase in the drain current and, consequently, an enhanced electrical signal.

The wavelength range to which the organic phototransistor responds is determined by the optical absorption properties of the OSC, particularly its optical bandgap. The optical bandgap is related to the energy difference between the highest occupied molecular orbital (HOMO) and the lowest unoccupied molecular orbital (LUMO). Since most OSCs predominantly absorb UV and visible light, narrowing the optical bandgap is an effective strategy to extend their absorption capabilities into the near-infrared (NIR).

Co-crystals, formed through the combination of charge donating and charge accepting materials, are a promising approach to modifying the electronic and optoelectronic properties of OSCs [2]. The intermolecular interactions within these materials can give rise to properties that are absent in the parent compounds, such as the polarity and extended optical absorption, the latter potentially enabling NIR absorption.

In this study, we aim to fabricate donor–acceptor co-crystals for NIR photodetection and evaluate their potential for application in organic phototransistors. Their morphology, electrical properties and optical absorption are investigated using complementary characterization techniques, including Kelvin probe force microscopy (KPFM), atomic force microscopy (AFM) and optical spectroscopy.

[1] Huang, X.; Ji, D.; Fuchs H.; Hu, W.; Li, T. ChemPhotoChem 4, 9-38 (2020)

[2] Dar, A.; Rashid, S. CrystEngComm 23, 8007-8026 (2021)

Mimicking lymph node 3D architecture in a microfluidic platform

Rodríguez A.R.[1,2], Marrero D.[3,4], Villa R[3,4]., Alvarez M[3]., Guasch J.[1]

[1]Institut de Ciència de Materials de Barcelona (ICMAB-CSIC), Campus UAB, Bellaterra 08193, Spain; [2]Universidad Autónoma de Barcelona (UAB), Bellaterra, 08193, Barcelona, Spain; [3]Instituto de Microelectrónica de Barcelona (IMB-CNM, CSIC), Campus UAB, Bellaterra, 08193, Barcelona, Spain.; [4]Centro de Investigación Biomédica en Red en Bioingeniería Biomateriales y Nanomedicina, Madrid, 50018, Spain

arodriguez2@icmab.es

Keywords: Cell biology, Microfluidics, 3D culture

Introduction

In vitro models have contributed significantly to advances in cell biology and oncology. In recent years, tissue engineering has progressed considerably, enabling the development of complex systems that mimic the extracellular matrix and cell–matrix interactions, producing 3D models capable of reproducing many tissue characteristics. Meanwhile, microfluidic systems have introduced the component of flow into cell culture, resulting in models that more closely represent physiological conditions. Combining both approaches yield a system consisting of a 3D artificial extracellular matrix subjected to flow generated by a peristaltic pump. In our case, we harnessed this potential to create a system that is inspired by the lymph nodes due to their interest in immunotherapy.

Aim

Engineering a 3D lymph node-on-a-chip under flow conditions for investigating healthy and oncologic cell behavior in a physiologically relevant environment.

Materials and Methods

An IOPAL PEG-heparin hydrogel was synthesized, following a previous protocol (1), and characterized by rheology and environmental scanning electron microscopy (ESEM). A microfluidic chip was also designed according to a prior publication (2) and operated with a pulsatile flow.Cellular responses were studied by flow cytometry and confocal microscopy.

Results

The hydrogel allows immune cells to infiltrate the scaffold, preventing them from being displaced by fluid flow. Cells cultured in the chip exhibited high viability compared to controls (cells in suspension and in hydrogel under static culture). Additionally, morphological changes were observed, reflecting adaptation to the flow conditions.

Conclusion

Our 3D platform allows to investigate healthy and oncologic immune cell behavior in a physiologically relevant microfluidic environment.

(1) Santos, F., Valderas-Gutiérrez, J., Del Río, E. P., Castellote-Borrell, M., Rodriguez, X. R., Veciana, J., ... & Guasch, J. (2022). Enhanced human T cell expansion with inverse opal hydrogels. Biomaterials science, 10(14), 3730-3738.

(2) Marrero, D., Guimera, A., Maes, L., Villa, R., Alvarez, M., & Illa, X. (2023). Organ-on-a-chip with integrated semitransparent organic electrodes for barrier function monitoring. Lab on a Chip, 23(7), 1825-1834.

Investigation of Electrolyte Composition and Solvation Chemistry for Improved SEI Stability in Sodium-Ion Batteries

Youssef Salhi, Deyana S. Tchitchekova, Alexandre Ponrouch
Institut de Ciència de Materials de Barcelona, ICMAB-CSIC,
Campus UAB, Bellaterra, 08193 Spain
ysalhi@icmab.es

Sodium-based batteries represent a sustainable and cost-effective alternative to lithium-based systems, particularly for large-scale energy storage. However, their widespread adoption is hindered by sodium's high reactivity, which accelerates electrolyte decomposition and results in an inherently unstable and soluble Solid Electrolyte Interphase (SEI) [1]. To mitigate this, strategic electrolyte design utilizing specialized salts, solvents, and film-forming additives is essential to engineering a more robust and insoluble SEI [2], [3].

In this study, we systematically investigate the impact of electrolyte formulation and ion solvation structure on the formation and stability of the SEI layer. By optimizing solvation environments to promote the generation of stable SEI products, we aim to enhance the electrochemical performance and lifecycle of sodium-based batteries. The formulated electrolytes are evaluated based on their transport properties, including ionic conductivity, density, and viscosity. Furthermore, the chemical composition and structural features of the resulting SEI are analyzed to assess its effectiveness in suppressing continuous electrolyte consumption and improving overall battery performance.

[1] D. I. Iermakova, R. Dugas, M. R. Palacín, and A. Ponrouch, “On the Comparative Stability of Li and Na Metal Anode Interfaces in Conventional Alkyl Carbonate Electrolytes,” *J. Electrochem. Soc.*, vol. 162, no. 13, pp. A7060–A7066, 2015, doi: 10.1149/2.0091513jes.
[2] R. Mogensen, D. Brandell, and R. Younesi, “Solubility of the Solid Electrolyte Interphase (SEI) in Sodium Ion Batteries,” *ACS Energy Lett.*, vol. 1, no. 6, pp. 1173–1178, Dec. 2016, doi: 10.1021/acsenergylett.6b00491.
[3] C. Li *et al.*, “Nonaqueous Liquid Electrolytes for Sodium-Ion Batteries: Fundamentals, Progress and Perspectives,” *Adv. Energy Mater.*, vol. 13, no. 40, pp. 1–21, 2023, doi: 10.1002/aenm.202301758

Silicon Microdosimeters for Hadron Therapy: Experimental Characterization and Monte Carlo Simulations

Andrea Sanchis[1], Ivan López-Paz[1], Carla Riera-Llobet[1], Celeste Fleta[1] and Consuelo Guardiola[1]

[1]*Centro Nacional de Microelectrónica (IMB-CNM, CSIC), Bellaterra, 08193, Spain*

andrea.sanchis@imb-cnm.csic.es

Keywords: radiation detectors, Hadron Therapy, Monte-Carlo simulations, microdosimeters

Particle therapy is becoming increasingly important in cancer treatment due to its ability to spare more the healthy tissues while maintaining tumour control, in comparison with conventional radiotherapy. The effectiveness of Hadron Therapy (HT) relies on the use of charged particles, such as protons or heavy ions, which present a high linear energy transfer (LET) and allow a more precise dose delivery to the tumour volume. As these advanced therapies evolve, accurate dosimetric and microdosimetic characterization of therapeutic beams and online dose monitoring becomes essential for treatment optimization and ensuring patient's outcome.

Microdosimetry enables the study of radiation effects at the micrometric scale, comparable to the dimensions of biological cells. The detailed study of the stochastic nature of energy deposition and the biological damage at the cellular level allows for the development of biologically optimized treatment plans. In this context, silicon microdosimeters have emerged as an alternative to the previous existing gas-filled tissue equivalent proportional counters, offering high spatial resolution, compactness and real-time operation, making them suitable for clinical environments**.**

This work presents the characterization and simulation of advanced silicon microdosimeters based on three-dimensional cylindrical detectors fabricated at the Institute of Microelectronics of Barcelona (IMB-CNM) [1]. These detectors are arranged in arrays of 3x3 unit cells of silicon microdetectors, each featuring a 25 µm diameter, a 20 µm thickness and a 100 µm pitch. These dimensions are optimized to allow operation at the intensities in particle therapy centres (~10^9 protons/s). Experimental measurements were carried out to evaluate the detector performance. In particular, the detector response when exposed to 3-14 MeV proton beams at National Centre of Accelerators (CNA, Spain) has been measured as a way to characterise the device. In parallel, the detector response was simulated using a Monte Carlo framework (Allpix Squared [2]), enabling the direct comparison with the experimental results.

Overall, the combined use of experimental characterization and simulations allow for a deeper understanding of the physical mechanisms involved in the detector's response. This study contributes to show the potential of these devices as microdosimeters for Hadron Therapy treatments and contributes to the ongoing development of detector technologies for advanced radiotherapy applications.

(1) C. Fleta et al 2015 JINST 10 P10001

(2) S. Spannagel et al., "Allpix2: A modular simulation framework for silicon detectors", Nuclear Instruments and Methods in Physics Research Section A, vol. 901, pp. 164-172, 2018, doi: 10.1016/j.nima.2018.06.020

Sustainable and Green Electronic Devices for Disposable Smart Patches

Manasa Sreerama[12], Eloi Ramon Garcia[12], David Castells Rufas[2]

[1]*Integrated Circuits and Systems Group (ICAS), Institute of Microelectronics of Barcelona (IMB-CNM, CSIC)*

[2]*Universitat Autonoma de Barcelona (UAB)*

Manasa.Sreerama@imb-cnm.csic.es

Keywords: Sustainable Electronics, Printed Electronics, Wearable sensors, Physiological Monitoring, Additive Manufacturing, Machine Learning, Deep Learning

The importance of green electronics is growing as current electronic trends face sustainability challenges. They use hazardous substances, consume large amounts of energy during production, and offer limited options for recycling. Many metal- and plastic-based products are often disposed of after a short usable life, significantly contributing to rising electronic waste (e-waste) and creating serious environmental problems (1).

In order to address these issues, we have developed flexible strain sensors that are capable of identifying physiological signals. A variety of geometries were selected for the initial design, including serpentine shapes incorporating different curve types, such as straight, triangular, sine, and square. These curves were designed in CorelDRAW to create masks for the screen-printing process. We crafted two screens to meet the study's requirements, each designated for a different biodegradable ink type, which includes the commercial copper ink (CopInk01NP) and silver ink (Sink01NP). These sensor configurations form the basis for investigating strain sensing approaches suitable for wearable and disposable applications. To explore the data-processing and classification component of the research, publicly available datasets, including NinaPro DB9, KINE-ADL BE UJI, and KIN-MUS-UJI, were analyzed. These datasets provide human-motion, posture, and hand-gesture information relevant to wearable sensing applications. Several machine learning and deep learning approaches, including Random Forest, XGBoost, Artificial Neural Networks (ANN), Long Short-Term Memory (LSTM), and Convolutional Neural Networks (CNN), have been investigated for classification. We evaluated their performance using accuracy, classification reports, and confusion matrices.

The overall objective of this research is to establish the framework that combines screen-printed strain-sensing with intelligent data processing for disposable smart patches. The ongoing experimental and computational work will contribute to the development of low-cost and potentially more sustainable wearable electronic devices for physiological and human-motion monitoring.

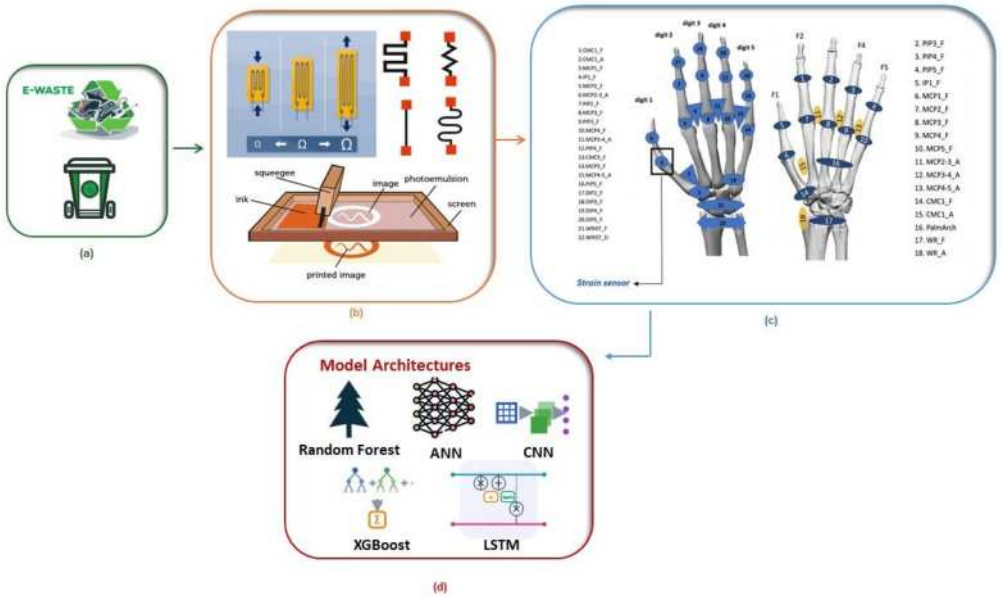

Figure 1 Graphical Abstract (a) Motivation (b) Screen-printed sensors (c) Implementation of sensors (d) Classification using ML/DL

(1) Guillemot, J.R.; Zhang, X.; Warner, M.E. Population Aging and Decline Will Happen Sooner Than We Think. Soc. Sci. 2024, 13, 190. https://doi.org/10.3390/socsci13040190

Tattoo electrodes for conformable biomedical applications

N. Termes-Español[1,2], A. Pascual-Valdunciel[3], Y. Castillo-Escario[2,4,6], E. Santamaría-Vázquez[5,6], R. Hornero[5,6], R. Jané[2,4,6], R. Villa[1,6], J. Ibáñez[3,6], A. Guimerà-Brunet[1,6], G. Gabriel[1,6]

[1] Institut de Microelectrònica de Barcelona, IMB-CNM (CSIC), Bellaterra, Spain

[2] Universitat Politècnica de Catalunya -BarcelonaTech (UPC), Barcelona, Spain

[3] Grupo BSICoS, I3A, Universidad de Zaragoza, IIS Aragón, Zaragoza, Spain

[4] Institute for Bioengineering of Catalonia (IBEC), Barcelona, Spain

[5] Biomedical Engineering Group, University of Valladolid, Valladolid, Spain

[6] Centro de Investigación Biomédica en Red en Bioingeniería, Biomateriales y Nanomedicina (CIBER-BBN)

Nuria.termes@i*mb-cnm.csic.es*

Keywords: tattoo electrodes, HD-sEMG, motor unit decomposition, electrophysiological monitoring

Abstract

High-density electrophysiological interfaces capable of maintaining conformal contact with moving skin are increasingly demanded for wearable biomedical applications. However, conventional gel electrodes and rigid HD arrays often compromise comfort, contact stability, and adaptability to anatomically complex regions. Here, we present an ultrathin screen-printed tattoo-electrode system (85 µm thick) for long-term electrophysiological monitoring and HD-sEMG. The system was fabricated using scalable screen-printing techniques on a stretchable thermoplastic polyurethane substrate and integrated silver/silver chloride sensing electrodes. Electrochemical characterization demonstrated low electrode-electrolyte impedance, while mechanical testing confirmed robustness under repeated bending. The system was evaluated in several physiological monitoring scenarios, including sleep bruxism assessment, respiratory monitoring, frontal EEG acquisition, and 32-channel HD-sEMG recordings. In particular, the proposed electrodes enabled successful motor unit decomposition in the first dorsal interosseous muscle, a challenging anatomical region for conventional HD-sEMG arrays [1,2]. These results support the use of ultrathin tattoo electrodes as a scalable and comfortable solution for advanced electrophysiological sensing, neuromuscular assessment, brain-computer interfaces, and home-based clinical monitoring.

[1] Y. Nishikawa et al., “Motor unit firing behavior of the first dorsal interosseous muscle,” Eur. J. Appl. Physiol., 2024.

[2] L. Bareket et al., “Temporary-tattoo for long-term high fidelity biopotential recordings,” Sci. Rep., 2016.

2026 JPhD 10th edition

Polarization-Controlled Multilevel Resistance States in Epitaxial Ferroelectric HfO_2 Films

Ye Tu, Ignasi Fina, Florencio Sánchez

[1]*Institut de Ciència de Materials de Barcelona (ICMAB-CSIC), Campus UAB, Bellaterra, 08193 Barcelona, Spain*

Abstract

Ferroelectric hafnia has attracted considerable interest because of its compatibility with CMOS technology. In metal-ferroelectric-metal junctions, polarization can modulate electrical resistance through interface-limited transport. Here, we investigate the thickness dependence of polarization-driven resistance modulation by electric field (electroresistance) in doped epitaxial HfO_2 films. In ultrathin films, the modulation is weak because of the limited polarization, making the overall electroresistance not sizeable. With increasing thickness, the polarization is enhanced, leading to a stronger resistive switching response and allowing to detect multilevel resistance states. In even thicker films, the resistance becomes extremely large and bulk-limited, while ferroelectric polarization vanishes, preventing the observation of electroresitance. A strong correlation between electroresistance and ferroelectric polarization further supports the dominant role of polarization switching and suggests only minor contributions from extrinsic effects. These results clarify the thickness window allowing large electroresistance driven by polarization switching in epitaxial HfO_2 films and therefore highlighting their potential for memory applications.

Key Words: Ferroelectric HfO_2, thin films, epitaxial

Template-Assisted Electrodeposition of FeMn Nanowires: Composition, Magnetic Properties, and Biodegradation

Carolina Ugarte-Pereyra[1]*, Luis Martínez Armesto[1,2], Alberto Quintana[1,2], Jordi Sort[1,2,3], Eva Pellicer[1]

[1] Departament de Física, Universitat Autònoma de Barcelona, Bellaterra 08193, Spain

[2] Catalan Institute of Nanoscience and Nanotechnology (ICN2), CSIC and BIST, 08193 Barcelona, Spain

[3] Institució Catalana de Recerca i Estudis Avançats (ICREA), Pg. Lluís Companys 23, Barcelona, Spain

carolina.ugarte@uab.cat

Keywords: *FeMn nanowires; electrodeposition; template-assisted synthesis; magnetic anisotropy; biodegradation.*

Magnetic nanowires (NWs) have attracted considerable interest in sensing, actuation, and biomedical technologies. Fe-based NWs combine high magnetic performance with tunable properties through alloying. Incorporating Mn is especially interesting for biomedical applications, as it can influence both the magnetic response and degradation behavior of Fe-based materials [1,2]. In this work, FeMn NWs were synthesized by template-assisted electrodeposition using Au-coated polycarbonate (PC) membranes. The NWs were deposited from an aqueous sulphate-chloride electrolyte in a three-electrode cell at a constant potential of −1.2 V vs. Ag/AgCl.

Scanning electron microscopy (SEM) showed homogeneous NWs with an average length of 4.11 ± 0.87 µm (Figure 1). Energy-dispersive X-ray spectroscopy (EDX) confirmed the incorporation of Mn and its homogeneous distribution within the nanowire population. Furthermore, HAADF-STEM combined with electron energy-loss spectroscopy (EELS) confirmed the simultaneous presence of Fe and Mn within individual NWs, supporting the formation of a FeMn alloy. Quantitative EELS analysis yielded a local composition of 76.5 at. % Fe and 23.5 at. % Mn.

The magnetic properties of the as-deposited NWs embedded in the PC template were subsequently investigated by vibrating sample magnetometry (VSM), with the magnetic field applied both parallel and perpendicular to the template surface. The resulting hysteresis loops revealed a preferential magnetic anisotropy along the NW axis, indicating an easy axis parallel to the nanowire length. This magnetic anisotropy is of particular interest for subsequent magnetic-guiding experiments.

Finally, the biodegradation behavior of the FeMn NWs was investigated by incubation in Hank's balanced salt solution at 37.5 °C for different periods of time. The evolution of the NWs during incubation provides insight into the influence of the FeMn composition on their degradation behavior and their potential suitability for transient biomedical applications.

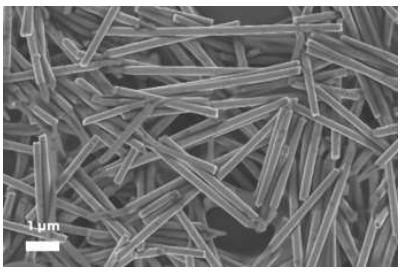

Figure 1: SEM images of FeMn nanowires

(1) Fernández-Barcia, M., Kurdi, S., Terzopoulou, A., Barber, Z. H., Hoffmann, V., Damm, C., ... & Gebert, A. (2019). Comparative study of the sustainable preparation of FeMn thin films via electrodeposition and magnetron co-sputtering. Surface and Coatings Technology, 375, 182-196.

(2) [2] Ogura, Y., Mori, H., Takigawa, Y., Uesugi, T., & Higashi, K. (2018). Fabrication of defect-free Fe–Mn alloys by using electrodeposition. Materials Transactions, 59(6), 935-938.

Growing Microneedles: Biolithography as a Growth-Directed Strategy for Fabricating Bacterial Cellulose Microneedles

G.Wetherell[1], L.Perez[1], A.Tuan[2], A.Mihi[1], J.Puigmartí[2], A.Roig[1]

[1] Institut de Ciència de Materials de Barcelona (ICMAB-CSIC), Campus UAB, 08193, Bellaterra, Spain

[2] Universitat de Barcelona

*gwetherell@icmab.es

Keywords: Bacterial Cellulose, Guided Assembly Biolithography, Micro Needles, Post-Synthesis Modifications

Transdermal delivery is limited by the stratum corneum, which reduces topical drug efficacy and confines effective drug administration to invasive hypodermic injection [1]. Microneedles (MNs) overcome this barrier through a minimally invasive, self-administrable skin-penetration route [2]. Bacterial cellulose (BC), a biomaterial with two decades of dermatological use, has never been fabricated as a microneedle, probably because conventional MN fabrication usually shapes a pre-formed material, whereas BC is synthesized *in situ* by living bacteria. We resolve this mismatch by guided assembly biolithography (GAB), a growth-directed strategy that uses a MN mold to template BC's native growth rather than shaping BC after synthesis [3]. Oxygen-permeable, micropatterned PDMS molds placed at the culture interface direct bacterial pellicle growth into microneedle geometries as it forms. This single-step, low-energy process yields the first reported BC-based microneedle array, generated entirely through guided biological self-assembly. Native BC-MNs are too soft to penetrate skin. We therefore developed three post-modification routes: biomineralized, sugar-glass, and sugar-immersed BC; and compared all four formulations for penetration, rehydration, and drug-release performance (Figure 1). Sugar-glass MNs showed the best performance overall. Together, these results establish biolithography as a scalable platform for growth-directed biofabrication of BC-Microneedles.

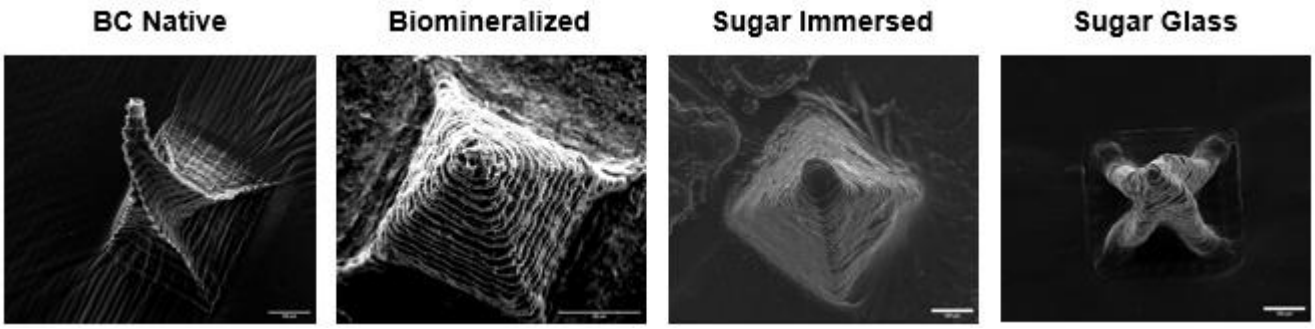

Figure 1. Bacterial cellulose (BC) microneedle arrays biosynthesized via guided assembly biolithography: native BC, biomineralized BC, sugar-immersed BC, and sugar-glass BC microneedles.

(1) Prausnitz, M. R.; Mitragotri, S.; Langer, R. *Nature Reviews Drug Discovery*, 3, 115-124 (2004).

(2) Henry, S.; McAllister, D. V.; Allen, M. G.; Prausnitz, M. R. *Journal of Pharmaceutical Sciences*, 87, 922-925 (1998).

(3) Bottan, S.; Robotti, F.; Jayathissa, P.; Hegglin, A.; Bahamonde, N.; Heredia-Guerrero, J. A.; Bayer, I. S.; Scarpellini, A.; Merker, H.; Lindenblatt, N.; Poulikakos, D.; Ferrari, A. *ACS Nano*, 9, 206-219 (2015).

One-pot room-temperature and microwave-assisted synthesis of $Ce_{1-x}Zr_xO_2$ NPs with enhanced ROS scavenging properties

Chuanli Zhang[1], Saúl Estandía[1], Huixia Lu[1], Jordi Faraudo[1], Juan Pellico[1], Anna Roig[1], Muling Zeng[1]*,

[1] Materials Science Institute of Barcelona (ICMAB-CSIC), Bellaterra, 08193, Barcelona, Spain

czhang@icmab.es

Keywords: CeO_2 nanoparticles; Zr doping; nanozymes; ROS scavenging; ABTS

Cerium oxide nano-enzymes have emerged as highly promising candidates for biomedical applications, offering superior stability, lower production costs, and enhanced environmental adaptability than natural enzymes. Their main advantage arises from their intrinsic redox activity, driven by reversible cycling between Ce3+ and Ce4+ oxidation states. [1] To further improve their antioxidant efficiency, Zr4+ doping has been employed to increase oxygen vacancy concentration and enhance redox performance. [2-3] However, there remains a lack of methodologies for synthesizing Ce1-xZr_xO_2 nanoparticles across different compositions to optimize and compare their reactive oxygen species (ROS) scavenging capabilities.
Here, we developed two simple and economical one-pot synthesis methods, room temperature (RT) and microwave-assisted (MW), to produce hydrophilic (RT) and hydrophobic (MW) Ce1-xZr_xO_2 nano-enzymes with different Ce:Zr ratios.[3-4] By controlling precursor ratios and fine-tuning parameters such as temperature, reaction time, and addition rate, we achieved different levels of Zr doping within the CeO_2 framework. Transmission electron microscopy (TEM) revealed average particle sizes of 3.9 ± 0.1 nm for RT-CeO_2 NPs (Fig. 1a). X-ray diffraction (XRD) analysis confirmed successful incorporation of Zr into the CeO_2 lattice through systematic peak shifts toward higher angles (Fig. c-d). The Ce^{3+}/Ce^{4+} valence states in ceria NPs and zirconium-doped ceria NPs were characterized using electron energy-loss spectroscopy (EELS) (Fig. b and f). Atomistic simulations based on the DFT-trained MACE-MP machine-learning potential were employed to investigate the effect of Zr doping on the stability of CeO_2 NPs (Fig. g). In Fig. h, ABTS radical scavenging activities for RT-CeO_2 and RT-CeZr-5/5 reached 40 ± 4% and 72 ± 4% respectively, indicating that Zr doping significantly enhanced the antioxidant activity. Future work will focus on encapsulation within PLGA nanoparticles for targeted liver disease.

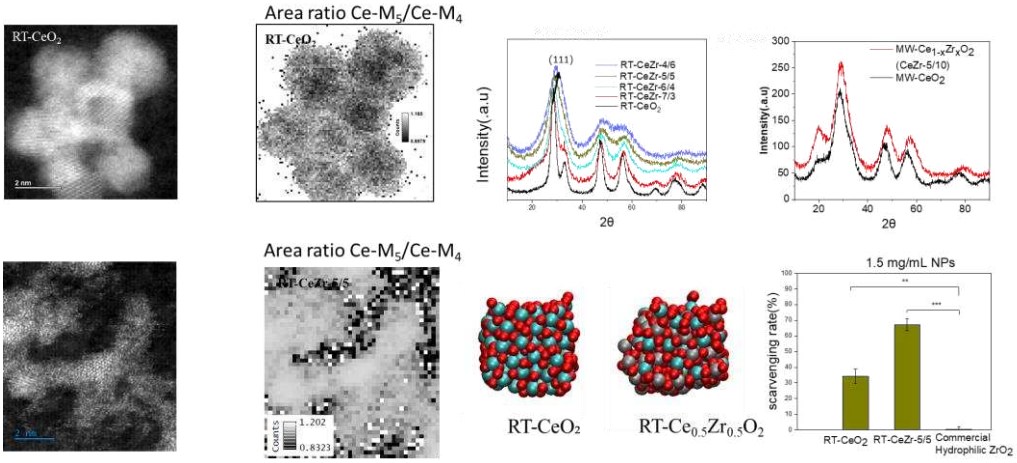

Figure 1. (a,b) TEM and EELS of RT-CeO_2; (c) diffraction of RT-CeO_2 and RT-$Ce_{1-x}Zr_xO_2$; (d) diffraction of MW samples; (e,f) TEM and EELS of RT-$Ce_{0.5}Zr_{0.5}O_2$; (g) theoretical calculations; (h) ABTS scavenging activity.

[1] Kim, Y.G., et al., Adv. Mater., 2024, 36, 2210819.
[2] Liu Y, Chen H, Chai L, et al. Sensors and Actuators B: Chemical, 2025, 437: 137709
[3] van Gent, J. and A. Roig, Nanoscale, 2023. 15(31): p. 13018-13024.
[4] Parra-Robert, M., et al. Biomolecules 2019, 9, 425.

Alkyl-Chain-Length and Packing Frustration Control of Single-Layer to Bilayer Polymorphism in Ph-BTBT-Cn Thin Films

Min Zhang[1], Alexandra Harbuzaru[1], Marta Mas Torrent[1]

[1] *Institut de Ciència de Materials de Barcelona, ICMAB-CSIC, Campus de la UAB, 08193 Bellaterra, Spain*

Email address: mzhang@icmab.es

Keywords:

Solution-processed molecular semiconductor thin films are highly sensitive to the molecular packing and polymorphic state, which in turn govern the performance and reproducibility of organic field-effect transistors. Here, we investigate the single-layer to bilayer transition in a homologous series of Ph-BTBT-Cn thin films, with n = 4-12, prepared by bar-assisted meniscus shearing. By combining thermal annealing, polymer blending, molecular mixing, and structural and electrical characterization, we establish alkyl-chain length as a molecular parameter governing the accessibility and stability of bilayer packing. Thermal annealing promotes coherent bilayer formation from Ph-BTBT-C6 onward, whereas Ph-BTBT-C4 undergoes vertical aggregation without stabilizing an ordered bilayer structure. Polymer blending with polystyrene improves film continuity and OFET performance, highlighting the importance of morphology optimization in addition to polymorphism control. Molecular mixing provides an additional route to tune vertical polymorphism via controlled packing frustration, yielding more reproducible device characteristics within specific chain-length mismatch and composition windows. Overall, these results show that efficient and reproducible charge transport requires the simultaneous optimization of vertical molecular packing and a continuous in-plane transport network, providing molecular-level design guidelines for controlling polymorphism in solution-processed molecular semiconductor thin films.

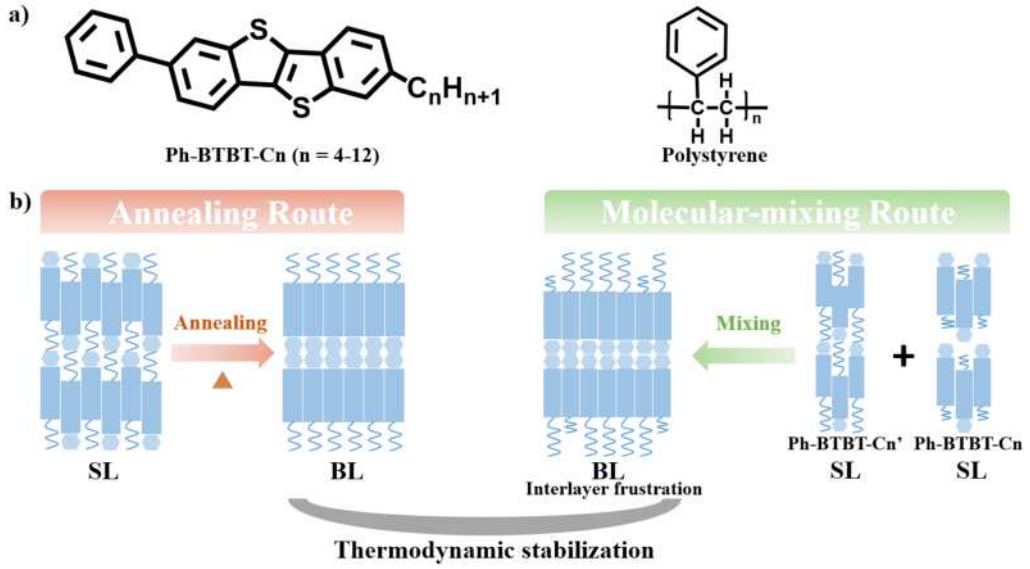

Figure 1: a) Molecular structures of the used organic semiconductors and binder polymer. b) Schematic illustration of the two pathways toward thermodynamic stabilization: the structural phase transition from single-layer to bilayer packing by the thermal annealing route (left), and the formation of a frustrated bilayer structure through the molecular mixing route of distinct Ph-BTBT derivatives (right).

(1) S. Inoue et al., Chem. Mater., 2015, 27, 3809–3812.

(2) S. Arai et al., Adv. Mater., 2018, 30, 1707256.

(3) G. Kitahara et al., Sci. Adv., 2020, 6, eabc8847.

Metal-Free Radical Dendrimersomes for Dual-Modal (MRI/Fluorescence) Imaging

Chuanting Zhou[1], Xuejiao Wang[1], Ehsan Shirdel[1], Vega Lloveras[1,2,*], José Vidal-Gancedo[1,2,*].

[1] Institut de Ciència de Materials de Barcelona, ICMAB-CSIC,Carrer dels Til.lers, , 08193 Cerdanyola del Vallès, Spain.

[2] CIBER de Bioingeniería, Biomateriales y Nanomedicina, Instituto de Salud Carlos III, 08913 Cerdanyola del Vallès, Spain.

chuantingzho@icmab.es

Keywords: Radical dendrimers, organic radicals, contrast agents, nanovesicles, MRI, OFI.

Dual-modality or multi-modality imaging has emerged as a powerful tool for enhancing the detection sensitivity and accuracy of disease diagnostic imaging technologies. Magnetic Resonance Imaging (MRI) and Optical Fluorescence Imaging (OFI) represent two complementary imaging modalities that do not utilize ionizing radiation.

This work introduces a Radical Dendrimer [1-6] precursor system: a PEG-Linear Dendritic structure fully functionalized with PROXYL organic radicals. This platform enables the spontaneous assembly of uniform and stable nanostructures (dendrimersome nanovesicles) simply upon dissolution in aqueous media. In addition, through the simple aqueous mixing of the radical dendrimer with fluorescent molecules we obtain nanovesicles that exhibit both magnetic and fluorescent properties, serving as a proof-of-concept for potential dual-modality MRI and OFI probe materials. We have successfully encapsulated both the hydrophilic Indocyanine Green (ICG) and the hydrophobic DiR' fluorescent probes in such nanovesicles. Through self-assembly, we have prepared nanovesicles containing varying concentrations of fluorescent molecules and characterized them using DLS, TEM or cryo-TEM, electron paramagnetic resonance (EPR), UV-Vis, fluorimetry, fluorescence optical microscopy, and MRI.

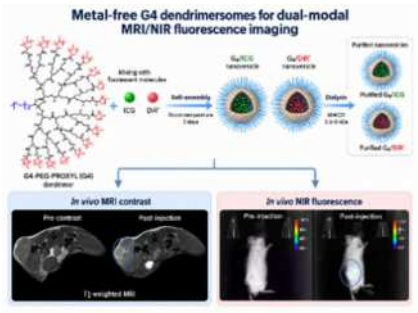

Significantly, this work not only demonstrates the successful assembly of dual-modal imaging nanomaterials but also highlights the potential of radical dendrimersomes as nanocarriers for the encapsulation of active molecules.

References

(1) S. Zhang, V. Lloveras, Y. Wu, J. Tolosa, J. C. García-Martínez, J. Vidal-Gancedo. Pharmaceutics, 2023, 15, 1776.

(2) Ch. Tian, S. Zhang, V. Lloveras, J. Vidal-Gancedo. Adv. Ind. Eng. Polym. Res. 2024, 7, 255-261.

(3) Y. Wu, V. Lloveras, A. Morgado, E. Perez-Inestrosa, E. Babaliari, S. Psilodimitrakopoulos, Y. Vida, J. Vidal-Gancedo. ACS Appl. Mater. Interfaces 2024,16 (47), 65295-65306.

(4) Y. Wu, V. Lloveras, S. Lope-Piedrafita, M. Mulero-Acevedo, A.P. Candiota, J. Vidal-Gancedo. Acta Biomaterialia 2025,192, 461-472.

(5) Y. Wu, V. Lloveras, S. Zhang, J. Tolosa, J. C García-Martínez, J. Vidal-Gancedo. Dyes Pigm. 2025, 232, 11248.

(6) S. Zhang, V. Lloveras, Y. Wu, J. Vidal-Gancedo. Eur. Polym. J. 2025, 235, 113691.

POSTER PRESENTATIONS

DFT/TD-DFT-Guided Molecular Design of Organic Semiconductors: From Attachment-Site Engineering to Excited-State Screening

Sana Abbas[1,2], Usman Ali[3], Abdessamad Tounsi[1]

[1] LGEEI, Faculty of Science and Technology, Sultan Moulay Slimane University, Beni-Mellal, Morocco

[2]Physics Department,Universidad Autónoma de Barcelona, 08193 Bellaterra, Spain.

[3]Department of Physics, University of Rome Tor Vergata, Rome, Italy

Email address: sana.abbas@usms.ma

Keywords: DFT/TD-DFT; Organic Semiconductors; Molecular Design; Excited States; Charge-transport properties.

Organic semiconductors are attractive materials for optoelectronic and photovoltaic applications because their electronic and optical properties can be tuned through molecular design. In our research work, we are using density functional theory (DFT) and time-dependent density functional theory (TD-DFT) to examine how structural changes influence the electronic structure, excited-state behaviour and charge-transport properties of π-conjugated organic molecules. In our previous study, four isomeric A-D-A molecules based on a pentathiophene donor core and trimethylxanthine acceptor units were investigated by changing only the attachment positions of the acceptor groups. This structural variation produced clear differences in frontier molecular orbital energies, optical absorption, intramolecular charge transfer and charge-transport descriptors. Among the investigated structures, PTP-b_2-TMX showed the most red-shifted absorption with λ_{max} = 491.82 nm, a light-harvesting efficiency of 0.96 and a low hole reorganization energy of 0.30 eV [1], showing that the attachment position of donor and acceptor units can strongly influence molecular performance. Building on these results and on our recent work on DFT/TD-DFT approaches for small-molecule organic solar cells, the current research study extends the analysis to a new series of π-conjugated organic molecules [2]. The computational workflow includes functional benchmarking, ground- and excited-state geometry optimization, solvent effects, frontier orbital analysis, absorption and emission properties, natural transition orbitals, density of states and electron and hole reorganization energies. Based on our research, we can predict how relatively small structural changes can modify the electronic and excited-state properties of organic semiconductors. The combined DFT/TD-DFT approach therefore provides a useful way to understand structure/property relationships and to identify promising molecular structures before experimental synthesis and device fabrication.

[1] Abbas, S.; Hachlaf, B.; Ali, U.; El Ghazali, A.; Baila, F.; Tounsi, A. Computational and Theoretical Chemistry 1256 (2026) 115639.

[2] Abbas, S.; Ali, U.; El Ghazali, A.; Baila, F.; Tounsi, A. International Journal of Quantum Chemistry 126 (2026) e70273.

Synthesis of polymeric particles for applications in Positron Emission Particle Tracking (PEPT)

M.P. Agustín-Mahiques[1], A. Fàbregas-Niño[1], J. Pellico[1]*

[1] *Institute of Materials Science of Barcelona (ICMAB-CSIC), 08193 Bellaterra, Catalonia, Spain*

magustin@icmab.es

Keywords: Positron Emission Particle Tracking (PEPT), polymeric microparticles, PLGA, PLA, emulsion-solvent evaporation method, nuclear imaging

Positron Emission Particle Tracking (PEPT) is a nuclear imaging technique that allows the study of the flow dynamics of a given system with high spatio-temporal resolution using tracers based on single particles radiolabeled with positron emitters. Although promising, the use of PEPT in medical imaging has been hindered due to the lack of effective methods to develop single particle tracers with sufficient activity. Recent advances have enabled the tracking of inorganic particles (1) and living cells (2); however, these single-particle tracers have shown poor blood circulation, which remains a persistent limitation.

In this work, we have focused on the development of polymeric microparticles as potential candidates for PEPT due their biodegradability, biocompatibility and tunable mechanical properties that we hypothesize, will facilitate better integration within biological environments and prolong the circulation upon administration of a single radiolabeled particle. For that, we have optimized emulsion-solvent evaporation methods to synthesize two types of polymeric particles based on Poly(lactide-co-glycolide acid) (PLGA) and Poly(lactide acid) (PLA) polymers. The characterization of their physicochemical properties revealed homogeneous particles with spherical morphology (Figure 1 (A) and (B)) and sizes of 1.8 ± 0.5 µm for PLGA and 1.7 ± 0.5 µm for PLA (Figure 1C).

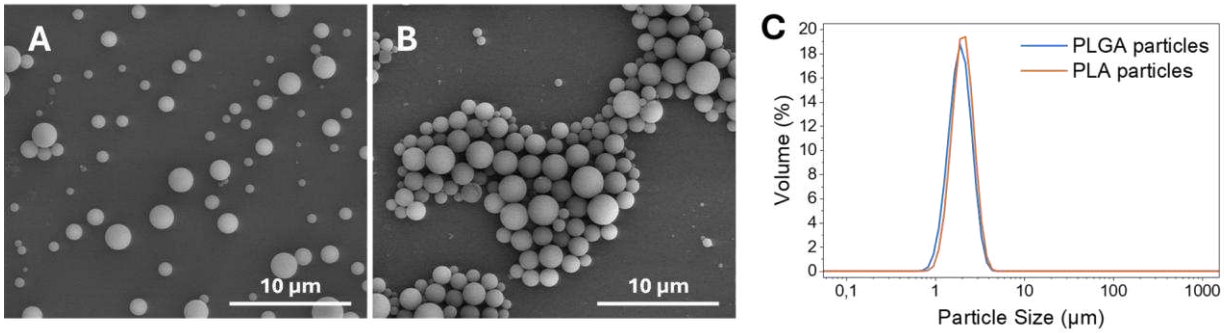

Figure 1. Scanning Electron Microscopy (SEM) images of (A) PLGA microparticles and (B) PLA microparticles. (C) Hydrodynamic diameter distribution for PLGA and PLA microparticles.

Overall, this work represents an important first step towards the development of single particle tracers based on polymeric materials with enhanced *in vivo* performance for PEPT, to ultimately enable the evaluation of blood flow dynamics.

(1) J. Pellico et al., Nature Nanotechnology, **2024**, 19, 668–676

(2) K.O. Jung et al., Nature Biomedical Engineering, **2020**, volume 4, 835–844

2026 JPh 10th edition

Catalytic nanotemplates for the direct growth of graphene nanoribbons

M. Àlava-Galarza, M. de la Vega, O. Muntada-López, J. Serrano, F. Pérez-Murano, I. Martin-Fernandez

Institute of Microelectronics of Barcelona (IMB-CNM, CSIC), Bellaterra, 08193, Spain

marck.alava@imb-cnm.csic.es

Keywords: graphene nanoribbons, chemical vapor deposition

Graphene nanoribbons (GNRs), the one-dimensional form of graphene, exhibit electronic properties, such as the appearance of a bandgap, that are highly dependent on their atomic structure, particularly their width and edge structure. Thus, they can display semiconducting behavior, making them promising candidates for future nanoelectronic and quantum devices. However, the integration of GNRs with simultaneous control over atomic structure, position, and orientation on a substrate still remains an outstanding challenge [1, 2]. Among the proposed alternatives, it has been reported that by fabricating a patterned catalyst template structure, the dimensions, position and orientation of the GNRs can be controlled in a chemical vapor deposition (CVD) growth [3]. However, GNRs in that work were 20 nm wide, above the estimated 10 nm width for the GNR to show a bandgap similar to that of Si (1.1 eV) [4].

The objective of this thesis is to provide solutions to the deterministic growth and integration of GNRs. Based on the work of reference [3], here we report the early stage fabrication of templates with an exposed catalyst section less than 10 nm wide. Our approach employs a multilayer sandwich architecture in which a catalytic thin film is confined between two non-catalytic materials (Figure 1a). The localized fabrication of the stacks on the wafer will allow to study catalyst confinement and to evaluate its potential for the direct CVD growth of GNRs (Figure 1b).

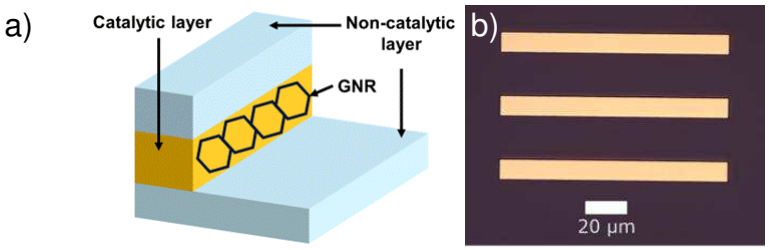

Figure 1: a) Design of the template platform, and b) Optical image of Ti/Au structures on a Si/SiO_2 wafer.

(1) J. Zhang et al., Nature Reviews Materials 11, 2026.

(2) X. Zheng et al., APL Materials, 14 (071108), 2026.

(3) I. Martin-Fernandez et al., Nano Letters 12 (12), 2012.

(4) M. Y. Han et al., Physical Review Letters 98 (206805), 2007.

Mitigating electronic limitations in Co_3O_4 via rational dopant integration for multifunctional sustainable energy applications

Ahmed Munawir Albarkani,[1] Ibrahim Hotan Alsohaimi,[2] et al.

[1] *Department of Chemistry, Faculty of Sciences, Autonomous University of Barcelona, 08193 Bellaterra, Spain*

[2] *Department of Chemistry, College of Science, Jouf University, Sakaka 2014, Saudi Arabia*

ahmed.albarkani@autonoma.cat

Keywords: Thin Films, Photocathode, Oxygen-Evolution Reaction, Solar Light Harvesting, Band Gap Alignment.

Cost-effective Co_3O_4 thin films, engineered via spray pyrolysis and rationally doped with Cu, Na, Cr, and Mo, exhibit exceptional bifunctional performance for sustainable energy conversion. Structural and spectroscopic analyses confirmed phase-pure spinel Co_3O_4, with dopants occupying specific lattice sites that finely tune the electronic structure and morphology. As oxygen-evolution reaction (OER) electrocatalysts, the optimized Cu, Na co-doped films exhibited a low Tafel slope of 69.2 mV·dec^{-1} and a specific activity of 2.94 mA·cm^{-2} at 350 mV, matching or exceeding noble-metal benchmarks. Strategic multielement doping induced pronounced bandgap narrowing (to 1.33/1.83 eV for Cu,Na, and 1.28/1.78 eV for Cr,Na, and Mo systems) and increased absorption coefficients (up to 1.1 × 104 cm^{-1}), thereby enhancing solar light harvesting. This band-structure engineering optimized the conduction-band alignment for water reduction, directly boosting photoelectrochemical hydrogen evolution. Remarkably, FeOx-passivated Cu,Na–Co_3O_4 photocathodes achieved a photocurrent of –106 μA·cm^{-2} at 0.024 V vs. RHE in alkaline media , five times higher than unmodified Co_3O_4 and attained without hetero-junctions or sacrificial agents. These results demonstrate that rational dopant integration in spray pyrolyzed Co_3O_4 effectively overcomes intrinsic electronic limitations, establishing a versatile, noble-metal-free platform for efficient electrocatalysis and solar-driven hydrogen production.

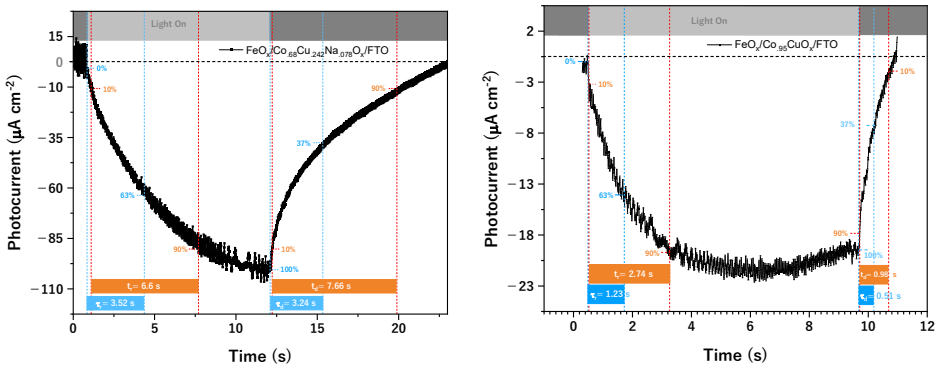

Figure 1. Photocurrent transient and corresponding semi-logarithmic plot in 1 M NaOH.

Reference:

[1] Ahmed Munawir Albarkani, Ibrahim Hotan Alsohaimi, Mosaed S. Alhumaimess, Meshal Alzaid, Qiao Chen, Mohammed A. El-Hashemy, Hassan M.A. Hassan, Electrochimica Acta, 2026, 549, 148085. https://doi.org/10.1016/j.electacta.2025.148085.

2026 JPh 10th edition

Co-Crystallization in Organic Thin Films for Tunable Near-Infrared Sensing

Georgios Atsas[1], Daniel Martin-Jimenez[1], Shunya Yan[1], Alba Cazorla[1], E. Solano[2], Esther Barrena[1]

[1][1]Institut de Ciència de Materials de Barcelona (ICMAB-CSIC), Campus UAB, Bellaterra, E-08193, Barcelona

[2]BL11-NCD-SWEET Beamline, ALBA Synchrotron Light Facility CELLS, Barcelona 08290, Spain

Email: gatsas@icmab.es

Keywords: charge-transfer complex, organic semiconductors, thin films, organic field-effect transistors, near-infrared absorption, GIWAXS

Charge-transfer complexes (CTCs) formed by the co-assembly of small conjugated molecules, typically an electron donor and acceptor, enable organic semiconductors with enhanced electrical and optical properties compared to their individual components, while avoiding complex synthetic routes [1–3]. Understanding and controlling co-crystallization in thin films is critical to exploit their properties in devices. Here, we investigate the formation of co-crystalline thin films comprising 2,7-bis(octyloxy)[1]benzothieno[3,2-b]benzothiophene (C8O-BTBT-OC8) and 1,3,4,5,7,8-hexafluoro-tetracyanonaphthoquinodimethane (F6TCNNQ) by sequential deposition of F6TCNNQ on C8O-BTBT-OC8 films, both vacuum sublimated. Grazing-Incidence Wide-Angle X-ray Scattering (GIWAXS) during acceptor deposition reveals the emergence and growth of the (001) Bragg peak associated with co-crystal formation. Atomic Force Microscopy (AFM) and Kelvin Probe Force Microscopy (KPFM) performed after acceptor growth confirms a morphological change in the films and an increase of the local work function. UV–vis spectroscopy demonstrates the formation of the CTC with a new absorption band in the near-infrared (NIR) absorption. We show that this approach is a viable strategy to grow uniform co-crystalline thin films, with potential application in NIR sensing applications

References:

(1) L. Sun et al. Adv. Mater. 31, 1902328 (2019).

(2) W. Wang et al. Chem. Eur. J. 27, 464 (2021)

(3) Y. Wang et al. Angew. Chem. Int. Ed. 57, 3963 (2018).

2026 JPhD 10th edition

Combined Enhanced Conformational Sampling and Protein-Ligand Dockings on CYP3A4 Improves in Silico Prediction of Drug Metabolism

Yassir Boulaamane[1], Christopher M. Baker[2], Lea Talmann[3], Jean-Didier Maréchal[1]

[1]*InSiliChem, Departament de Química, Universitat Autònoma de Barcelona, 08193, Bellaterra (Barcelona), Spain*

[2]*Syngenta, Jealott's Hill International Research Centre, Bracknell, RG42 6EY, UK*

[3]*Syngenta Crop Protection, Schaffhauserstrasse 101, 4332 Stein, Switzerland*

E-mail: yassir.boulaamane@uab.cat

Cytochrome P450 3A4 (CYP3A4) is the primary drug-metabolizing enzyme in humans. This is largely due to its highly flexible structure, which enables it to bind a broad spectrum of xenobiotics with a wide variety of shapes and physicochemical properties. This plasticity, however, presents challenges for in silico substrate prediction methods, in particular those that consider only a limited conformational space of the receptor or that rely on static crystal structures. In this study, we aim to explore the conformational landscape of CYP3A4 using Gaussian accelerated Molecular Dynamics (GaMD) and then to assess the viability of using this method to identify pro-reactive conformations through protein-ligand docking. GaMD simulations were initiated from distinct X-ray structures in triplicate 500 ns runs. The results demonstrate that the simulations cover a very large conformational space, including all reported X-ray structures as well as conformations with significantly expanded active-site geometries unseen in the experimental data. Protein-ligand docking of known CYP3A4 substrates onto the main cluster representatives from GaMD simulations allows the identification of metabolically active poses of the substrates. This is true even in cases where substrate-bound X-ray structures or docking against a single structure fails to yield productive results, as in the case of CYP3A4–Erythromycin. Furthermore, a classifier trained on ensemble docking scores discriminates CYP3A4 substrates from non-substrates better than any single conformation (ROC-AUC 0.735 vs 0.697), with performance increasing with ensemble size.

Overall, the study shows that enhanced conformational sampling is crucial for accurately modelling highly flexible enzymes like CYP3A4 and can significantly improve metabolic predictions.

Keywords: Cytochrome P450 3A4, Gaussian accelerated molecular dynamics, Ensemble Docking, Conformational sampling, Drug metabolism.

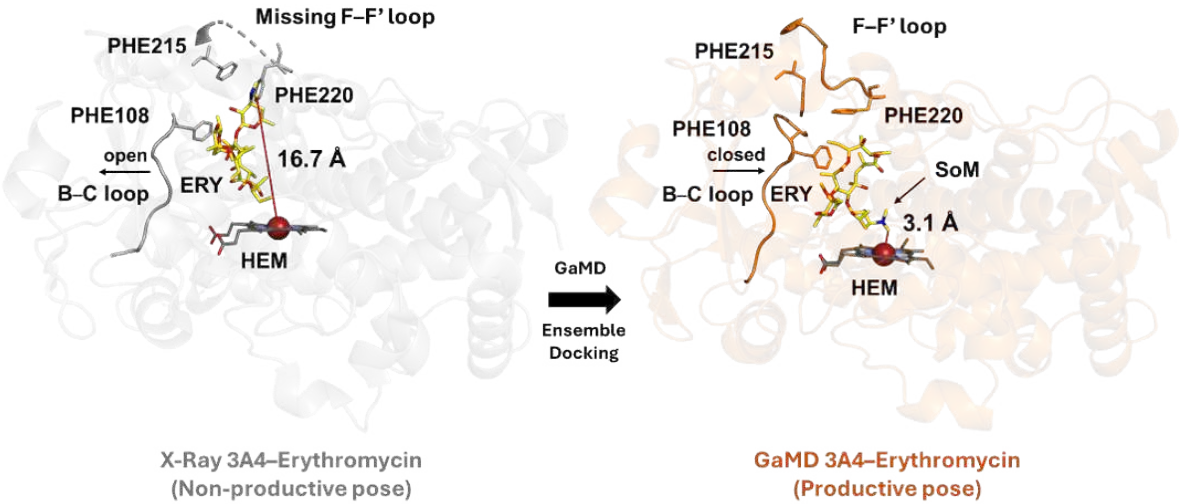

Phytoremediation and biomass valorization as a circular strategy: Recovering Copper from vineyards

C.Cazorla-Ares[1]; E.Cardo-Reyes[1]; J.Leiva[1,] I.H.Valido[1]; M.Valiente[1]; M.Llugany[2]; M.López-Mesas[1]

[1]*GTS Research Group, Department of Chemistry, Faculty of Science, Universitat Autònoma de Barcelona, Cerdanyola del Vallès, 08193 Barcelona, Spain.*

[2]*Plant Physiology Group (BABVE), Faculty of Biosciences, Universitat Autònoma de Barcelona, Cerdanyola del Vallès, 08193 Barcelona, Spain*

camila.cazorla@uab.cat

Keywords: Copper, Phytoremediation, plant tissue analysis, circular economy, soil contamination

One of the main threats affecting grapevine cultivation is downy mildew, a disease caused by *Plasmopara viticola* that primarily affects vine leaves. The long-term application of Cu-based fungicides has led to increasing Cu accumulation in vineyard soils. To mitigate Cu accumulation while avoiding excavation or chemical treatments, phytoremediation has been proposed as a sustainable alternative [1].

This study was structured into three main parts aimed at evaluating Cu behavior in different contexts, within the framework of a circular economy strategy. First, the potential of *Plantago lanceolata,* a promising candidate for phytoremediation [2], was assessed under controlled laboratory conditions by exposing plants to different Cu concentrations in both hydroponic nutrient solutions and universal substrate.

In parallel, a screening study involving 6 weed species commonly present in vineyards from Banyeres de Penedès was conducted to compare Cu accumulation patterns in native plants from ecological and conventional vineyards.

Finally, an incineration method for plant biomass was developed as a strategy for Cu recovery from harvested weeds. BCR and Tessier sequential extractions were conducted to the resulting ashes as an indirect speciation approach to support future Cu recovery and valorization strategies. In all cases, total Cu concentrations were analyzed by Inductively Coupled Plasma Mass Spectrometry (ICP-MS).

(1) V. Kumar et.al, Copper Bioavailability, Uptake, Toxicity and Tolerance in Plants: A Comprehensive Review, *Chemosphere* 2021, 262, 127810.

(2) J. Widmer, L. Norgrove, Identifying Candidates for the Phytoremediation of Copper in Viticultural Soils: A Systematic Review. *Environ. Res*. 2023, 216, 114518.

Engineering MIEC Oxide Thin Films for Low-Temperature Proton-Coupled Charge Storage

Chirag Chotai, Francesco Chiabrera, Alex Morata, Federico Baiutti, Albert Tarancon

Mixed ionic–electronic conducting oxides capable of reversible proton uptake are promising electrodes for low-temperature electrochemical energy storage. Understanding proton uptake, charge compensation, and electrochemical stability across different electrolyte environments is important for the development of proton-active oxide electrodes.

Here, $La_{0.6}Sr_{0.4}FeO_{3-}\delta$ (LSF40) thin films are investigated as a model proton-active perovskite electrode. Dense films with controlled thickness are prepared by pulsed laser deposition and characterized in acidic and alkaline aqueous electrolytes. Proton insertion coupled with electron transfer (PICET) is examined using cyclic voltammetry, coulometric titration, and galvanostatic cycling to evaluate reversible charge insertion, electrochemical stability, and electrolyte-dependent behavior. LSF40 exhibits reversible proton-coupled charge storage across different electrolyte environments, including stable operation under acidic conditions. Charge insertion reaches approximately 0.4 e^- per unit cell, corresponding to a volumetric capacity of approximately 314 mAh cm^{-3}.

These results establish LSF40 thin films as a model platform for investigating proton insertion and charge storage in MIEC oxides and provide a basis for integrating proton-active electrodes with solid-state proton-conducting electrolytes.

References

1. Tang, Y. *et al.* **ACS Appl. Mater. Interfaces** 14 (2022).

2. Zhao, B. *et al.* **Nano Lett.** 26 (2026).

3. Rocca, T. *et al.* **ACS Appl. Mater. Interfaces** 16 (2024).

4. Hwang, S. H. *et al.* **Int. J. Hydrogen Energy** 46 (2021).

5. Makivić, N. *et al.* **Chem. Mater.** 33 (2021).

Computational Insights into a Diels–Alder Rate Enhancement inside a $[Pd_6L_4]^{12+}$ Cage

I. Cuesta[1], G. Sciortino[1], G. Norjmaa[1] and G. Ujaque[1]

[1]*Departament de Química, Universitat autònoma de Barcelona, Cerdanyola del Vallès, Catalunya, Spain.*

Email: irina.cuesta@uab.cat

Keywords: Supramolecular Chemistry, Metallorganic cages, Computational Chemistry

Metallocages act as effective enzyme mimics, in which the interior cavity provides a environment capable of strongly modulating the reactivity of encapsulated substrates. A well-known case is the Diels–Alder reaction ocurring within the Fujita metallocage (Figure 1), which exhibits markedly faster kinetics tan in bulk solution. [1] To clarify the origin of this rate enhancement and the observed selectivity, a computational study combining molecular dynamics (MD) simulations and hybrid QM/MM was performed. [2]. MD simulations show that the cage is not a passive host, but actively promotes pro-reactive conformations. QM/MM calculations provide Gibbs energy profiles for the reaction in solution and inside the cage, allowing the contributions of confinement, microsolvation, and the metallocage framework to be separated. Comparison of the activation barriers obtained reveals the factors driving the catalytic acceleration are identified. Notably, the same approach reproduces the substrate-dependent behavior seen experimentally: upon encapsulation, the intrinsic barriers of the different dienes converge, so reactivity is governed only by conformational accessibility within the cavity.

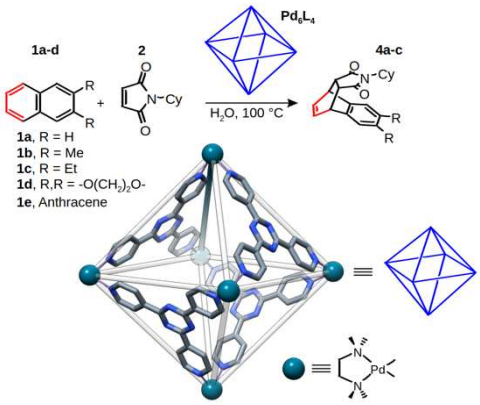

Figure 1: Diels-Alder reaction of naphthalene with maleimide within $[Pd_6L_4]^{12+}$ analyzed in this work.

(1) Takeda, N.; Umemoto, K.; Yamaguchi, K.; Fujita, M. Nature, 794-796.

(2) Sciortino, G.; Cuesta, I.; Norjmaa, G.; Ujaque, G. Inorganic Chemistry, 16163-16172.

Acknowledgment: Project PID2023-150881NB-I00 funded by AEI/10.13039/501100011033.

Spectroscopic and electrochemical characterization of compounds with UV-vis spectroelectrochemistry in reflection mode

Alessandra Cutillo-Foraster[1,2*], Julio Bastos-Arrieta[1,2], Núria Serrano[1,2], José Manuel Díaz-Cruz[1,2]

[1]*Department of Chemical Engineering and Analytical Chemistry, Universitat de Barcelona (UB), Martí i Franquès 1-11, 08028-Barcelona, Spain.*

[2]*Water Research Institute (IdRA), University of Barcelona (UB), Martí i Franquès 1-11, 08028- Barcelona, Spain.*

alessandra.cutillo@ub.edu

Keywords: UV-vis spectroelectrochemistry, spectroscopic characterization, electrochemical characterization

UV-vis spectroelectrochemical chronoamperometry in reflection mode is a technique within the field of spectroelectrochemistry (SEC) that enables the monitoring of changes in the UV-vis absorption spectrum of a compound upon the application of a constant potential for a defined period of time. These measurements are performed by combining an optical and electrochemical sensor, which in our case are a reflection probe and screen-printed carbon electrode (SPCE), respectively.

One of the main advantages of this technique is its ability to provide spectroscopic and electrochemical information simultaneously in a single experiment, while requiring a sample volume of less than 100 µL.

This makes the technique particularly attractive for the characterization of compounds electrochemically and spectroscopically active. In this work, UV-vis SEC was employed to characterize the spectroscopic behavior of different redox systems during electrochemical reduction and/or oxidation processes. The spectroscopic responses obtained during these processes were subsequently used for analytical studies (obtention of calibration curve and determination of analytical parameters) with the aim of assessing the feasibility of using this technique as an analytical tool[1,2,3].

(1) Ustabasi, S.; Bastos-Arrieta, J.; Pérez-Ràfols, C.; Serrano, N.; Díaz-Cruz, J.M. Microchemical Journal, 107678.

(2) Cutillo-Foraster, A.; Özbek, N.; Otero-de-Muller, Ll.; Bastos-Arrieta, J.; Serrano, N.; Díaz-Cruz, J.M. Microchemica Acta, 546.

(3) Cutillo-Foraster, A.; Özbek, N.; Bastos-Arrieta, J.; Serrano, N.; Díaz-Cruz, J.M. Talanta, 2026, 129768.

Benzanthrone-based photosensitizers for visible-light harvesting in solid-state molecular solar thermal systems and phase change materials

David B. Amabilino[1], David De Francesco

[1]*Institut de Ciència de Materials de Barcelona (ICMAB-CSIC), Campus UAB, 08193 Bellaterra, Spain*

dfrancesco@icmab.es

Keywords: photosensitizers; benzanthrone; molecular solar thermal storage; phase change materials; triplet energy transfer

Molecular solar thermal (MOST) systems and phase change materials (PCMs) are efficient light and heat energy stores, and their combination is a promising route to solar energy storage [1]. However, most photoswitches are activated by UV-blue light. Triplet-sensitized photoswitching, in which a visible-absorbing photosensitizer transfers its triplet energy to the photoswitch, can extend their activation across the visible spectrum [2]. In the RESHAPE project, we design new amphiphilic organic photosensitizers that localize at the PCM/polymer interface of solid nanocomposites and cover the visible range without rare elements.

Benzanthrones are ketone chromophores with fast intersystem crossing, which makes them attractive triplet sensitizers [3]. Here we report the synthesis of benzanthrone **1** (Figure 1), methyl 3-methoxy-7-oxo-7*H*-benzo[*de*]anthracene-9-carboxylate, following the two-step route of An *et al.* [4]: Suzuki–Miyaura coupling of methyl 8-bromo-5-methoxy-1-naphthoate with 4-(methoxycarbonyl)phenylboronic acid, then BBr_3-promoted intramolecular Friedel–Crafts acylation at room temperature. The ester group of compound 1 can be saponified to the carboxylic acid, the polar anchor of the amphiphilic sensitizer. Current work addresses its photophysical characterization and the introduction of lipophilic chains.

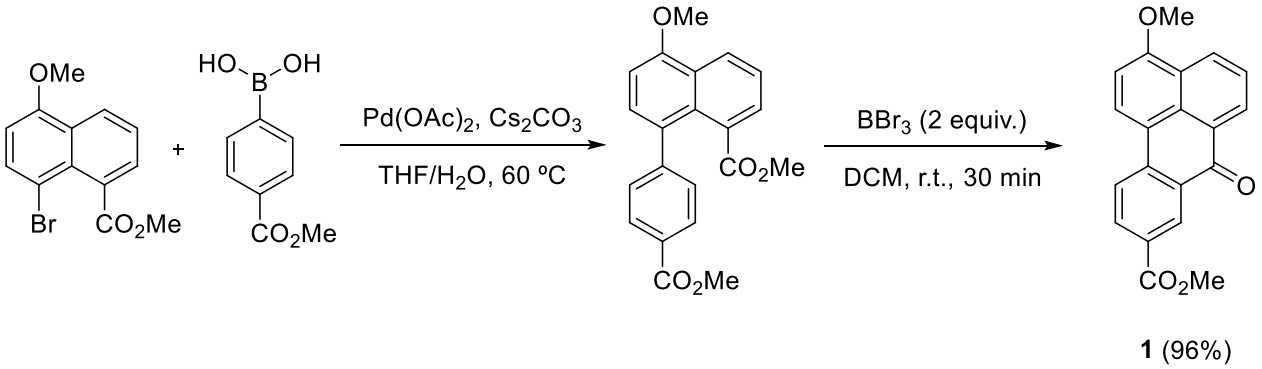

1 (96%)

Figure 1: Synthesis of benzanthrone **1**

(1) Han, G. G. D.; *et al. Nat. Commun.* **2017**, *8*, 1446.
(2) Bharmoria, P.; *et al. Chem. Sci.* **2022**, *13*, 11904.
(3) Maleckis, A.; *et al. Molecules* **2024**, *29*, 1143.
(4) An, X.; Ma, H.; Cui, G.; Zhang, T.; Xu, L.; Wang, M. *New J. Chem.* **2024**, *48*, 1741.

Direct Growth of Graphene Ribbons

M de la Vega, M Alava-Galarza, O Muntada-López, T Cuesta**,** J Serrano, I Martín-Fernandez, F Perez-Murano

Institut de Microelectrònica de Barcelona (IMB-CNM, CSIC). Campus UAB, 08193 Bellaterra, Spain

marcel.delavega@imb-cnm.csic.es

Keywords: Graphene ribbons; Direct growth; Chemical vapour deposition; Nanoelectronics

Scalable fabrication of devices based on graphene is a laborious and technically demanding process. Among the principal challenges is that graphene is typically grown on a separate substrate and then transferred onto the device substrate, and this is likely to result in mechanical damage and chemical contamination on graphene. The following patterning by lithography and etching also needs to be finely adjusted to minimise any additional degradation [1].

Several bottom-up approaches have been reported for the direct growth of graphene ribbons (GRs) to avoid the transfer and patterning processes, including surface-catalytic selectivity growth [2], the direct growth on Ge [3] or the growths within boron nitride trenches [4]. However, they have not reached a high enough readiness level and a scalable solution is still required.

The objective of my thesis is to define solutions to the integration of GRs into electronic devices for applications in sensor technology, analogue electronics and digital logic. During my first year, my work focuses on the direct growth of GRs on the cross sections of Cu/Al_2O_3 stacks to control their morphology and position (Figure 1-a, b), and on the development of a platform for their later structural and electrical characterization (Figure 1-c).

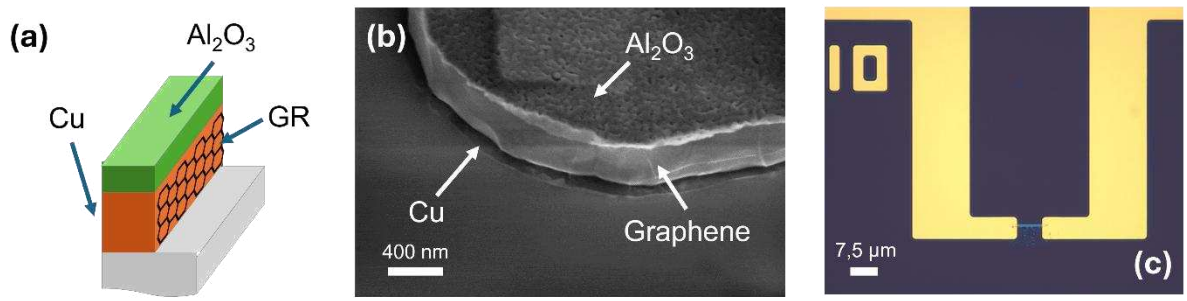

Figure 1: (a) Schematic of direct GR growth on Cu/Al_2O_3. (b) SEM image of a directly grown GR. (c) Optical image of the GR characterization platform.

(1) Khadem, A. H.; Diaz, C. B.; Lou, L. *Small Science* 5, 2025

(2) Martin-Fernandez, I.; Wang, D.; Zhang, Y. *Nano Letters* 12, 2012, 6175–6179

(3) Zheng, X.; Wang, J.; Su, K. A.; Arnold, M. S. *APL Materials* 14, 2026, 071108.

(4) Lyu, B., Chen, J., Wang, S. *et al. Nature* 628, 2024, 758–764.

Microstructural Evolution and Hardness Mapping of Submerged Arc Welded P265NB Steel

Rime Djellabi, Zakaria Boumerzoug

[1]*Department of Mechanical Engineering, University of Biskra, Biskra, Algeria*

Rime.djellabi@univ-biskra.dz

Keywords: P265NB steel; submerged arc welding; microstructure; heat affected zone; microhardness; grain size

The present study investigates the microstructural evolution and hardness distribution in P265NB low-carbon steel welded by the submerged arc welding (SAW) process. Optical microscopy was used to characterize the microstructural features across the base metal (BM), heat-affected zone (HAZ), and fusion zone (FZ). Grain size measurements were performed using ImageJ software after image calibration to provide quantitative information on the microstructural changes induced by the welding thermal cycle [1]. Vickers microhardness measurements were carried out using a 300 gf load to evaluate the mechanical heterogeneity across the welded joint. The microstructural observations revealed a ferrite–pearlite structure in the BM, whereas significant microstructural modifications occurred in the HAZ and FZ as a consequence of the thermal cycle [2]. The HAZ exhibited the coarsest average grain size, approximately 17.59 µm, compared with 13.54 µm in the BM and 13.49 µm in the FZ. The hardness profile also showed a clear variation between the different regions of the welded joint, with the BM exhibiting the highest hardness values, while lower values were measured in the HAZ and FZ. These results demonstrate the strong influence of the welding thermal cycle on grain structure and local mechanical properties, particularly within the HAZ. The combined use of optical microscopy, quantitative image analysis, and microhardness mapping provides a useful approach for correlating microstructural changes with local mechanical behavior in welded P265NB steel used for LPG cylinder applications[3].

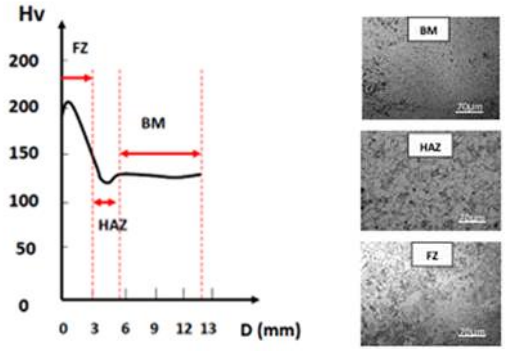

Figure 1: Microstructures and hardness distribution across the SAW-welded P265NB steel joint.

References

[1] Morris Jr., J.W. The influence of grain size on the mechanical properties of steel. Revue de Métallurgie, 2001, 98(10), 909–918.

[2] Cioroagă, B.D.; Socalici, A.V.; George, V. Submerged arc welding effect of welding speed on pressure vessel steel P355N tensile strength and microstructure. 2024.

[3] Khalfallah, A.; Moradi, M.; Beygi, R. Welding and Joining of Metallic Materials: Microstructure and Mechanical Properties. Crystals, 2024, 14(10), 839.

Eliminating Critical Metals: Electrochemical Reversibility of Organic Cathodes for Aqueous Zinc-Ion Batteries

Jairo Andrés Eraso-Narváez[1,3], Agostina Lina Capodilupo[2], Dino Tonti[3]

[1]*Instituto de Energías Renovables, Universidad Nacional Autónoma de México, Privada Xochicalco S/N, C.P. 62580, Temixco, Morelos, México.*

[2]*Consiglio Nazionale delle Ricerche, Istituto Di Nanotecnologia, Strada provinciale Lecce-Monteroni, Km 1,200, 73100 – Lecce, Italy*

[3]*Institut de Ciència de Materials de Barcelona, Consejo Superior de Investigaciones Científicas, Carrer dels Til·lers sn ES 08193 Cerdanyola del Vallès, Spain*

jaen@ier.unam.mx

Keywords: Aqueous Zinc-Ion Batteries, Organic Cathodes, Quinones and Dianhydrides, Heavy-Metal-Free Batteries, Electrochemical Reversibility.

Large-scale energy storage must prioritize inherently safe systems free of critical transition metals. As a result, aqueous zinc-ion batteries (AZIBs) with organic cathodes have gained attention over inorganic materials due to their structural designability, lattice flexibility, and resource renewability [1]. This work evaluates slurry-cast organic cathodes based on quinone and dianhydride families. Cyclic voltammetry (CV) revealed distinct redox peaks, demonstrating excellent electrochemical reversibility and stable kinetics during zinc-ion coordination. Consequently, the cells exhibited highly defined voltage-capacity profiles (Figure 1). These initial findings successfully validate the fundamental viability of these compounds as reversible active materials. Future work will optimize the electrode formulation and cell architecture to increase specific capacity, advancing toward a practical system free of critical metals.

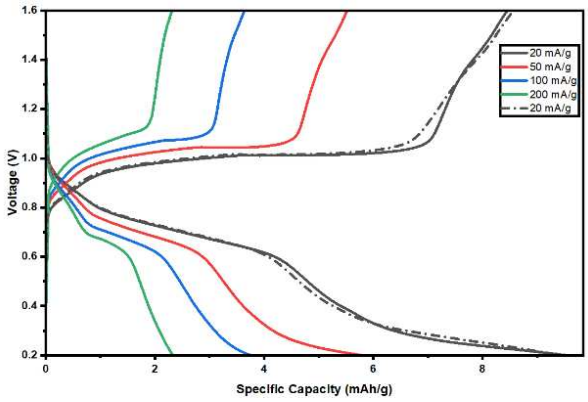

Figure 1: Galvanostatic charge-discharge profiles of the quinone-based cathode at various current densities.

(1) Dai, Y.; Yao, Y.; Feng, L.; Qiu, Z.; Deng, M.; Peng, Q. Advanced Science, 202503156.

Two-Step RF Sputtering and Sulfurization Process for Large-Area MoS_2 thin films

Abril A. Garcia-Soriano[1], Isai S. Hernandez-Luna[2], Norberto Hernandez-Como[2], Osvaldo de Melo[3]
[1]*Escuela Superior de Ingeniería Química e Industrias Extractivas del Instituto Politécnico Nacional (ESIQIE-IPN)*
[2]*Centro de Nanociencias Micro y Nanotecnologías del IPN (CNMN-IPN)*
[3]*Escuela Superior de Física y Matemáticas del IPN (ESFM-IPN)*
agarcias2500@alumno.ipn.mx

Keywords: MoS_2, Two-Dimensional Materials, RF Magnetron Sputtering, Sulfurization, Raman Spectroscopy, Thin-Film Transistors.

In this work, a two-step process based on RF sputtering and sulfurization was investigated for the fabrication of large-area MoS_2 thin films. MoS_2 precursor films were deposited by RF sputtering at 100 W and subsequently sulfurized using sulfur powder under a thermal annealing treatment at 700 °C. Different sulfurization atmospheres, N_2 and H_2, were initially evaluated using Raman spectroscopy. H_2 was selected based on the greater consistency of the relative Raman peak intensities observed among the analyzed samples. The precursor thickness was then progressively reduced from approximately 5 to 3 nm to investigate the minimum thickness suitable for sulfurization. A precursor thickness of 3 nm was identified as the minimum condition yielding consistent Raman signatures characteristic of crystalline MoS_2, with final film thicknesses of approximately 3 nm after sulfurization. The characteristic E^1_2g and A^1_1g Raman modes were observed in the analyzed samples, together with the LA(M) mode, which is associated with crystal imperfections. Repeated sulfurization experiments showed comparable Raman responses at multiple locations, supporting the reproducibility of the structural response. SEM characterization confirmed MoS_2 coverage across the substrate area, although local morphological variations were observed. These results demonstrate the potential of the proposed two-step approach for the fabrication of large-area MoS_2 thin films, while identifying morphological uniformity as an aspect for further process optimization.

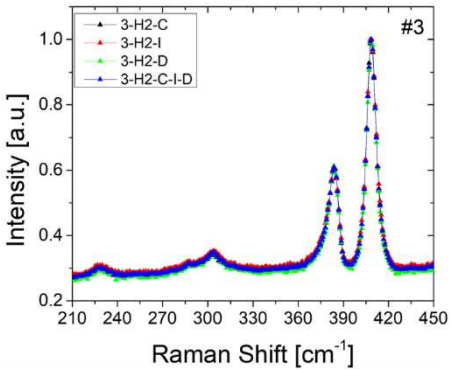

Figure 1: Raman spectra (532 nm laser) of ~5 nm MoS_2 sulfurized with H_2 on Si/SiO_2(300 nm) substrates.

(1) F. Tumino et al., Crystals 13, 1271 (2023). DOI: 10.3390/cryst13081271.

2026 JPhD 10th edition

Photoswitchable poly(ethylene imine) gels

Oriol Gonzalez-Prats[1]; Joan Freitas[1]; Marc Villabona[1]; Gonzalo Guirado[1]; Rosa Mª Sebastián[1]; Jordi Hernando[1]

[1]*Departament of Chemistry, Universidad Autònoma de Barcelona, Cerdanyola del Vallès, 08193, Spain.*
oriol.gonzalez@uab.cat

Keywords: CO_2 capture, photoswitches, PEI gels, photomodulation

The incorporation of molecular photoswitches into soft matter allows the preparation of light-responsive materials for a variety of applications, which range from optoelectronics to sensors, drug delivery, and soft robotics.[1,2] This is the case of photoswitchable gels, which are often developed to generate mechanical motions upon stimulation with external light.[3] In this work we focus our attention on poly(ethylene imine) (PEI) gels, which are widely employed in different fields such as cell culture[4] or CO_2 capture.[5]

To make PEI gels photoswitchable, suitable light-responsive cross-linkers must be introduced to their structure. Herein we explored the use of two different types of crosslinking agents to accomplish this goal: (a) azobenzenes, which are known to undergo reversible photoisomerization between their initial extended *trans* configuration and their thermally unstable folded *cis* form upon exposure to light;[6] and (b) diarylethenes, which reversibly photoconvert between *open* and *closed* states under irradiation. In both cases, terminal carboxylic acid groups were attached to the photoswitches through spacers of variable length to promote PEI cross-linking and gel formation. In this presentation we describe the synthesis of these photoswitchable cross-linkers and of the corresponding PEI gels, as well as the evaluation of their photoswitching properties.

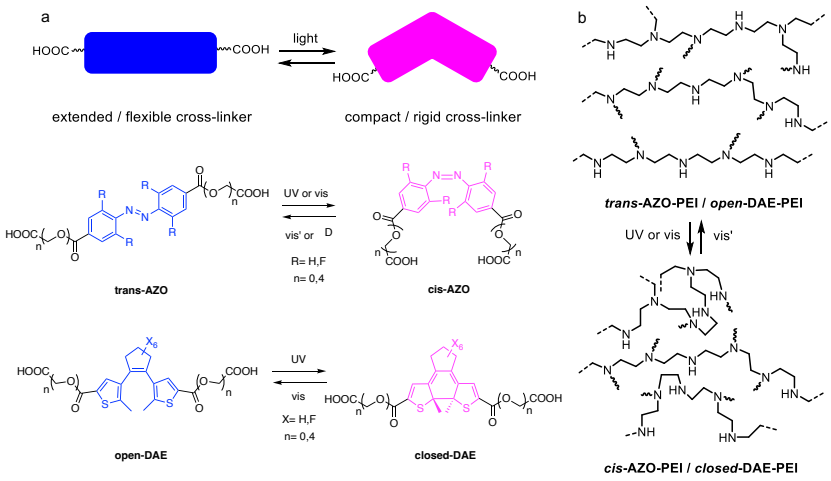

Figure 1: A) Structures of the photoswitchable azobenzene- and diarylethene-based cross-linkers synthesized. B) Photomodulation of the PEI cross-linked polymer gels upon irradiation.

(1) Russew, M.-M.; Hecht, S. Adv. Mater. ***2010****, 22, 3348–3360.*
(2) Yu, Y.; Nakano, M.; Ikeda, T. Nature ***2003****, 425, 145–145.*
(3) Luo, P.-F.; Xiang, S.-L.; Li, C.; Zhu, M.-Q. J. Polym. Sci. ***2021****, 59, 2246–2264.*
(4) Chen, Z.; Lv, Z.; Sun, Y.; Chi, Z.; Qing, G. J. Mater. Chem. B ***2020****, 8 , 2951–2973.*
(5) Shen, X.; Du, H.; Mullins, R. H.; Kommalapati, R. R. Energy Technol. ***2017****, 5, 822–833.*
(6) Bandara, H. M. D.; Burdette, S. C. Chem. Soc. Rev. ***2012****, 41, 1809–1825.*

2026 JPhD 10th edition

Oxygen Vacancy Modulation in $Hf_{0.5}Zr_{0.5}O_2$ Epitaxial Thin Films via Seed Layer and Redox Deposition conditions

Mostafa Habibi[1], Mehrdad Ghiasabadi Farahani[1], Jose P. B. Silva[2,3], Ignasi Fina[1] and Florencio Sanchez[1]

[1]Institute of Materials Science of Barcelona (ICMAB-CSIC), Carrer dels Til.lers, 08193 Cerdanyola del Vallès,, Spain

[2]Physics Center of Minho and Porto Universities (CF-UM-UP), University of Minho, Braga, Portugal

[3]Laboratory of Physics for Materials and Emergent Technologies, University of Minho, Braga, Portugal

Email: mhabibi@icmab.es

Keywords: ferroelectric, memory, Hafnia, endurance, polarization

***Abstract*—** Researchers first discovered ferroelectricity in HfO_2 in polycrystalline films doped with Si in 2011. Since then, ferroelectric HfO_2 has emerged as one of the most promising candidates for next-generation memory technologies due to its unique characteristics, including non-volatility, high polarization, fast switching, thickness scalability, and compatibility with three-dimensional architectures. Oxygen vacancies have since been identified as critical factor governing the stabilization of the metastable ferroelectric phase in HfO_2. Because epitaxial films provide precise control over microstructure, they offer an ideal model system for systematically investigating the role of oxygen vacancies in stabilizing and enhancing ferroelectricity. Herein, we employ a non-conventional approach in pulsed laser deposition to modulate oxygen vacancies by controlling the redox condition while adjusting plasma energy, following the deposition of a well-crystallized HZO seed layer. Thin films grown under controlled redox conditions on $SrTiO_3$ (001) and $SrTiO_3$ (110) substrates exhibit enhanced remanent polarization compared with a reference sample without growth redox regulation. In addition, improved enhancement is achieved through the mitigation of fatigue, resulting in a larger technological memory window and more stable device operation.

Acknowledgment: This work has received funding from the European Union's Horizon Europe (HORIZON) Marie Skłodowska-Curie Actions Doctoral Networks (MSCA-DN) HORIZON-MSCA-2023-DN-01 call, under the Grant Agreement number 101168161.

Design of a Three-Interface Voltammetric Electronic Tongue for the simultaneous quantification of Serotonin, Folic Acid and Paracetamol

Jing Huang[1,2*], Julio Bastos-Arrieta[1,2], Núria Serrano[1,2], José Manuel Díaz-Cruz[1,2]

[1]*Department of Chemical Engineering and Analytical Chemistry, Universitat de Barcelona (UB), Martí i Franquès 1-11, 08028 Barcelona, Spain.*

[2]*Water Research Institute (IdRA), University of Barcelona (UB), Martí i Franquès 1-11, 08028 Barcelona, Spain.*

jing.huang@ub.edu

Keywords: screen-printed electrodes, electronic tongue, electroanalysis, surface modification, emerging pollutants.

Overlapping voltammetric signals challenge the simultaneous determination of electroactive compounds. This study developed a compact electronic tongue combining three screen-printed carbon electrode (SPCE) interfaces with chemometric analysis to quantify serotonin (SE), folic acid (FA), and paracetamol (PA) in ternary mixtures.

The sensing array comprised bare SPCE, SPCE modified with poly(diallyldimethylammonium chloride) (PDDA), and an electrochemically activated PDDA/poly(styrene sulfonate) (PSS) interface. We performed differential pulse voltammetry in phosphate-buffered saline at pH 7.0, where SE, FA, and PA are predominantly cationic, anionic, and neutral, respectively. The activated PSS-terminated interface markedly enhanced the SE response, whereas SPCE/PDDA enhanced the measurable FA response. These differentiated profiles provided complementary information despite substantial signal overlap.

Separate partial least squares regression (PLS-1) models were developed using 27 calibration mixtures covering 1–5 $\mu mol \cdot L^{-1}$ SE, 5–25 $\mu mol \cdot L^{-1}$ FA, and 2–20 $\mu mol \cdot L^{-1}$ PA. Model complexity was selected by Venetian-blinds cross-validation, retaining eight, five, and seven latent variables for SE, FA, and PA, respectively. The SE and PA models incorporated all three electrode blocks, while the FA model used the bare SPCE and SPCE/PDDA blocks. Independent external validation with 15 mixtures measured on a separate day yielded R^2 values of 0.933, 0.905, and 0.962, and root mean square errors of prediction of 0.385, 1.677, and 1.237 $\mu mol \cdot L^{-1}$ for SE, FA, and PA, respectively. Corresponding range-normalised prediction errors were 9.61%, 8.38%, and 6.87%. Variable importance in projection analysis identified influential regions across the retained electrode blocks. A positive constant offset was observed for FA during external validation.

These findings demonstrate that controlled interfacial diversity coupled with multivariate calibration supports simultaneous quantification of compounds with overlapping voltammetric responses. The results establish a proof of concept in buffered ternary mixtures and provide a basis for subsequent evaluation in complex sample matrices.

2026 JPh 10th edition

Evaluating Alternative Culture Media for Enhanced Bacterial Cellulose Production

Guillem Wetherell Mateu[1], Asier R. Muguruza[1], Muling Zeng[1], Sergi Diaz-Permanyer[1], **Nicole Jiménez-Majano[1]***, Nastassia Knödlseder[2,3], Pablo Guardia[1], Anna Laromaine[1], Anna Roig[1]

[1]ICMAB-CSIC, Campus UAB, 08193, Bellaterra, Spain
[2]Department of Medicine and Life Sciences, Universitat Pompeu Fabra (UPF), 08003, Barcelona, Spain
[3]Department of Biomedicine, Aarhus Universitet, 8000, Aarhus, Denmark
njimenez2@icmab.es

Keywords: Bacterial Cellulose, Culture Media, Biomaterials

Bacterial cellulose (BC) is a promising biopolymer for biomedical and advanced material applications due to its nanofibrillar structure, purity, mechanical strength, and biocompatibility [1]. *Komagataeibacter xylinus* (*K. xylinus*) is one of the most widely used BC producers due to its well-characterized metabolism, stable cellulose production, and scalability. Although conventional Hestrin–Schramm (HS) medium has been extensively optimized, studies combining HS with alternative microbiological culture media remain limited.

In this study, Lysogeny Broth (LB), Brain Heart Infusion (BHI), and de Man–Rogosa–Sharpe (MRS) media were evaluated individually and in combination with HS, with or without 5% (v/v) glycerol supplementation. BC production was quantified, and the resulting films were characterized for structural, physicochemical, and functional properties.

HS:MRS supplemented with 5% glycerol achieved the highest BC yield, approximately four-fold higher than conventional HS. BC retained comparable crystallinity, morphology, and chemical composition across conditions (Figure 1). Moreover, selected culture conditions enabled the incorporation of *E. coli* into BC without compromising BC production, supporting their potential for the development of BC-based living materials. Overall, alternative microbiological media provide a simple strategy to enhance BC production while preserving key material properties.



Figure 1: Image of oven-dried BC samples in different media compositions showing different transparencies.

(1) Klemm, D., Heublein, B., Fink, H. P. & Bohn, A. Cellulose: Fascinating biopolymer and sustainable raw material. Angew. Chem. Int. Ed. 44, 3358–3393 (2005).

2026 JPhD 10th edition

Development of micropillar structures towards spatially resolved electrophysiological interrogation of the paracellular pathway

Irene Martínez-Aguilera [1,2], Xavi Illa [1,3], Jose Yeste [1,3]

[1] *Instiut de Microelectrònica de Barcelona, IMB-CNM (CSIC), Campus UAB, 08193 Bellaterra, Spain*

[2] *Doctoral Program in Biomedical Engineering, Universitat Politècnica de Catalunya - BarcelonaTech (UPC), Barcelona, Spain.*

[3] *Centro de Investigación Biomédica en Red en Bioingeniería, Biomateriales y Nanomedicina (CIBER-BBN), Instituto de Salud Carlos III, Madrid, Spain*

irene.martinez@imb-cnm.csic.es

Keywords: Paracellular pathway, tight junctions, micropillar electrodes, MDCK II

Epithelial barriers separate tissue and organ compartments and regulate the exchange of ions and solutes between them. Part of this transport occurs through nanometre-scale pores in the paracellular pathway, between adjacent cells [1]. Conventional electrophysiological techniques measure the averaged response of large epithelial areas [2], masking local variations and the rapid dynamics observed at the level of individual paracellular channels [3]. To investigate these local phenomena, we are developing a micropillar electrode array chip designed to facilitate the integration of pillars into the intercellular space, with close contact between their electrode tips in and the paracellular channels. The chip, fabricated using silicon-on-insulator (SOI) technology, integrates 64 micropillar electrodes of ~1 µm in diameter and 5.5 µm in height. As a first step towards its implementation, we first evaluated whether epithelial cells could form an intact barrier while accommodating the micropillar structures. Madin-Darby Canine Kidney II (MDCK II) cells formed confluent monolayers, and ZO-1 immunostaining and confocal microscopy confirmed continuous intercellular contacts over the micropillars (Figure 1A). In addition, the electrical properties of the microelectrodes were characterized. Because of their small dimensions, optimization of the electrode–electrolyte interface is required to achieve suitable electrical performance (Figure 1B). Platinum black coatings were explored to increase the effective electrode surface area and improve electrode capacitance. Although the coatings enhanced the electrical response, substantial electrode-to-electrode variability was observed in both capacitance and coating morphology for the 1 µm in diameter electrodes, limiting their reproducibility. Alternatively, a process based on evaporation of TiN is currently being evaluated [4]. Together, these results establish the biological and technological foundations required for future spatially resolved measurements of paracellular conductance.

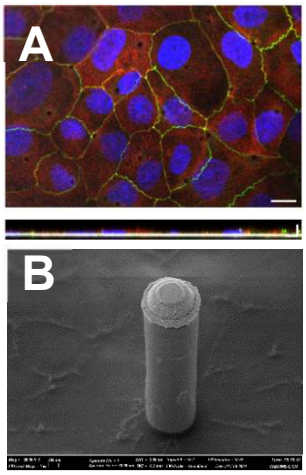

Figure 1: MDCK II monolayers stained for ZO-1, F-actin, and nuclei (A; scale bars: XY, 10 µm; XZ, 5 µm) and SEM image of the Pt-electrode pillar (B).

(1) Günzel, D.; Yu, A.S.L. Physiological Reviews, 93, 525–569.
(2) Srinivasan, B.; Kolli, A.R.; Esch, M.B.; Abaci, H.E.; Shuler, M.L.; Hickman, J.J. Journal of Laboratory Automation, 20, 107–126.
(3) Weber, C.R.; Liang, G.H.; Wang, Y.; Das, S.; Shen, L.; Yu, A.S.L.; Nelson, D.J.; Turner, J.R. eLife, 4, e09906.
(4) Ryynänen, T.; Toivanen, M.; Salminen, T.; Ylä-Outinen, L.; Narkilahti, S.; Lekkala, J. Front. Neurosci. 12, 882.

2026 JPhD 10th edition

Nucleation process in lithium–sulfur batteries: effects of experimental conditions

Irina Martynova[1], Andreu Cabot[1,2]

[1]*Catalonia Institute for Energy Research - IREC, Sant Adrià de Besòs, Barcelona 08930, Catalonia, Spain,*
[2]*ICREA, Pg. Lluis Companys, Barcelona 08010, Catalonia, Spain*

imartynova@irec.cat

Keywords: lithium–sulfur batteries; Li_2S nucleation; redox mediator; diphenyl diselenide

Lithium–sulfur (Li–S) batteries are attractive for next-generation energy storage because sulfur is inexpensive, abundant and environmentally safer than cobalt and nickel, while the theoretical energy density reaches 2600 Wh kg^{-1}. Their practical development is limited by capacity loss during cycling, the polysulfide shuttle effect, lithium dendrites and cathode volume expansion.

In this work, the Li_2S nucleation process was systematically evaluated in dependence on time, overpotential, substrate and electrolyte composition. Nucleation is the initial formation of Li_2S during discharge and controls subsequent particle growth, sulfur utilization and reaction kinetics. During experiments It was used a carbon cloth substrate with 30 µL of 0.25 M Li_2S_6 solution. The time dependence was examined at 2.06 V after 3 and 15 h. The effect of overpotential was studied at 2.04, 2.00 and 1.98 V for 2 h, showing changes in nucleation morphology and electrochemical response.

The substrate effect was investigated using Al foil, carbon cloth and carbon cloth with a hydrophobic layer. The SEM observations and electrochemical response demonstrate that the substrate changes the nucleation behavior. Finally, 0.1 M diphenyl diselenide was used as a redox-mediator additive at 2.04 V for 2 h. The additive changed the nucleation morphology and current response (Figure 1). Galvanostatic charge–discharge and cyclic-voltammetry measurements were also performed for Li–S cells with and without the mediator.

Overall, the results show that Li_2S nucleation is strongly dependent on experimental conditions. The study provides a basis for further morphology analysis after the initial nucleation peaks and for evaluating electrolyte additives with a pure redox-mediator mechanism, linking fundamental nucleation behavior with Li–S battery performance, cycle life and safety.

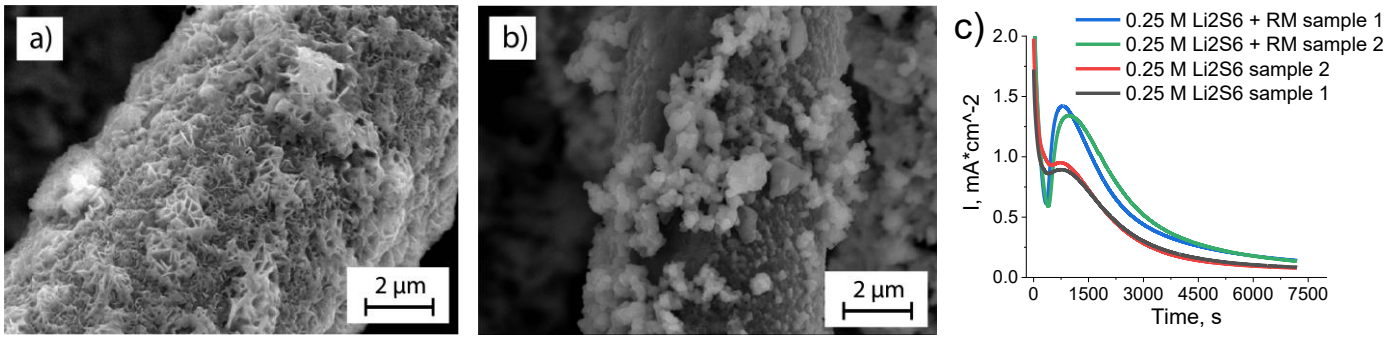

Figure 1: SEM images of nucleation process with redox mediator (a) and without (b), electrochemical curves for the processes (c)

Acknowledgments: This work was supported by European Union's Horizon Europe research and innovation programme under the Marie Skłodowska-Curie grant agreement No 101081337.

Epoxy Replication of Silicon-Based Electrospray Thrusters

P.Mercier[1,2], B.Sepúlveda[1], J.Cruz[2]

[1] *Institut de Microelectrònica de Barcelona IMB CNM*

[2] *IENAI SPACE S.L.*

pau.mercier@cisc.es

Keywords: Epoxy replication, Electrospray thrusters, Space mobility

Electrospray thrusters are a novel technology for highly efficient orbital maneuvering. Passively fed electrospray thrusters rely on capillary forces to transport the propellant (ionic liquid) from the reservoir in which it is stored to the emitter itself. In our case, we fabricate silicon-based arrays of sharp micropyramids to locally intensify the electric field that promotes the electrospray emission. To vertically transport the ionic liquid, each pyramid is intersected by two microholes (Figure 1 a). On top of this, the surface of the whole emitter, including the pyramids, is coated with nanowires (Figure 1 b). This nanocoating enhances the hydrophilicity of the surface and at the same time it imposes a fluidic resistance to promote ionic emission regimes.

Producing these silicon-based systems requires access to a specialized infrastructure such as a microfabrication cleanroom, where it might take from a couple of weeks to several months -depending on the availability of certain equipment- to produce a small number of emitters at a high economical cost. Because of this, in my phD, I am studying the feasibility of creating flexible molds of these silicon-based emitters and then casting curable materials such as epoxies or UV resins to obtain replicas. This would not only decrease the fabrication times and costs of the manufacturing process, but it would also open door to large scale production of emitters that have exactly the same features, as they would be manufactured using the same mold.

The preliminary results obtained are promising. In the epoxy replicas, the overall geometry of the emitters is preserved, from the sharpness of the micropyramids (Figure 1 c), to the presence of the nanowires (Figure 1 d). To open the vertical microchannels that go through the whole thickness of the polymeric replica two different techniques have been studied: the alignment of a second silicone mold with micropillars and the usage of a UV laser to cut the holes.

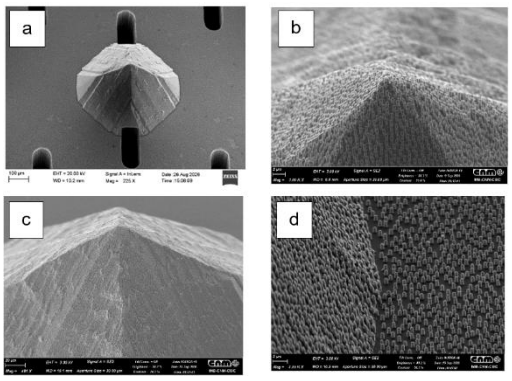

Figure 1: (a,b) SEM images of the Si-based micropyramids coated with NWs. (c,d) SEM images of the epoxy replicated pyramids.

Radiation Hardness of 4H-SiC Detectors and Their Development Towards Radiation Detection Applications

J. Nickson[1], J.M. Rafí[1], J. Montserrat[1] and G. Pellegrini[1]

[1] *Instituto de Microelectrónica de Barcelona, CNM-CSIC,*

Bellaterra, Spain

jack.nickson@imb-cnm.csic.es

Keywords: Silicon Carbide, Radiation Detection, Wide-Band Gap Materials.

Radiation is everywhere, the movement of energy as particles or waves is part of the fabric of the world around us. Since the discovery of X-rays, humankind has progressively developed the ability to understand, exploit, and detect different forms of radiation. Today, radiation detection is fundamental to a wide range of applications, from medical imaging and scientific research to space exploration and energy production. As these applications continue to advance, there is an increasing need for detector technologies capable of operating reliably under harsh conditions. Wide-band-gap (WBG) semiconductor materials are promising candidates for next-generation solid-state radiation detectors, with silicon carbide (SiC) at the forefront. Compared with conventional silicon, SiC combines a wide band gap, high breakdown electric field, low intrinsic carrier concentration, and high radiation hardness, providing the potential for operation at elevated temperatures and in high-radiation environments. Despite these advantages, much of the development of SiC has historically focused on power electronics, while its application as a radiation detection material remains comparatively less mature. Further investigation of its properties is therefore required to establish its potential as a robust alternative to conventional silicon-based detectors [1].

In this work, SiC PiN and Schottky diodes are investigated using a range of experimental techniques to assess their electrical characteristics, temperature-dependent performance, radiation hardness, and radiation detection response. Electrical characterisation is performed over a range of temperatures, while transient current technique (TCT) measurements and alpha particle detection are used to investigate the charge collection and detection response of the devices. Radiation hardness is evaluated following exposure to a range of proton and electron fluences. The potential application of SiC detectors in recoil-separator systems, where radiation tolerance and reliable charge collection are critical is also studied. In addition, a potential way to mitigate the radiation effects is investigated by studying the response of operating devices under illumination at different wavelengths.

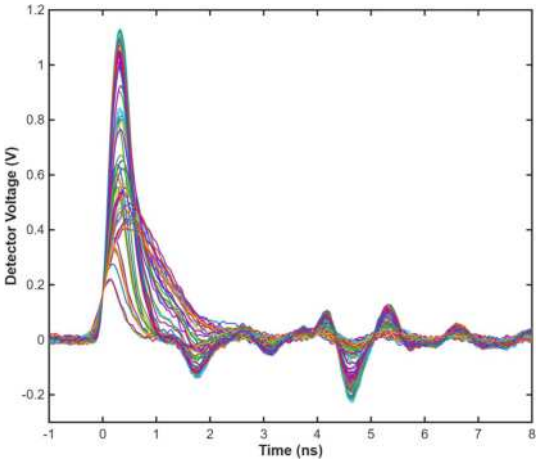

Figure 1: Detection Signal of an Alpha particle from a Triple Alpha source. Detected by a 4H-SiC 1mm PiN diode that was irradiated by protons at a fluence of 1.36×10^{13} p/cm^2.

(1) De Napoli, M., 2022. SiC detectors: A review on the use of silicon carbide as radiation detection material. Frontiers in physics, 10, p.898833.

Computational Modelling of Au-Based Asymmetric Catalysis in Artificial Metalloenzymes

Maria Fernanda Peralta-Morales[1], Giuseppe Sciortino[1], Jean-Didier Maréchal[1]

[1]*Department of Chemistry, Universitat Autònoma de Barcelona, Cerdanyola del Vallès, 08193, Spain*

MariaFernanda.Peralta@uab.cat

Keywords: Artificial metalloenzyme, biocatalysis, multiscale modelling, protein design, gold.

Artificial metalloenzymes (ArMs) are engineered biocatalysts that incorporate non-native metal ions or synthetic cofactors into protein scaffolds, combining enzymatic selectivity with the catalytic versatility of transition metals [1]. Among emerging scaffolds, the *Lactococcal multidrug resistance regulator* (LmrR) has gained prominence as a versatile scaffold for ArM design. Recently, targeted mutations (such as V15pSHF) enabled site-specific Au(I) coordination, yielding a gold–LmrR system capable of catalyzing complex organic transformations [2].

In this study, the alkenynone cyclization was evaluated using a single-cysteine LmrR variant. While the initial LmrR_V15C scaffold provided a catalytic environment, achieving high enantioselectivity remained challenging. Through a directed evolution campaign, an optimized variant (LmrR_CVITQ) was developed, establishing a tailored asymmetric microenvironment that enhances enantioselectivity.

To gain deeper mechanistic insights, a multiscale computational protocol was implemented to elucidate the structural differences between LmrR_V15C and LmrR_CVITQ. Our analysis reveals that the most active evolved mutant has altered properties regarding the LmrR_V15C in terms of substrate orientation, distinct hydrophobic profiles, and active-site cavity conformation. Together, these findings provide an explanation for the enantioselectivity measured experimentally.

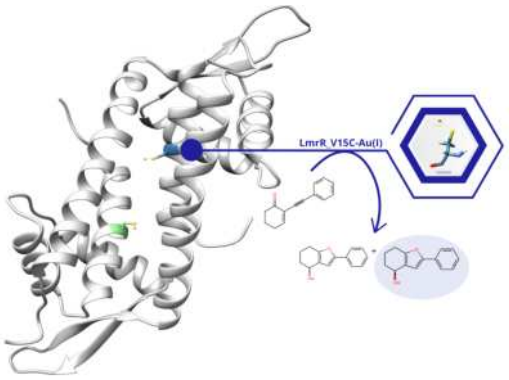

Figure 1: LmrR_V15C and the alkenynone reaction.

[1] L. Alonso-Cotchico, J. Rodríguez-Guerra, A. Lledós, J.-D. Maréchal, Acc. Chem. Res. 2020, 53 (4), 896–905. https://doi.org/10.1021/acs.accounts.0c0003

[2] M. J. Veen, F. S. Aalbers, H. J. Rozeboom, A.-M. W. H. Thunnissen, D. F. Sauer, G. Roelfes, Angew. Chem. Int. Ed. 2025, 64, e202421912. https://doi.org/10.1002/anie.202421912

Exploring polar metallicity in transition metal oxides

Gustavo Pinedo-Cuba[1], J.M. Caicedo[1], H. Yokota[2], K. Cordero-Edwards[1], F. Sandiumenge[3], G. Catalán[1] and D. Pesquera[1]

[1]*Catalan Institute of Nanoscience and Nanotechnology (ICN2), Barcelona, Spain*
[2]*Institute of science Tokyo, 4259 Nagatsuta-cho, Midori-ku, Yokohama, 226-8501, Japan*
[3]*Institute of Materials Science of Barcelona (ICMAB-CSIC), Campus UAB, Bellaterra, Barcelona, 08193 Catalonia, Spain*

Email: manuelgustavo.pinedo@icn2.cat

Keywords: Polar metals, flexoelectricity, membranes

An inhomogeneous mechanical deformation, or strain gradient, is well known to break the inversion symmetry of centrosymmetric insulators, thereby inducing an electric polarization [1]. This effect, known as flexoelectric, can be understood as the intrinsic polarization response of a material to a spatially varying strain, analogous to the polarization induced by an electric field through the conventional dielectric response. Metals, which are typically centrosymmetric, may also undergo symmetry breaking under strain gradients. In epitaxial films, large strain gradients can be produced by mechanical deformation with a probe tip, by stoichiometry gradients or by strain relaxation. The latter has been exploited to demonstrate polar displacements in $SrRuO_3$ (SRO), a metallic and magnetic perovskite [2]. Here we take advantage of the flexibility of freestanding epitaxial oxide membranes released from their substrate, which, in bilayer form, can bend into micrometre-scale roller structures with large strain gradients [3].

We combine two metallic perovskites, $LaNiO_3$ (LNO) and SRO, in a bilayer and study how it rolls up when the underlying $Sr_3Al_2O_6$ sacrificial layer is etched, which yields LNO/SRO microtubes. Second harmonic generation microscopy reveals inversion symmetry breaking in the rolled structures, which remain metallic down to cryogenic temperatures. We then examine the depth-dependent microstructure of the rolls by high-resolution scanning transmission electron microscopy (HR-STEM). Finally, I will discuss how the curvature and morphology of the rolls can be engineered with this approach, and their potential for nonlinear and nonreciprocal transport and photovoltaic effects.

(1) P. Zubko, G. Catalan, and A. K. Tagantsev, Flexoelectric Effect in Solids, Annu. Rev. Mater. Res. 43, 387 (2013).

(2) W. Peng et al., Flexoelectric polarizing and control of a ferromagnetic metal, Nat. Phys. 20, 450 (2024).

(3) Y. Lun, S. Xu, X. Wang, and J. Hong, Flexoelectricity in self-rolling freestanding heterogeneous films, International Journal of Solids and Structures 271–272, 112223 (2023).

Evaluation of graphene degradation in graphene based- solution gated field effect transistors technology: implications in biomedical applications

Leo Salgado-Chane [1,2], Marta Delgà-Fernández, Sergi Valero, Xavi Illa, Elena Del Corro, Rosa Villa, Elisabet Prats-Alfonso, Sergi Brosel-Oliu, Anton Guimerà-Brunet.

[1] *Institute of Microelectronics of Barcelona (IMB-CNM), Bellaterra, 08193, Spain*
[2] *Universitat Autonoma de Barcelona (UAB), Bellaterra, 08193, Spain*

e-mail: leo.salgado@csic.es

Keywords: graphene, electrochemical stability, Raman spectroscopy, solution-gated devices

Graphene solution-gated field-effect transistors (gSGFETs) are promising interfaces for neural recording and biomedical sensing, but long-term operation may be limited by electrochemical modification of the graphene–electrolyte interface. Although potentials within the water-stability window are often considered safe, the stability of monolayer graphene under sustained polarization remains insufficiently defined [1–3]. In this work, I used a simplified graphene macroelectrode structure as a model system to study how electrochemical polarization affects graphene stability, correlating how this behavior depends on the initial defect density of the material.

Graphene stability was evaluated using chronoamperometry and Raman spectroscopy techniques. Using a three-electrode configuration, an Ag/AgCl reference and a Pt counter electrode were placed in 10 mM PBS, in contact with the active area of the PCE, acting as the working electrode. The graphene was held at 0 V for 12 hours, and then at 400 mV for 12 hours, while the current between the PCE and counter electrode was continuously monitored. Raman measures of the same region were done at each step (start, after 0 V and after 400 mV) to study the defects evolution. Two graphene conditions were compared: bare CVD-grown graphene as transferred from the Cu foil and CVD-grown graphene previously treated by ultraviolet-ozone (UVO) to introduce a controlled initial D/G Raman peaks ratio of ~0.5.

Chronoamperometry at 0 V produced a negligible increase in defect density as expected, whereas the 400 mV step led to a clear D/G increase in both cases, showing a significant degradation of the graphene layer. This increase was more pronounced in UVO-treated samples, suggesting that initial defects make graphene more vulnerable to electrochemical degradation under positive bias. Similarly, Raman analysis also showed shifts in the 2D/G peaks positions, consistent with strain and doping induced effects in the graphene layer.

The results observed demonstrate that graphene electrochemical stability depends strongly on its initial state and the voltage bias applied, where long periods of time can induce significant degradation even for working potential typically considered safe such as 400 mV. The simplified model allows us to assess graphene stability in devices where the graphene-electrolyte interface directly affects performance and electrical readout, also demonstrating the importance in long-term operation of gSGFETs.

[1] A. Bonaccini et al., Nature Nanotechnology 17 (2022) 301-309.
[2] R. Joshi et al., J. Phys.: Condens. Matter 37 (2025) 143001.
[3] A. Ambrosi et al., Chemical Reviews 114 (2014) 7150-7188
[4] M. Delgà-Fernández et al., Nano Lett. 24 (2024) 11376-11384.

Silicon Microstructures for an X-ray Dark-Field Detector

Clàudia Sellarès[1], Giulio Pellegrini[1]

[1] *Instituto de Microelectrónica de Barcelona (IMB-CNM, CSIC), Cerdanyola del Vallès, Barcelona, España*

claudia.sellares@imb-cnm.csic.es

Keywords: High-aspect-ratio silicon microstructures, DRIE, X-ray dark-field imaging.

Chronic obstructive pulmonary disease (COPD) is the third leading cause of death worldwide [1]. Conventional X-ray imaging cannot detect alveolar obstruction, limiting its diagnostic potential. However, X-rays undergo slight diffraction when interacting with alveolar walls, producing a pattern detectable with sufficiently high spatial resolution [2]. Within the SmartX project, a novel X-ray dark-field detector is being developed to detect this pattern. This requires 3-5 µm pixels and deep silicon trenches, later filled with scintillator material at a partner institution (Figure 1).

This work investigates deep reactive ion etching (DRIE) of 200 µm-thick p-type silicon wafers. Bosch etching produced trenches up to 194 µm deep, but mask undercut, wall thinning and scalloping were observed. Shallower etching preserved the walls, whereas near-target depths led to thinning and partial collapse, highlighting the difficulty of combining high depth and structural stability (Figure 1a-d).

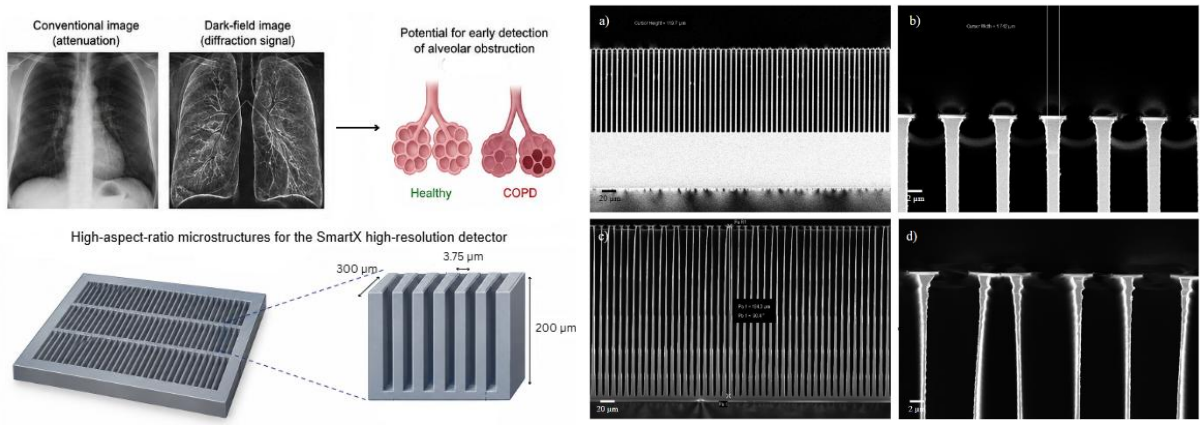

Figure 1: Concept of the SmartX detector (left) and SEM images of the trenches (right, a-d)

Funding was provided by the European Research Council (ERC Synergy Grant SmartX, SyG 101167328).

(1) World Health Organization. Chronic obstructive pulmonary disease (COPD).
(2) Willer, K. et al. PLoS One, e0204565.

2026 JPhD 10th edition

Volatile Filamentary Switching in Solution-Processed Ag/cPVP/Ag Organic Memristors

Z. Su[a], O. Duque[a], A. Cantudo[b], J.A. Jiménez-Tejada[b], C. Acal[c], C. Ferreyra[a], J.B. Roldan[b], M.B. Gonzalez[a*], C. Martínez-Domingo[a*]

[a]*Institut de Microelectrònica de Barcelona (IMB-CNM-CSIC), Campus UAB, 08193 Bellaterra, Spain*
[b]*Departamento de Electrónica y Tecnología de Computadores, Universidad de Granada, 18071 Granada, Spain*
[c]*Departamento de Estadística e Investigación Operativa, Universidad de Granada, 18071 Granada, Spain*

[a]*zhenhua.su@imb-cnm.csic.es,* [a*]*mireia.bargallo.gonzalez@imb-cnm.csic.es,* [a*]*carme.martinez@csic.es*

Keywords: Organic memristors, volatile resistive switching, cPVP, conductive filaments.

Most memristors are based on inorganic materials such as metal oxides, 2D materials and halide perovskites, some of which require high-temperature processing or raise toxicity and stability concerns. Organic materials are attractive for memristors due to their chemical tunability, solution processability, and mechanical flexibility [1,2]. Their molecular structure enables tailored resistive switching, while low-temperature solution processing (<180 °C) allows nanometer-scale films on flexible substrates, making them promising for memory and neuromorphic applications.

In this work, fully solution-processed Ag/cross-linked poly(4-vinylphenol)/Ag memristors were fabricated using inkjet-printed Ag bottom and top electrodes and a spin-coated cPVP as switching layer with a thickness of approximately 650 nm (Fig. 1a,b). The devices exhibit reproducible resistive switching over 1000 cycles with a memory window approaching two orders of magnitude (Fig. 1c). The threshold-voltage distribution, ranging from 0.5 to 2.2 V, reveals the stochastic nature of conductive-path formation in the polymer layer. Volatile operation is demonstrated by the spontaneous recovery of the high-resistance state within 400 ms under a 0.1 V read bias after SET switching (Figure 1d). This self-recovery is consistent with the formation and rupture of transient Ag conductive filaments within the cPVP layer, highlighting the potential of fully solution-processed organic memristors for neuromorphic applications.

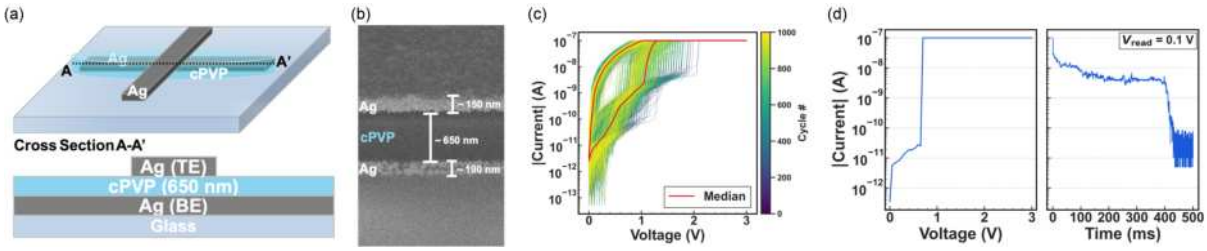

Figure 1: (a) Schematic and (b) cross-sectional SEM image of the Ag/cPVP/Ag device. (c) I - V curves over 1000 RS cycles with the median (red). (d) Single-cycle I - V curve and current relaxation at V_{read} = 0.1 V.

(1) Yuan, L.; Liu, S.; Chen, W.; Fan, F.; Liu, G. Organic Memory and Memristors: From Mechanisms, Materials to Devices. *Adv. Electron. Mater.* **2021**, *7*, 2100432.
(2) Gao, S.; Yi, X.; Shang, J.; Liu, G.; Li, R.-W. Organic and Hybrid Resistive Switching Materials and Devices. *Chem. Soc. Rev.* **2019**, *48*, 1531 - 1565.

2026 JPhD 10th edition

Designing Organic Radical Adducts to Enhance MRI Contrast in Radical Dendrimers

Xuejiao wang[1], Ehsan Shirdel[1], Chuanting Zhou[1], Silvia Lope-Piedrafita,[2] Vega Lloveras,[1,3,*] José Vidal-Gancedo.[1,3,*]

[1] Institut de Ciència de Materials de Barcelona, ICMAB-CSIC, Campus UAB, 08193 Bellaterra, Spain.

[2] Departament de Bioquímica i Biologia Molecular, Unitat de Bioquímica de Biociències, Edifici Cs, Universitat Autònoma de Barcelona, 08193 Bellaterra, Spain

[3] CIBER de Bioingeniería, Biomateriales y Nanomedicina, Instituto de Salud Carlos III, 08913 Bellaterra, Spain.

xwang2@icamb.es; *vega@icmab.es; *j.vidal@icmab.es

Keywords: organic radicals; MRI contrast agents; relaxivity; dendrimers.

Organic radical-based contrast agents, in particular radical dendrimers—dendrimers fully functionalized with organic radicals—have emerged as promising alternatives to conventional Gd(III) chelates for magnetic resonance imaging (MRI), motivated by concerns regarding gadolinium accumulation in the brain and associated toxicity.[1-6] In this work, we synthesized a series of mono-, di-, and tri-TEMPO radical adducts with different structural rigidity, radical–radical spacing, and molecular weights to evaluate key factors affecting their MRI behaviour. These structural variations are systematically investigated using EPR spectroscopy and MRI measurements. Additionally, the most effective radical adduct is being anchored onto a dendrimer scaffold to further enhance relaxivity and maximize MRI contrast performance in radical dendrimers.

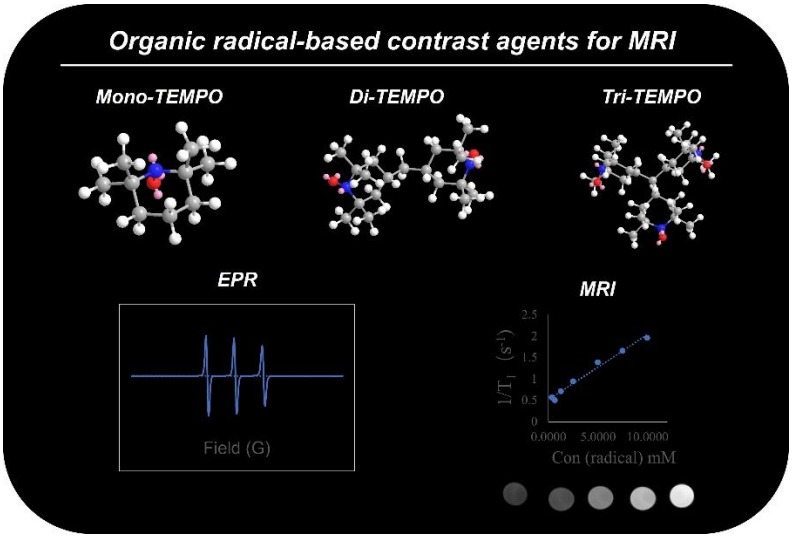

Figure 1: organic radical-based contrast agents for MRI

(1) S. Zhang, et al. *Pharmaceutics*, 2023, **15**, 1776.
(2) Ch. Tian, et al. *Adv. Ind. Eng. Polym. Res*. 2024, **7**, 255-261.
(3) Y. Wu, et al. *ACS Appl. Mater. Interfaces*. 2024,**16**, 65295-65306.
(4) Y. Wu, et al. *Acta Biomaterialia*. 2025,**192**, 461-472.
(5) Y. Wu, et al. *Dyes Pigm*. 2025, **232**, 11248.
(6) S. Zhang, et al. *Eur. Polym. J*. 2025, **235**, 113691..

Facile Ambient-Condition Synthesis of High-Entropy Alloy Nanoparticles by Colloidal Coreduction for Bifunctional Oxygen Electrocatalysis

Chenxin Yang[1], Muriel Freixanet[1], Jielin Zhang[1], Aziz Genç[1], Hamid Mollania[2], Pu Chen[2], Andreu Cabot[2,3,*], Jordi Arbiol[1,3,*], Neus Bastús[1*]

[1] *Catalan Institute of Nanoscience and Nanotechnology (ICN2), CSIC and BIST, 08193, Barcelona, Catalonia, Spain*

[2] *Catalonia Institute for Energy Research (IREC), Sant Adrià de Besòs, 08930, Catalonia, Spain*

[3] *ICREA, Pg. Lluis Companys, 08010 Barcelona, Catalonia, Spain*

Email address: chenxin.yang@icn2.cat

Keywords: High-entropy alloys; Nanoparticles; Wet-chemical synthesis; Electrocatalysis

High-entropy alloys (HEAs) have emerged as promising electrocatalysts due to their compositional complexity and tunable electronic structures and surface properties. However, the synthesis of HEA nanoparticles often requires harsh conditions, like high temperature and pressure, limiting their systematic optimization at the nanoscale.

Here, we investigate a facile strategy for synthesizing multimetallic HEA nanoparticles under ambient conditions. A series of noble-metal-based HEAs with different compositions and synthesis conditions was prepared by chemical coreduction. The effects of metal concentration, reducing agent concentration, polymer stabilization, were systematically investigated. The resulting materials were characterized by transmission electron microscopy(TEM), dynamic light scattering(DLS), X-ray photoelectron spectroscopy(XPS), and elemental analysis to correlate synthesis conditions with particle size, morphology, composition, and surface chemistry.

The synthesized HEAs are further evaluating for the oxygen evolution reaction (OER) and oxygen reduction reaction (ORR), and will continuously conduct theoretical computation like DFT, aiming to establish structure-composition-activity relationships finally. This work provides a mild and systematic approach for controlling the synthesis and surface properties of HEA nanoparticles for electrocatalytic applications.



Figure 1: Route of the project: synthesis, applications and theoretical inductively analysis

2026 JPhD 10th edition